Casing Wear Study on Gullfaks Field

Establishing a Relevant Casing Wear Model for Gullfaks

Department of Mineral Recourses

and Petroleum Engineering

Montanuniversität Leoben, Austria

Statoil

Benedikt Bindl, BSc

Leoben, November 2010

Affidavit

I declare in lieu of oath, that I wrote this thesis and performed the associated research myself, using only literature cited in this volume.

Eidesstattliche Erklärung

Ich erkläre an Eides statt, dass ich diese Arbeit selbständig verfasst, andere als die angegebenen Quellen und Hilfsmittel nicht benutzt und mich auch sonst keiner unerlaubten Hilfsmittel bedient habe.

Leoben, 28.03.2011

Benedikt Bindl

Acknowledgement

This thesis is carried out at the Mining University of Leoben, Department of Mineral Recourses and Petroleum Engineering for Statoil ASA.

I thank Univ.-Prof. Dipl.-Ing. Dr. mont. Gerhard Thonhauser for great guidance and co-operation throughout the developing and outlining of this thesis.

Thank you to Benjamin Bourgeois for his general expertise and his excellent guidance. In addition, he has been of great support to develop this thesis.

A very special thanks goes to my family for believing in me and the continuing support during all my study.

I also would like to thank my friends for endorsing me and for all the great times we had.

Abstract

The drilling industry in Norway faces new problems nowadays. The operators are reaching the capacity limits for existing installations and therefore need to re-use mature surface and intermediate casing sections of old wells. It is necessary to know the precise casing condition to make sure, that this worn casing can withstand the applied drilling loads. Therefore an extensive casing wear simulation has to be carried out before planning a new sidetrack.

The scope of this master thesis was to develop a relevant casing wear model for the Gullfaks field on the Norwegian continental shelf. The work presented is split in three parts.

The first chapters deal with general information about Gullfaks and different casing wear mechanisms and basics. This part also contains the results of extensive laboratory tests with several muds, additives and casing materials. An introduction to casing wear logging and in special to USIT logging, including detailed information on ultra sonic imaging, is also included.

The following chapters describe the theoretical background of the used prediction software package Cwear and how it is operated. Special attention is put on the result output and how this is processed to compare it with existing USIT logs.

The last part includes the simulation process workflow, the data acquisition and log processing. A detailed discussion about the presented outcome is included and possible software and procedure improvements and outlooks into the future presented.

Kurzfassung

Die norwegische Erdölindustrie ist heut zu Tage mit immer neuen Problemen konfrontiert. Die Firmen erreichen die Kapazitätsgrenzen der existierenden Plattformen und müssen daher Sektionen alter Bohrlöcher wiederverwenden. Dabei ist es sehr wichtig den Zustand des Casings zu kennen, um sicher zu stellen, dass ein abgenutztes Casing auch den auftretenden Kräften standhalten kann. Aus diesem Grund muss die Abnutzung sehr genau simuliert werden, bevor mit der Planung einer neuen Ablenkung begonnen wird.

Ziel dieser Diplomarbeit ist es, ein relevantes Vorhersagemodell dieser Abnutzung für das norwegische Ölfeld Gullfaks zu erstellen.

Die hier präsentierte Arbeit teilt sich grob in drei Teile. Die ersten Kapitel behandeln generelle Informationen über das Gullfaks Öl und Gasfeld, die verschiedenen Arten der Casingabnützung und deren Grundlagen. Dieser Teil enthält auch die Ergebnisse ausgiebiger Labortest mit verschiedenen Bohrspülungen, Zusätzen und Casingmaterialien. Eine Einleitung in die Abnützungsmessung und im Speziellen in USIT-Messungen ist ebenfalls in diesem Kapitel enthalten.

Die folgenden Kapitel behandeln den theoretischen Hintergrund der verwendeten Vorhersagesoftware „Cwear" und ihre Funktionsweise. Spezielle Aufmerksamkeit wird dabei auf die Ergebnisausgabe und den Vergleich der Simulation mit der gemessenen Abnützung gelegt.

Der letzte Teil der Arbeit beinhaltet den Arbeitsablauf einer Simulation, die Zusammenstellung der nötigen Daten und die Aufbereitung der Bohrlochmessungen. Außerdem wird das Ergebnis der Arbeit diskutiert und mögliche Verbesserungen der Software und Arbeitsabläufe sowie ein Ausblick in die Zukunft präsentiert.

Contents

AFFIDAVIT I

EIDESSTATTLICHE ERKLÄRUNG I

ACKNOWLEDGEMENT II

ABSTRACT III

KURZFASSUNG IV

1 INTRODUCTION 1

1.1 The Gullfaks field 1

1.2 Gullfaks blend 3

1.3 Gullfaks Reservoir 4

2 CASING WEAR BASICS 6

2.1 Casing wear model 6

2.1.1 Volumetric wear rate 6

2.1.2 Wear depth and volume 8

2.1.3 Contact pressure 10

2.1.4 Weight of steel particles 11

2.1.5 Casing wear in doglegs 11

2.1.6 Casing wear during tripping 13

2.2 Laboratory tests 15

2.2.1 Test procedure 16

2.3 Casing wear mechanisms 17

2.3.1 Machining wear 18
2.3.2 Galling wear 18
2.3.3 Grinding wear 20
2.3.4 Polishing wear 22

2.4 Influences on casing wear 22
2.4.1 Mud properties 22
2.4.1.1 Effect of additives 25
2.4.1.2 Effect of barite 27
2.4.1.2.1 Effect of barite in different muds 27
2.4.1.2.2 Effect of barite concentration 30
2.4.1.3 Effect of mud weight 32
2.4.2 Lubricants 34
2.4.3 Casing properties 36
2.4.3.1 Effect of casing material in water based mud 36
2.4.3.2 Effect of casing material in oil based mud 38
2.4.4 Tool joint material 40
2.4.4.1 Smooth steel 41
2.4.4.2 Tungsten-carbide hardbanding 41
2.4.4.3 Non-tungsten-carbide hardfacing 42
2.4.5 Buckling 44
2.4.6 Doglegs 45
2.4.6.1 Effect of dogleg location 45
2.4.6.2 Effect of dogleg magnitude 47
2.4.6.3 Type of dogleg 48
2.4.7 Lateral loads 48
2.4.8 Tripping 51

2.5 Effects of wear on casing strength 51
2.5.1 Types of casing failures 52
2.5.2 Failure due to internal pressure 53
2.5.2.1 Failure modes 53
2.5.2.2 Internal pressure thread leakage 53

2.5.2.3 Burst failure 55
2.5.3 Failure due to external pressure 56
2.5.3.1 External pressure thread leakage 56
2.5.3.2 Collapse failure 57
2.6 Casing wear logging 58
2.6.1 Logging principles 59
3 ULTRA-SONIC-IMAGING 60
3.1 Tool principle 60
3.2 USIT measurement 61
4 INTRODUCTION TO CWEAR 64
4.1 Theoretical Background 64
4.1.1 Nonlinear correction factor 65
4.1.2 Drag and lateral loads 66
4.1.3 Burst and collapse of worn casing 67
4.1.3.1 Biaxial equations 67
4.1.3.2 API equations 67
4.1.3.3 OTS equations 68
4.2 Input parameters 68
4.2.1 Tool bar 68
4.2.2 Units 69
4.2.3 Project page 69
4.2.3.1 Drill 70
4.2.3.2 Redrill 70
4.2.3.3 Ream Upward 70
4.2.3.4 Rotate Off Bottom 71
4.2.4 Survey page 71
4.2.5 Tubular page 72

4.2.6 Wellbore page 72
4.2.7 Operation page 73
4.2.7.1 Drill / Redrill 73
4.2.7.2 Ream upwards 74
4.2.7.3 Rotate off bottom 74
4.2.8 Wear factor page 75
4.2.8.1 Wear Factor Expert System 76
4.2.8.2 Wear Factor Database 76
4.2.9 Wear history page 77

4.3 Result output 77
4.3.1.1 Main output window 78
4.3.2 Casing wear schematic graph 79

5 GULLFAKS WEAR MODEL 81

5.1 Data acquisition 81
5.1.1 Well information 81
5.1.1.1 Wellbore survey data 82
5.1.1.2 Casing sizes and depths 84
5.1.1.3 Operations data 84
5.1.1.4 Drill string composition data 85
5.1.2 Log data 85
5.1.2.1 Simulation matching 91
5.1.2.2 Comparison with Schlumberger wear report 92
5.1.3 Operation simplification 93

5.2 Simulations 95
5.2.1 Uncertainties 95
5.2.1.1 Tool joint outside diameter 95
5.2.1.2 Tool joint length 96
5.2.1.3 Drillpipe outside diameter 97
5.2.1.4 Hardbanding material 99

5.2.1.5 Operational parameters 100
5.2.2 Workflow 101

5.3 Results 104

5.4 Discussion on the analysis 106
5.4.1 Cwear 106
5.4.1.1 Operation Limitations 106
5.4.1.2 Cwear workflow 107
5.4.1.3 Input data 107
5.4.1.4 Wear history 108
5.4.2 USIT logs 108
5.4.3 Uncertain drilling parameters 108
5.4.3.1 Comparison measured and reported operations 108

6 CONCLUSION 111

7 NOMENCLATURE I

8 REFERENCES II

APPENDIX A: INPUT FOR EXAMPLE WELL 34/10 B-14A T3 V

APPENDIX B: RESULTS FOR EXAMPLE WELL 34/10 B-14A T3 X

APPENDIX C: CWEAR OUTPUT FOR EXAMPLE WELL 34/10 B-14A T3 XIV

List of Figures

Figure 1: Gullfaks general information [1] [3] 1
Figure 2: Gullfaks structures [3] 2
Figure 3: Gullfaks geological information I [3] 4
Figure 4: Gullfaks geological information II [3] 5
Figure 5: Volumetric wear theory [4] 6
Figure 6: Wear geometry [5] 9
Figure 7: Relationship wear depth – wear volume [5] 9
Figure 8: Volumetric wear groove [4] 11
Figure 9: Casing wear test machine – schematic [7] 15
Figure 10: Casing wear test machine [7] 15
Figure 11: Wear testing analysis [7] 16
Figure 12: Machining wear [7] 18
Figure 13: Machining wear – debris [7] 18
Figure 14: Galling wear [7] 19
Figure 15: Galling wear – debris [7] 19
Figure 16: Grinding wear I [7] 20
Figure 17: Grinding wear II [7] 20
Figure 18: Wear rate vs. contact pressure [7] 21
Figure 19: Grinding wear – debris [7] 21
Figure 20: Polishing wear [7] 22
Figure 21: Mud type – casing wear 23
Figure 22: Mud type – wear factor 24
Figure 23: Mud type – friction factor 24
Figure 24: Additives – casing wear 25
Figure 25: Additives – wear factor 26
Figure 26: Additives – friction factor 27
Figure 27: Effect of barite – casing wear 28
Figure 28: Effect of barite – wear factor 29

Figure 29: Effect of barite – friction factor 29
Figure 30: Effect of barite concentration – casing wear 30
Figure 31: Effect of barite concentration – wear factor 31
Figure 32: Effect of barite concentration – friction factor 31
Figure 33: Effect of mud weight – casing wear 32
Figure 34: Effect of mud weight – wear factor 33
Figure 35: Effect of mud weight – friction factor 33
Figure 36: Effect of lubricants – casing wear 35
Figure 37: Effect of lubricants – wear factor 35
Figure 38: Effect of lubricants – friction factor 36
Figure 39: Casing material in WBM – casing wear 37
Figure 40: Casing material in WBM – wear factor 38
Figure 41: Casing material in WBM – friction factor 38
Figure 42: Casing material in OBM – casing wear 39
Figure 43: Casing material in OBM – wear factor 40
Figure 44: Casing material in OBM – friction factor 40
Figure 45: Tooljoint hardfacing – casing wear 42
Figure 46: Tooljoint hardfacing – wear factor 43
Figure 47: Tooljoint hardfacing – friction factor 43
Figure 48: Effect of buckling I [9] 44
Figure 49: Effect of buckling II [9] 45
Figure 50: Effect of dogleg depth – casing wear 46
Figure 51: Effect of dogleg severity – casing wear 47
Figure 52: Types of doglegs [10] 48
Figure 53: Effect of lateral loads – casing wear 49
Figure 54: Effect of lateral loads – wear factor 50
Figure 55: Effect of lateral loads – friction factor 50
Figure 56: Variation of casing dimensions [12] 52
Figure 57: Internal pressure failure tc [7] 53
Figure 58: Internal pressure leakage [7] 54
Figure 59: Burst pressure comparison [7] 56
Figure 60: Collapse failure [7] 58

Figure 61: USIT tool description [13] 61
Figure 62: USIT processing[13]..62
Figure 63: Output description [13] 63
Figure 64: Wear factor vs. casing wear [16] 65
Figure 65: Nonlinear correction factor [16] 66
Figure 66: Drag and lateral loads [17] 67
Figure 67: Cwear project page 70
Figure 68: Cwear survey page 71
Figure 69: Cwear tubular page 72
Figure 70: Cwear wellbore page 73
Figure 71: Cwear operation page – drilling 74
Figure 72: Cwear operation page – backreaming 74
Figure 73: Cwear operation page – rotating 75
Figure 74: Cwear wear factor page 76
Figure 75: Cwear wear history page 77
Figure 76: Cwear result ouput 79
Figure 77: Cwear schematic graph 80
Figure 78: Influence of survey accuracy 83
Figure 79: Operation data 85
Figure 80: Drillstring composition 85
Figure 81: USIT data of C-38 original and removed connections 87
Figure 82: USIT data of B-28 removed connections and moving average 88
Figure 83: Wall thickness cross section 89
Figure 84: Wall thickness vs. angle 90
Figure 85: Cross section histogram 91
Figure 86: Schlumberger visual USIT log interpretation [21] 92
Figure 87: Original vs. simplified operations 94
Figure 88: Influence of tool joint OD 95
Figure 89: Wear trend for tool joint OD 96
Figure 90: Influence of tool joint length 97
Figure 91: Influence of drillpipe OD 98
Figure 92: Wear trend for drillpipe OD 99

Figure 93: Hardbanding ARNCO 300 XT [22] ... 100
Figure 94: Simulation workflow ... 103
Figure 95: Equivalent ProNova TxD – KPI – operation report [23] ... 110
Figure 96: ProNova time break down [23] ... 110
Figure 97: 30/10 B-14A T3 wellpath ... VI
Figure 98: 30/10 B-14A T3 BHA I ... VIII
Figure 99: 30/10 B-14A T3 BHA II ... VIII
Figure 100: 30/10 B-14A T3 BHA III ... VIII
Figure 101: 30/10 B-14A T3 original and cleaned USIT log ... IX
Figure 102: 30/10 B-14A T3 simulations WF 9 and 12 ... X
Figure 103: 30/10 B-14A T3 simulations WF 20 and 30 ... XI
Figure 104: 30/10 B-14A T3 Schlumberger log interpretation [24] ... XII
Figure 105: 30/10 B-14A T3 Output graph I ... XXXVIII
Figure 106: 30/10 B-14A T3 Output graph II ... XXXVIII
Figure 107: 30/10 B-14A T3 Output graph III ... XXXIX
Figure 108: 30/10 B-14A T3 Output graph IV ... XXXIX
Figure 109: 30/10 B-14A T3 Output graph V ... XL
Figure 110: 30/10 B-14A T3 Output graph VI ... XL

List of Tables

Table 1: Casing wear mechanisms 17

Table 2: Mud properties 23

Table 3: Effect of additives 25

Table 4: Effect of barite 27

Table 5: Effect of barite concentration 30

Table 6: Effect of mud weight 32

Table 7: Effect of lubricants 34

Table 8: Effect of casing material in WBM 37

Table 9: Effect of casing material in OBM 39

Table 10: Non-tungsten carbide hardfacing 42

Table 11: Effect of dogleg location 46

Table 12: Effect of dogleg severity 47

Table 13: Effect of lateral loads 49

Table 14: Operational parameters 101

Table 15: Well overview 104

Table 16: Simulation results 105

Table 17: DBR report [23] 109

Table 18: 30/10 B-14A T3 operational parameters VII

Table 19: 30/10 B-14A T3 project description 14

Table 20: 30/10 B-14A T3 general data XIV

Table 21: 30/10 B-14A T3 tabulated wear results XXI

Table 22: 30/10 B-14A T3 tabulated loads and forces XXIX

Table 23: 30/10 B-14A T3 tabulated pressures XXXVI

Table 24: 30/10 B-14A T3 results XXXVII

1 Introduction

1.1 The Gullfaks field

The main Gullfaks field is located in the Northern part of the Norwegian North Sea, in Block 34/10.

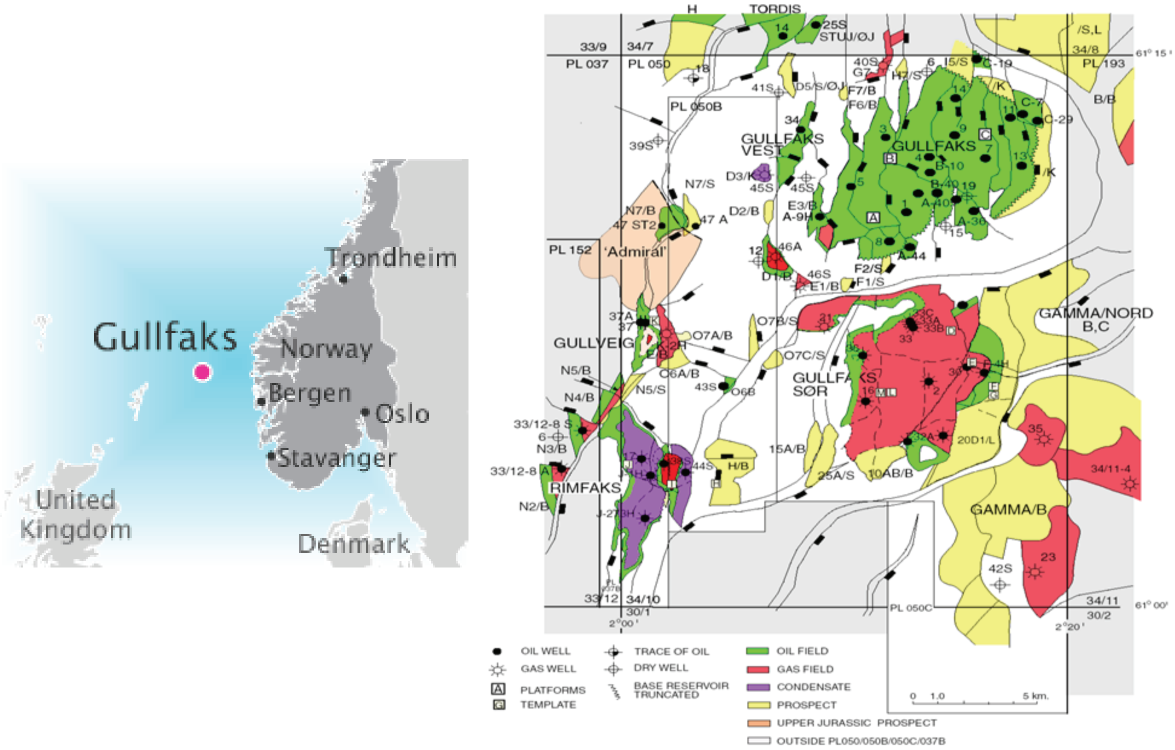

Figure 1: Gullfaks general information [1] [3]

It's development plan was to build three stationary concrete production platforms. The Gullfaks A platform began production on the 22nd of December 1986, with Gullfaks B following the 29th of February 1988 and the C platform the 4th of November 1989.

The oil transport to shore is ensured by shuttle tankers, while the gas is compressed and pumped to the Kårstø gas treatment plant north of Stavanger and from there to continental Europe. The A platform is used for storing and exporting stabilised crude from the Vigdis and Visund fields.

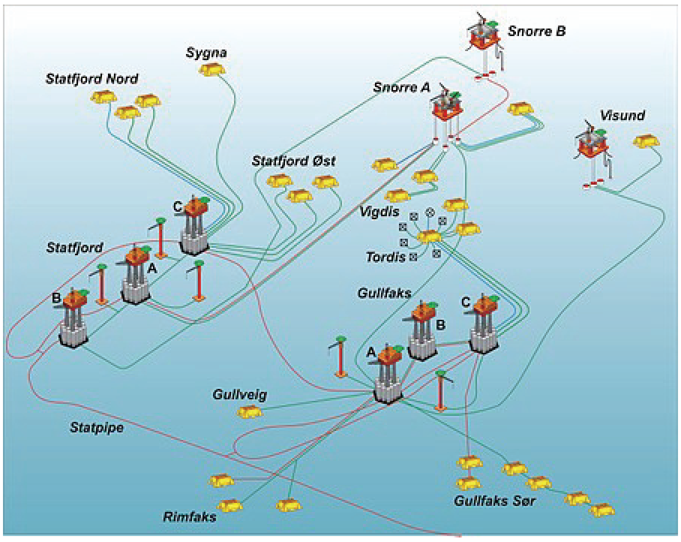

Figure 2: Gullfaks structures [3]

Oil and gas from Gullfaks B is transferred to the A and C platforms for processing, storage and export.

Since June 1994, Gullfaks C has received and processed oil from the Tordis field. The field set a production record of 605,965 barrels for a single day on the 7th of October 1994.

Three satellite fields – Gullfaks South, Rimfaks, Skinfaks and Gullveig – have been developed with subsea wells remotely controlled from the Gullfaks A and C platforms.

The recovery factor on Gullfaks is 59 per cent, with the goal is to increase it to 62 per cent. Measures to improve recovery include horizontal and extended-reach wells, new completion and sand control technology, and water alternating gas injection.

Block 34/10 was awarded in 1978 to three Norwegian companies:

- Statoil (operator)
- the former Norsk Hydro
- the former Saga Petroleum

This was the first time a purely domestic consortium had been awarded an offshore licence. [1]

1.2 Gullfaks blend

Gullfaks Blend is a light, low sulphur North Sea crude oil.

Gullfaks Blend facts:

- Commingling fields: Gullfaks A/B/C, Gullfaks satellites, Vigdis, Visund, Tordis and Gimle
- Operator: Statoil
- Location: Norway
- Loading port: Offshore
- Cargo size: Standard buoy loaders (855 000 bbl)
- Crude production: 192 000 bbl/day

Crude characteristics:

- API: 37.5°
- S.G.: 0.8372
- Sulphur: 0.22 mass%
- Pour Point: -15 °C
- TAN: 0.10 mg KOH/g
- Nickel: 1.0 wppm
- Vanadium: 1.0 wppm
- Visc. (20°C): 5.74 cSt

The produced crude is sometimes slightly lighter than the current assay. [2]

1.3 Gullfaks Reservoir

The Gullfaks Field lies to the west of the Viking Graben, and constitutes a structural high point in the Tampen area. The field comprises a number of rotated fault blocks, containing mainly pre-, but also syn-rift sediments as young as late Jurassic to early Cretaceous in age and is divided into three main structural domains. The central and western areas of the field consist of a domino system of westerly dipping rotated fault blocks. A nonrotated horst complex lies farthest to the east. Between these two areas lies a complex accommodation area, characterised by a fragmented antiformal fold structure. The structural architecture of Gullfaks is mainly the result of late Jurassic-early Cretaceous rifting, although earlier rift structures of Permian-Triassic age probably influenced the later structural development to some degree.

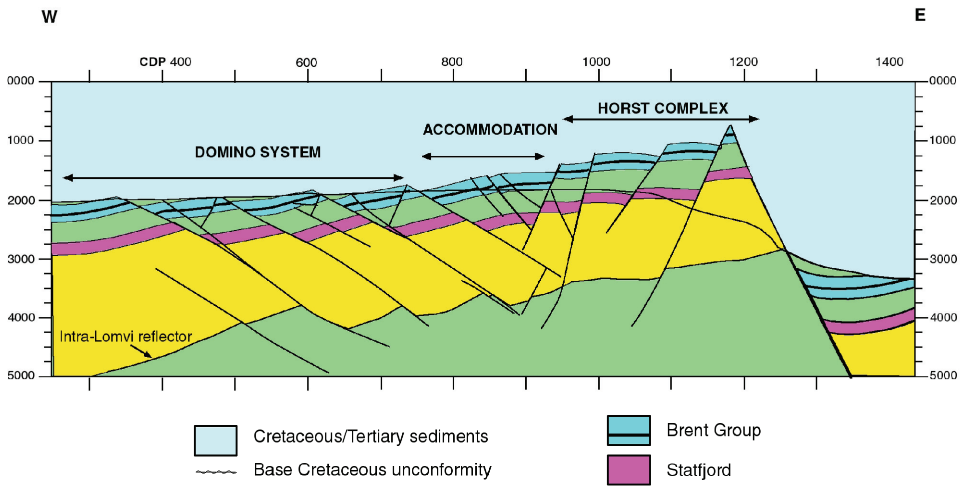

Figure 3: Gullfaks geological information I [3]

The field is dissected by a set of main faults which form an anastomosing pattern, with a dominant north-south orientation in map view. These faults typically have offsets of between 50 and 250 metres, although throws of almost 500 metres are recorded. The main faults in the domino system have an eastward dip of approximately 30°. In the horst complex, the faults have a westward dip of approximately 60-65°. [3]

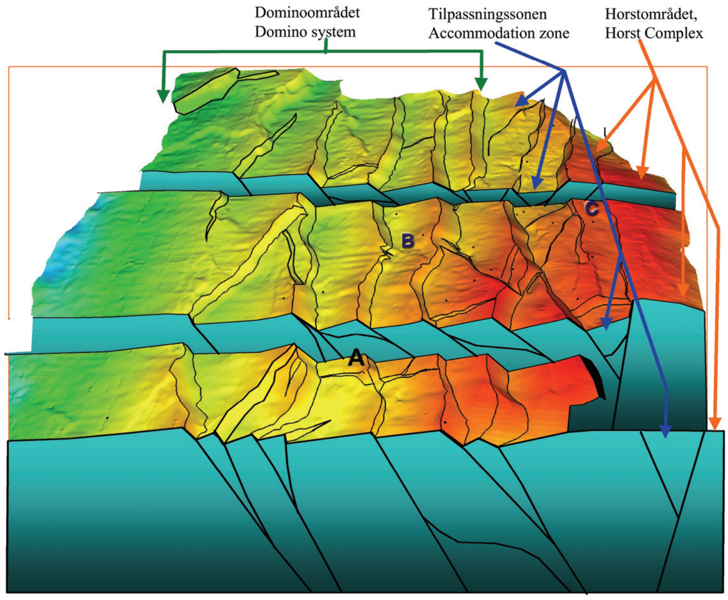

Figure 4: Gullfaks geological information II [3]

2 Casing wear basics

This chapter gives an overview of casing wear. It is vital to understand the different wear modes and where they differ. It is also necessary to know how the casing wear is dependent on several values.

2.1 Casing wear model

2.1.1 Volumetric wear rate

Rotating tool joints that are subjected to lateral loads will wear crescent ("moon-shaped") grooves in casing/risers. The model presented here calculates the volume of material worn away in the crescent wear groove and from this calculates the depth of the wear groove. [4]

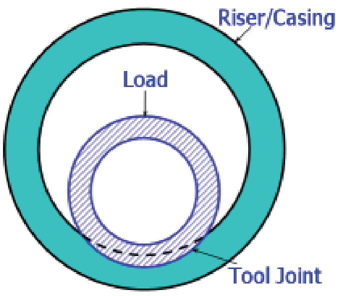

Figure 5: Volumetric wear theory [4]

The volume of casing worn away in a unit length of casing in time, t, by a rotating tool joint equals:

$$V = \frac{E}{e} \quad \left[\frac{in^3}{ft}\right] \qquad \text{Equation 1}$$

where

E = energy input per unit length [in*lb/ft]

e = specific energy [in*lb/in^3]

Specific energy is defined as the amount of energy required to remove a unit volume of metal.

The frictional energy, E, imparted to the casing/riser equals:

$$E = f \cdot F_{lat} \cdot D \quad \left[\frac{in \cdot lb}{ft}\right]$$

Equation 2

where

f = friction factor []

F_{lat} = lateral load on tool joint per unit length [lb/ft]

D = sliding distance [in]

Combining these Equations above shows that wear volume, V, equals:

$$V = \frac{f \cdot F_{lat} \cdot D}{e} \quad \left[\frac{in^3}{ft}\right]$$

Equation 3

The total sliding distance, D, between the tool joint and casing equals:

$$D = \pi \cdot N \cdot d \cdot t \quad [in]$$

Equation 4

where

N = rotary speed [rpm]

d = tool-joint diameter [in]

t = contact time [min]

Contact time t equals:

$$t = \frac{S \cdot L_{TJ}}{ROP \cdot L_{DP}} \quad [\min]$$

Equation 5

where

S = drilling distance [ft]

L_{TJ} = tool-joint length [ft]

ROP = rate of penetration [ft/min]

L_{DP} = drill-pipe joint length [ft]

Tool-joint lateral load per foot F_{lat} equals:

$$F_{lat} = \frac{F_{DP} \cdot L_{DP}}{L_{TJ}} \quad \left[\frac{lb}{ft}\right]$$

Equation 6

where

F_{DP} = average lateral load on the drill pipe [lb/ft]

Wear factor WF controls wear efficiency and is defined as:

$$WF = \frac{f}{e} \quad \left[\frac{in^2}{lb}\right]$$

Equation 7

The total wear volume can be calculated by dividing the total distance drilled into discrete intervals and estimating wear in each interval as follows:

$$V = \sum_{i=1}^{n} \Delta V_i$$

Equation 8

where

ΔV_i = incremental wear volume for each incremental drilling distance.

2.1.2 Wear depth and volume

Geometry of the crescent wear groove is a function of casing or riser inner diameter and tool-joint outer diameter (R and r), and depth of penetration into the casing wall (h). It is important to note that the volume of the worn crescent increases nonlinearly with wear depth because the wear groove becomes wider as wear depth increases. [5]

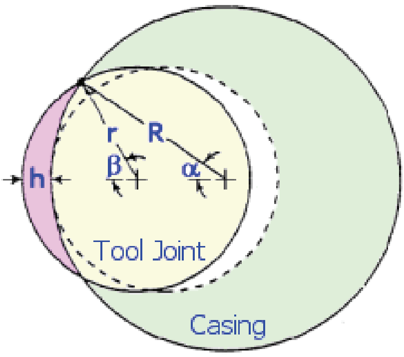

Figure 6: Wear geometry [5]

An example wear-depth/wear-volume relationship is shown for a 6 ½ in. tool joint rotating in 9 5/8 in, 47-lb/ft casing. The 0.47 in. thick casing is completely worn through when the groove wear volume reaches 22.1 in^3/ft.

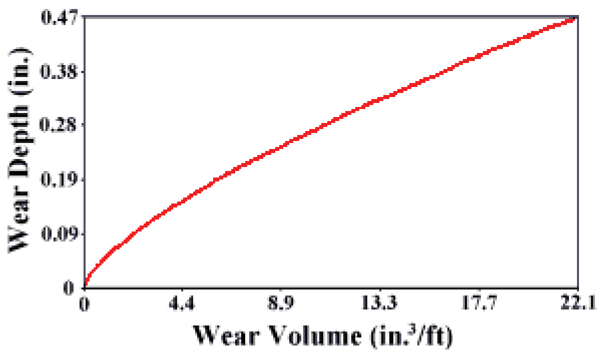

Figure 7: Relationship wear depth – wear volume [5]

The relationship between the volume and the wear depth is

$$V = 12 \cdot \left(\beta \cdot r^2 + R \cdot (s + h) \cdot \sin\alpha - \alpha \cdot R^2\right) \qquad \text{Equation 9}$$

where

V = volume [in^3/ft]

h = wear depth

R = casing inner radius [in]

r = tool joint outer radius [in]

s = offset distance

Angles α and β are in radians and calculated as follows:

$$\alpha = \arcsin\left[\frac{1}{2 \cdot R \cdot (s+h)} \cdot \sqrt{2 \cdot \left[R^2 \cdot (s+h)^2 + r^2 \cdot R^2 + r^2 \cdot (s+h)^2\right] - \left[R^4 + r^4 + (s+h)^4\right]}\right]$$

Equation 10

$$\beta = \arcsin\left(\frac{R \cdot \sin\alpha}{r}\right)$$

Equation 11

2.1.3 Contact pressure

Casing wear changes from abrasive wear, at casing pressures less than about 200 psi, to adhesive or galling wear, at contact pressures greater than 200 psi. Abrasive wear consists of the solids in the mud slowly wearing away the metal whereas adhesive wear consists of the tool joint welding to and wearing tearing away the casing metal in large pieces. The different wear types are discussed in a following chapter. [6]

Contact pressure between the tool joint and the casing is defined as:

$$p = \frac{L'}{12 \cdot w} \quad [psi]$$

Equation 12

where

p = contact pressure [psi]

L' = tool joint lateral load [lbs/ft]

w = maximum width of wear groove [in]

The width of the wear groove equals:

$$w = 2 \cdot R \cdot \sin\alpha$$

Equation 13

where

R = casing inner radius [in]

α = defined in the upper chapter

2.1.4 Weight of steel particles

The weight of steel, worn from the casing, equals:

$$W = V \cdot \rho \quad \left[{}^{lb}\!/_{ft} \right]$$ Equation 14

where

W = wear weight [lb/ft]

V = wear volume [in3/ft]

ρ = density [lb/in3]

The model predicts the total steel volume worn from the casing.

Several major operators routinely monitor steel particles in the mud stream as an indicator of casing wear. A magnet is positioned in the mud return line and is checked regularly. This information is used to provide a qualitative measure of the casing wear and to describe an overall trend. [4]

2.1.5 Casing wear in doglegs

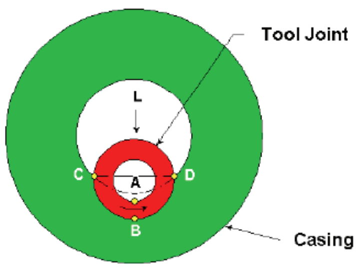

Figure 8: Volumetric wear groove [4]

The volume is proportional to the frictional energy and therefore varies as:

$$V = WF \cdot F_{DP} \cdot D \quad \left[{}^{in^3}\!/_{ft} \right]$$ Equation 15

where

V = wear volume [in^3/ft]

WF = wear factor [$pasi^{-1}$]

F_{DP} = drillpipe lateral load [lb/ft]

D = tool joint rotational sliding distance [in]

The lateral load between the drillpipe in the casing in doglegs equals:

$$F_{DP} = T \cdot \sin\Theta \quad \left[{lb}/{ft} \right]$$ Equation 16

where

T = drillstring tension load [lb/ft]

Θ = dogleg severity [°/ft]

Combining the equations equals:

$$V = WF \cdot T \cdot \sin\Theta \cdot D \quad \left[{in^3}/{ft} \right]$$ Equation 17

This equation shows that the casing wear volume is proportional to sinΘ. For small angles sinΘ ≈ Θ which shows that the wear volume is proportional to the dogleg severity. Therefore, if the dogleg severity doubles, the casing wear will double. This explains why major casing wear problems usually occurs at doglegs.

In a vertical well the drill string tension at the wear point is:

$$T_V = W_{DS} - W_{BIT} \quad [lbs]$$ Equation 18

where

T_V =drillstring tension [lbs]

W_{DS} = buoyant weight of drillstring below wear point [lbs]

W_{BIT} = weight applied to the bit [lbs]

In a deviated well, drillstring tension below the wear point, is affected by the hole angle and by drill string friction.

The tool joint rotational drilling distance for a rotating tool equals:

$$D = \pi \cdot 60 \cdot d \cdot N \cdot t \quad [in]$$ Equation 19

where

D = tool joint rotational sliding distance [in]

N = rotary speed [rpm]

d = tool-joint diameter [in]

t = contact time [min]

2.1.6 Casing wear during tripping

The wear model assumes that the wear volume is proportional to the frictional energy input.

$$V = \frac{E}{e} \quad [in^3]$$ Equation 20

where

E = energy input [in*lb]

e = specific energy [in*lb/in^3]

The frictional energy input imparted to the casing by a sliding tool joint equals:

$$E = f \cdot F_{lat} \cdot s \quad [in \cdot lb]$$ Equation 21

where

f = friction factor []

F_{lat} = lateral load [lb]

s = tool joint sliding distance [in]

The wear factor was defined in an earlier chapter but will be adapted as:

$$WF = \frac{f}{e} \quad \left[\frac{in^2}{lb}\right]$$ Equation 22

Combining these equations shows that the wear volume is:

$$V = WF \cdot F_{lat} \cdot s$$ Equation 23

When tripping the drillpipe a distance, the tool joint slides across a given wear point on the casing.

$$s = \left(\frac{x}{x_p} \right) \cdot s_p \quad [in]$$ Equation 24

where

s = tool joint sliding distance [in]

x = tool joint contact length [in]

x_p = drillpipe joint length including tool joint [in]

sp = drillpipe sliding distance [in]

It is important to notice that the wear factor in these equations is for the tool joint and therefore that it corresponds to the lateral loads on the tool joints, not the lateral loads on the drillpipe. [11]

The lateral load on a uniform diameter drillpipe bent around a curve equals:

$$F_{lat} = 2 \cdot W_{DS} \cdot \sin\left(\frac{\Theta}{2} \right) \quad \left[{}^{lbs}\!/_{ft} \right]$$ Equation 25

where

F_{lat} = lateral load [lbs/ft]

W_{DS} = buoyed weight of drillpipe below wear point [lbs]

Θ = dogleg severity [°/ft]

2.2 Laboratory tests

There are several casing wear test devices at universities and in the industry. All referred tests in this thesis were conducted with the 25 HP Drilco casing wear test machine as shown in the figure below.

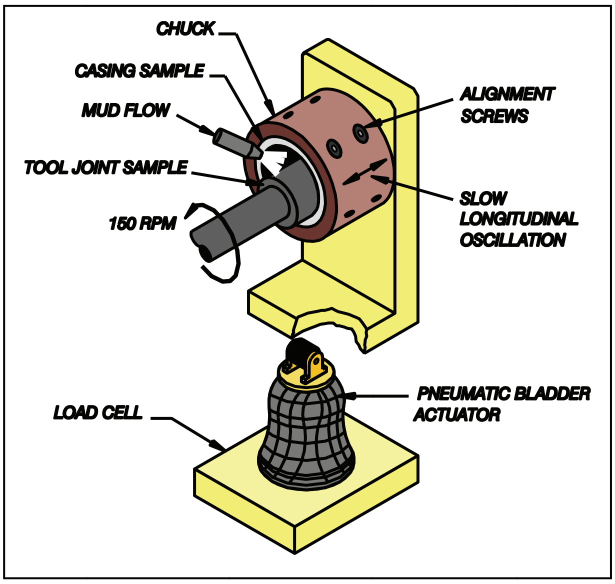

Figure 9: Casing wear test machine – schematic [7]

Figure 10: Casing wear test machine [7]

A tooljoint is rotated at 150 rpm and reciprocates the casing sample at a speed of 22 ft/hr to simulate movement of the drill pipe while drilling. A load of up to 7000 lb/ft is applied during these tests, to maintain uniform load between the casing and tool joint.

The automated machine utilizes:

- a large mud tank which eliminated the need to replace mud in short periods
- a linear transducer which measures casing wear continuously
- a computer controlled data acquisition system

The automated machine contains a feedback loop which allows the computer to monitor, vary and control the test conditions.

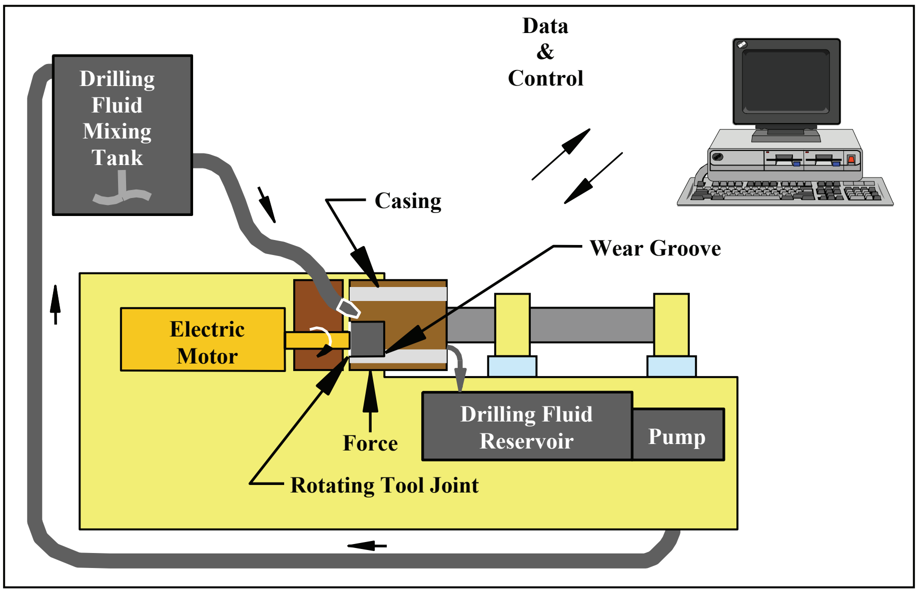

Figure 11: Wear testing analysis [7]

2.2.1 Test procedure

Following procedures were defined to get the most accurate and comparable measurements.

- It is very important to align the casing and the tool joint prior the test properly.
- If there are some aligning problems the grooves might become wider at one end.
- New batches of mud are mixed before every test to ensure the same mud composition.
- Every 30 minutes wear groove depth and width are measured during the test

- Following the test, the samples are cut up, measured and conserved

Most of the casing wear tests were conducted for 8 hours at 150 rpm which corresponds to 472 to 1912 hours rotating time in the field. The relationship between the field drilling time and the laboratory test time equals:

$$T = \frac{s}{S} \cdot \frac{L}{l} \cdot t \quad [hrs]$$

Equation 26

where

T = field rotating time [hrs]

t = laboratory test time [hrs]

L = drill pipe joint length including tool joint [ft]

l = tool joint / casing contact length [ft]

S = Field rotary speed [rpm]

s = laboratory rotary speed [rpm]

2.3 Casing wear mechanisms

Four basic types of wear are observed and shown in the following table.

Wear mechanisms	Wear debris	Wear factors
		[10^{-10} psi^{-1}]
Machining	Chips	400 – 1800
Galling	Flakes	20 – 50
Grinding	Powder	5-10
Polishing	Fine powder	0.1 - 1

Table 1: Casing wear mechanisms

The variation in wear rate by 2 to 3 orders of magnitude from grinding to machining wear was observed. The size of the debris is directly related to the wear rate, with the largest debris produced by the highest wear rate

2.3.1 Machining wear

Machining casing wear takes place when rough tungsten-carbide particles in the tool joint get exposed as the softer material, they are bedded in, wears away. Once they get exposed they act like a cutting tool, similar to the machining operation of a lathe.

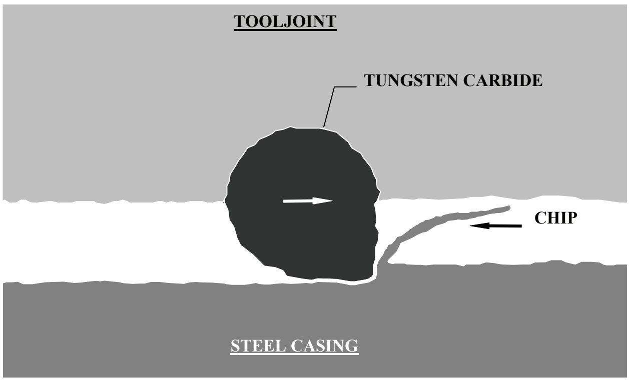

Figure 12: Machining wear [7]

The debris the cutting is producing looks like long chips. Some of them even look like steel wool. [7] [8]

Figure 13: Machining wear – debris [7]

2.3.2 Galling wear

Transferring steel in a solid-phase welding process from the casing to the tool joint due to higher strength of the tool joint is called galling wear.

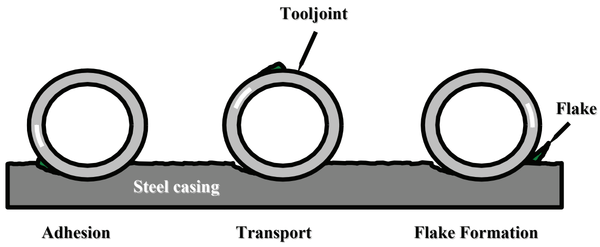

Figure 14: Galling wear [7]

The particles produced by this kind of wear mechanism look like flakes.

Three conditions must usually occur to produce galling wear:

- High lateral loads
- No solids in fluid
- Similar tooljoint – casing hardness

Galling wear often occurs with water or gel mud, when the metal surfaces get in intimate contact with high lateral loads without the presence of solids. A prevention of galling can be achieved by adding sand, barite or drill solids to the mud, to separate the sliding surfaces and keep them from coming in contact with each other. By adding sand to water based drilling fluid a reduction in wear by 50% to 75% can be gained. [7] [8]

Figure 15: Galling wear – debris [7]

2.3.3 Grinding wear

Another form of wear, where solid particles such as sand, barite or drill solids roll between the tool joint and the casing, is called grinding wear.

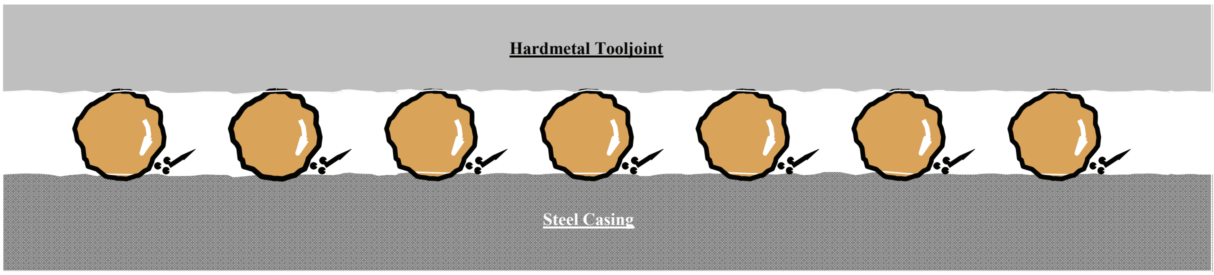

Figure 16: Grinding wear I [7]

The abrasive particles cause fractures at localized points because they exceed the strength of the steel. This is caused by high contact loads on these particles by the steel surfaces. A threshold force must be exceeded before the sand grains will cause brittle or plastic failure.

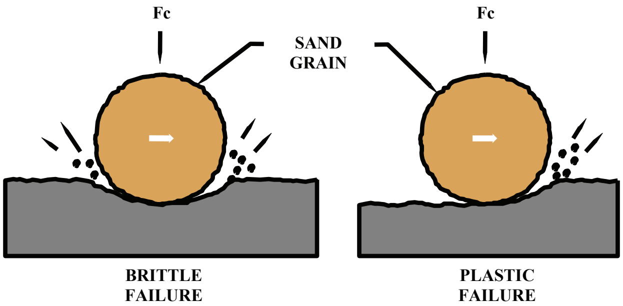

Figure 17: Grinding wear II [7]

Steel normally fails plastically, but heat generation during the wear process can cause the surface to fail in brittle manner.

High grinding wear rates require the following conditions:

- Solid particles with sufficient strength
- Solid particles with sufficient size
- The absence of softer solid particles to cushion the point loads on the harder grains
- Joint hardness greater than the casing hardness

- High lateral loads between tubing and casing

Grinding wear is low with very fine particles or heavy weight mud with sand, where the other solids prevent high loading of the individual sand grains. Fine steel powder is produced by grinding wear. [7] [8]

Casing wear changes from grinding or abrasive wear with low contact loads (below 250 psi) to galling or adhesive wear at high contact loads (above 250 psi). [6]

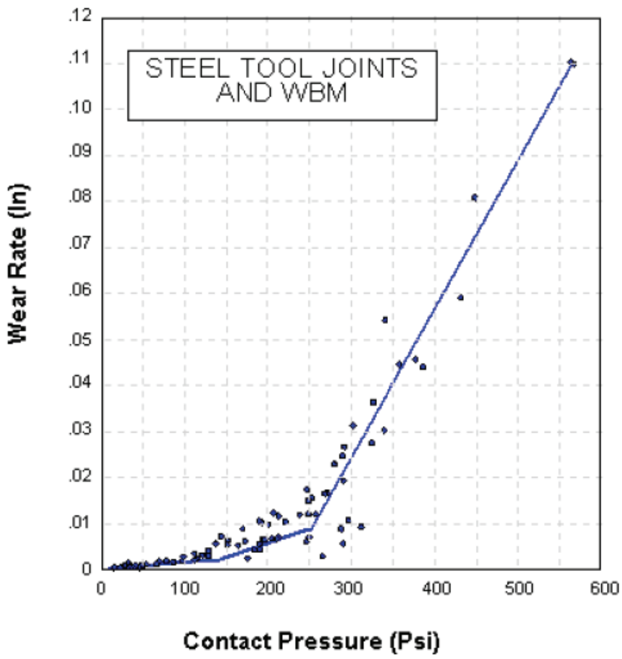

Figure 18: Wear rate vs. contact pressure [7]

These tests were conducted with steel joints and water based muds containing 6% sand.

Figure 19: Grinding wear – debris [7]

2.3.4 Polishing wear

When a particle is trapped in a soft material (e.g.: rubber) it produced a very smooth and polished surface, with very low wear rate. This is called polishing wear.

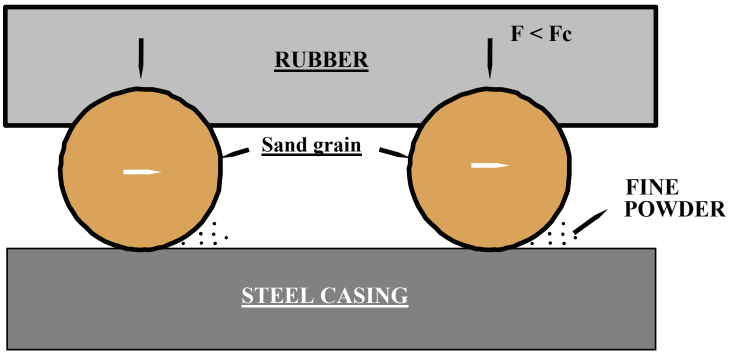

Figure 20: Polishing wear [7]

The soft material acts as cushioning medium, deforming and preventing the high particle contacts loading needed to abrasively remove steel particles as it is done with grinding wear. Polishing wear is observed with rubber drill pipe protectors in gel mud containing 2% sand. Wear rates with the rubber protectors were 90% lower than those with steel joints in the same mud.

Polishing produce very fine steel particles similar to those produced by grinding wear. [7] [8]

2.4 Influences on casing wear

To determine the influences of different properties on casing wear a lot of tests had to be carried out. All data in the following chapter is taken from various test reports and especially from the DEA-42 project. [7]

2.4.1 Mud properties

As seen in the table below, the mud type has a significant effect on casing wear.

Mud type	Mud weight		Sand vol.	Wear depth		Wear factor	Friction factor
	[ppg]	[sg]	[%]	[in]	[%]	[10^{-10} psi^{-1}]	
WB	10.0	1,20	7	0.084	18	5.5	0.20
HEC	9.5	1,14	7	0.179	38	16.8	0.30
XC	9.5	1,14	7	0.077	16	4.9	0.25
OB	9.7	1,16	7	0.041	9	1.9	0.09
Mineral oil	7.1	0,85	0	0.059	13	3.2	0.08
Mineral oil	8.6	1,03	7	0.043	9	2.1	0.10

Table 2: Mud properties

Wear with HEC polymer mud was 38% compared to 18% for water based mud. Wear with XC polymer mud (16%) was slightly lower than with the water based mud. The wear rate with oil based mud was only 9%. For mineral oil the wear rate was 9% with sand and 13% without sand. This shows that the use of oil based mud should greatly reduce casing wear.

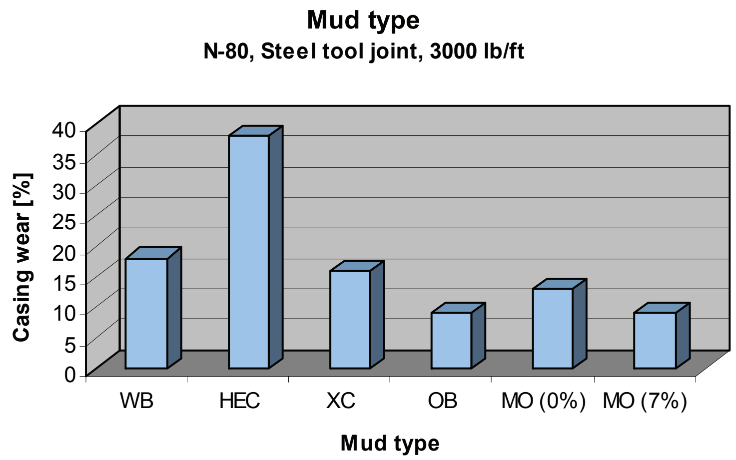

Figure 21: Mud type – casing wear

Wear factors ranged from 16.8 for the HEC mud to 1.9 for the oil based mud like seen in the figure below

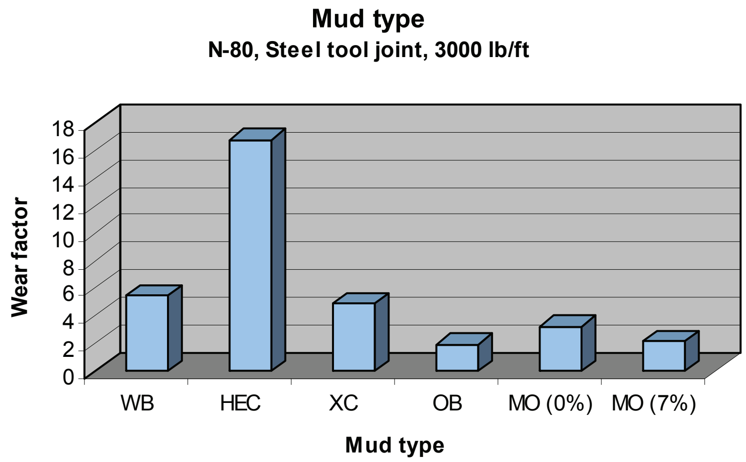

Figure 22: Mud type – wear factor

The friction factors for the HEC and XC polymer mud were higher than the water based mud whereas the friction coefficient for the oil and mineral oil based mud were much lower. This shows why oil based mud systems are often used in high angle and horizontal wells to overcome torque and drag problems.

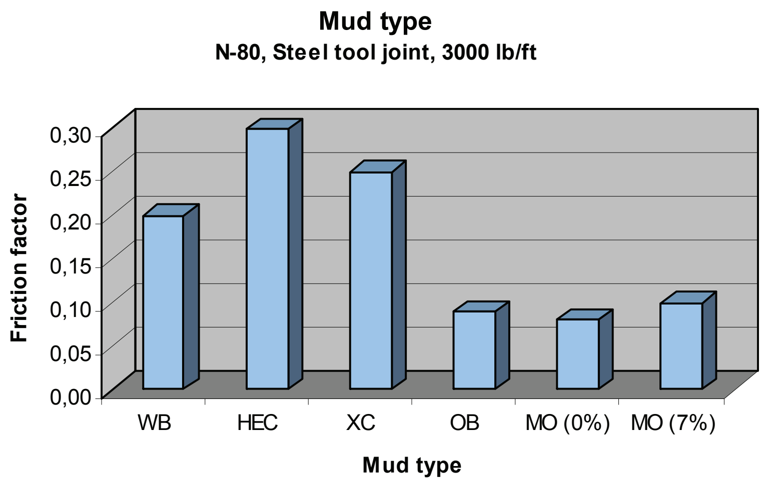

Figure 23: Mud type – friction factor

2.4.1.1 Effect of additives

The table and figures below show the effect of various mud additives on casing wear.

Additive	Mud type	Mud weight		Sand vol.	Wear depth		Wear factor	Friction factor
		[ppg]	[sg]	[%]	[in]	[%]	[10^{-10} psi^{-1}]	
None	W	8.3	1,00	0	0.260	55	29.00	0.32
None	WB	8.8	1,06	0	0.084	18	5.70	0.26
None	WB	10.0	1,20	7	0.086	18	5.60	0.21
Barite 5%	WB	10.0	1,20	0	0.012	3	0.33	0.19
Limestone 7%	WB	10.0	1,20	0	0.015	3	0.40	0.14
Gilsonite 5#/BBL	WB	10.0	1,20	7	0.024	5	0.90	0.15
Walnuts 6#/BBL	WB	10.0	1,20	7	0.045	10	2.20	0.16

Table 3: Effect of additives

The addition of bentonite to water reduced casing wear from 55% to 18%. The addition of barite, limestone, gilsonite or walnuts to the water bentonite mud caused a further reduction in casing wear.

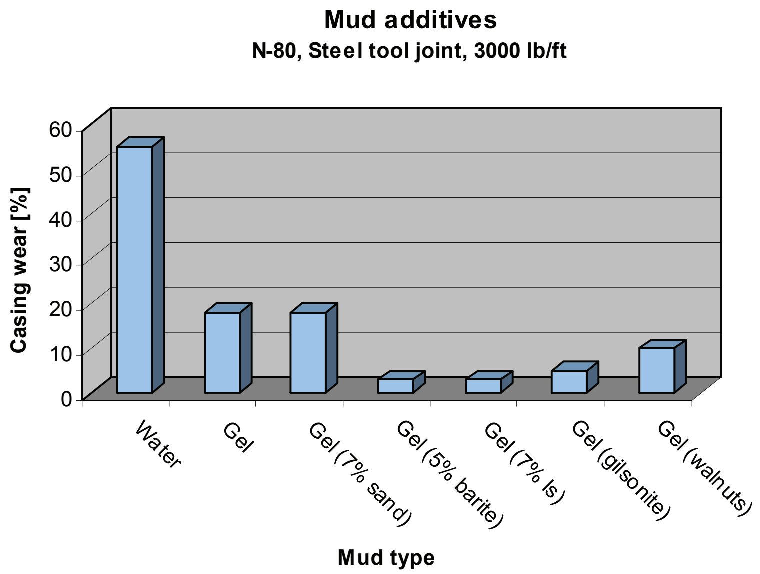

Figure 24: Additives – casing wear

The addition of 7% sand to the gel mud did not increase the casing wear above 18%. The addition of 5% barite reduced the wear by 3%. This shows the importance of weighting the mud with barite if casing wear problems exist.

The wear factor of water was reduced from 29 to 5.7 with the addition of bentonite as shown in the figure below. The addition of sand to the water and gel had very little effect on the wear factor, whereas the addition of barite results in a major reduction in wear factor. Reduced wear factors are also measured when gilsonite and limestone were added to water based mud.

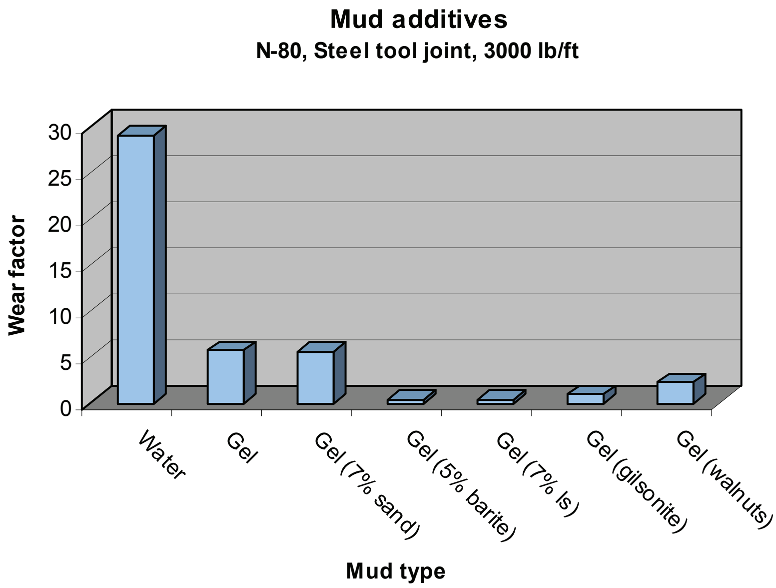

Figure 25: Additives – wear factor

The friction factors for all of these muds were in relatively broad range from 0.32 to 0.14. The weighted samples in general had a greater reduction in wear rate than in friction factor, as compared to un-weighted mud. This trend suggests that mechanical work is being input to the process, but not contributing to destruction of the casing wall. This work must be either converted into heat or used to disintegrate the solid materials in the mud.

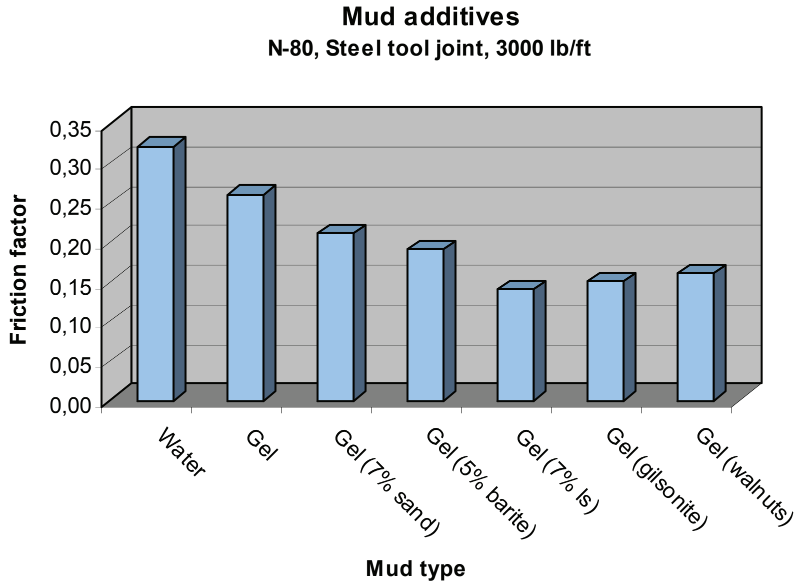

Figure 26: Additives – friction factor

2.4.1.2 Effect of barite

2.4.1.2.1 Effect of barite in different muds

Barite is commonly used to increase mud weight. In each test barite was found to effectively lower casing wear. When sand was added to a barite mud mixture, casing wear was increased as compared to mud without sand. Casing wear results with barite in three mud types are presented in the table below.

Mud type	Barite	Sand	Wear depth		Wear factor	Friction factor
	[%]	[%]	[in]	[%]	[10^{-10} psi^{-1}]	
Water based	0	0	0.084	18.0	5.70	0.26
Water based	5	0	0.012	2.5	0.30	0.19
Water based	5	2	0.020	4.2	0.67	0.16
Oil based	0	0	0.032	6.8	1.30	0.09
Oil based	5	0	0.010	2.1	0.24	0.04
Oil based	5	2	0.011	2.3	0.27	0.05
Petro free	5	0	0.012	2.5	0.31	0.07
Petro free	5	2	0.015	3.2	0.43	0.07

Table 4: Effect of barite

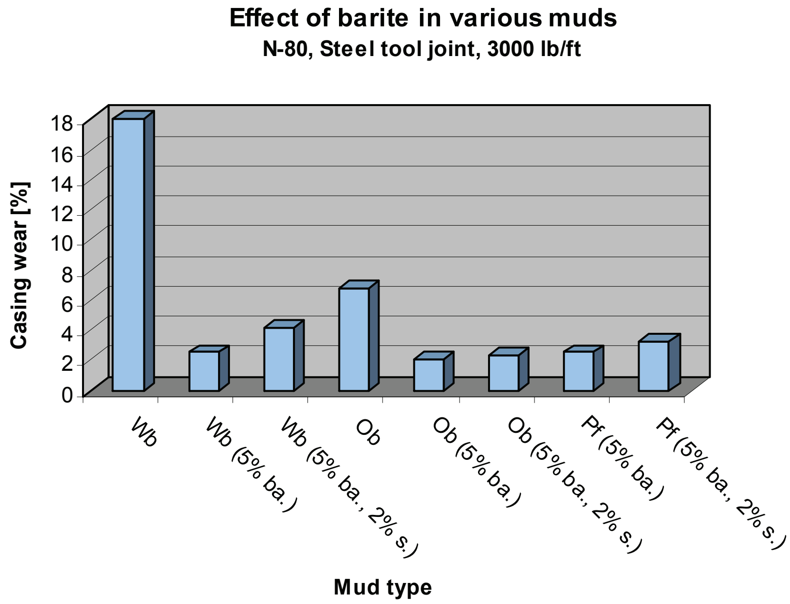

Figure 27: Effect of barite – casing wear

These barite test yielded interesting and unexpected results. The wear of unweighted oil based mud is less than half that with unweighted water based mud. However when barite is added to these muds the wear is reduced almost to the same value. This suggests, when barite is used, casing wear rate is controlled by barite content rather than mud type.

The addition of 2% sand to the mud resulted in a slightly increase in casing wear. Wear factors of the barite test are presented in the following table.

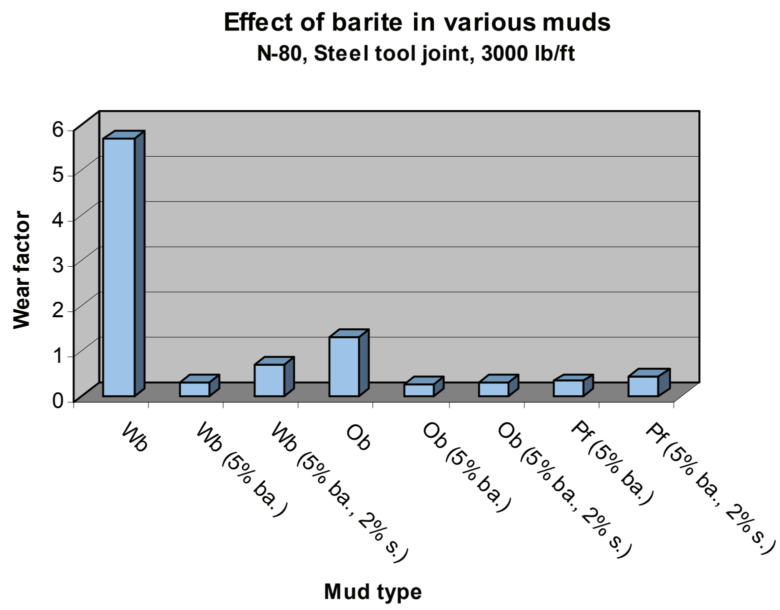

Figure 28: Effect of barite – wear factor

Friction factors were significantly less with oil based muds than with water based muds. Barite reduced the friction factor but sand had very little impact. The reduction in friction factor with barite can be an important benefit especially in highly deviated wells.

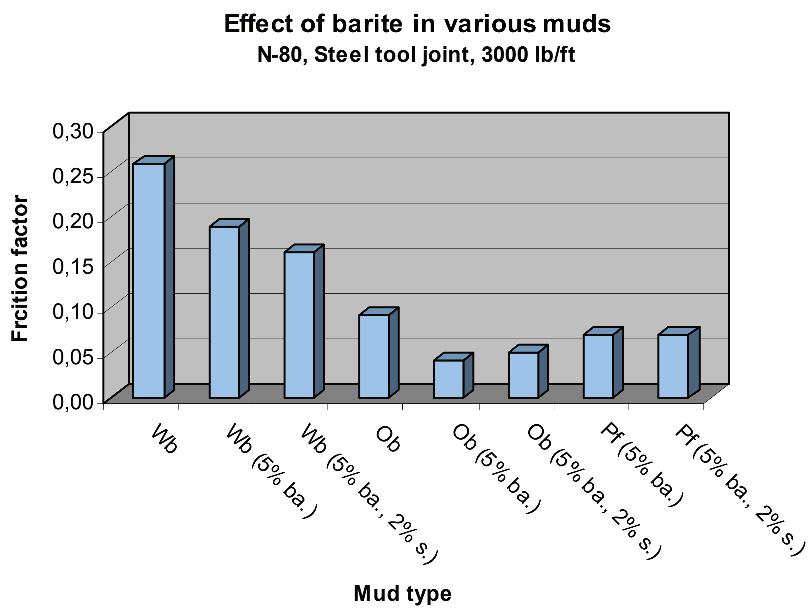

Figure 29: Effect of barite – friction factor

2.4.1.2.2 Effect of barite concentration

Several wear tests were run with different barite and sand concentrations to determine how the reduction in casing wear is affected by the barite concentration. The results are presented in the table below

Barite	Sand	Wear depth		Wear factor	Friction factor
[%]	[%]	[in]	[%]	[10^{-10} psi^{-1}]	
0	7.0	0.084	18.0	5.50	0.20
1	2.0	0.064	14.0	3.70	0.14
2	2.0	0.021	4.5	0.70	0.15
3	7.0	0.020	4.2	0.66	0.15
4	0.5	0.019	4.0	0.61	0.18
5	0.0	0.012	2.5	0.33	0.19
5	2.0	0.020	4.2	0.67	0.16
18	1.0	0.017	3.6	0.51	0.18

Table 5: Effect of barite concentration

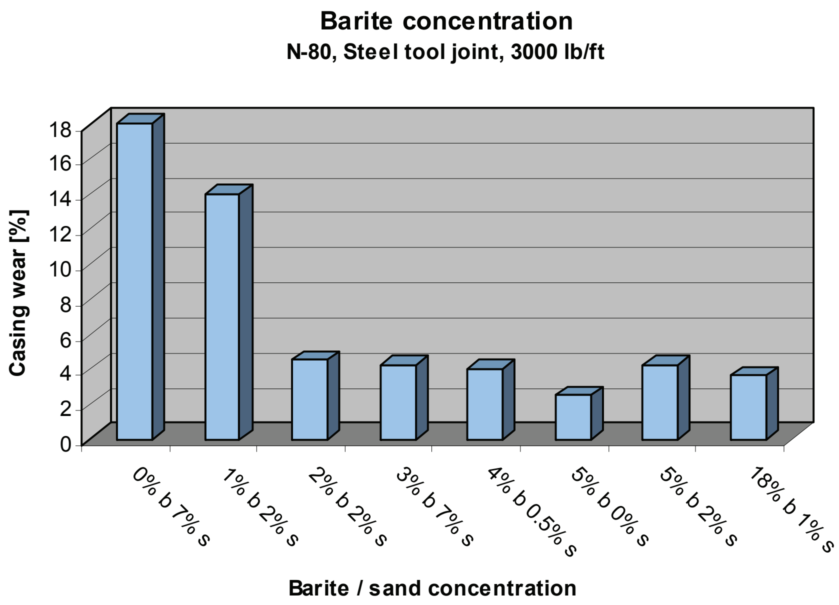

Figure 30: Effect of barite concentration – casing wear

An increase of the barite concentration above 2% was not found to appreciably decrease casing wear. 1% barite did not have an significant impact on wear. Therefore, for considerations of casing wear reduction, 2% to 4% barite will achieve optimal results. Higher concentrations will not further reduce casing wear. Sand content in barite weighted mud does increase wear slightly. Even if this increase is slight, it does illustrate the importance of good solids control in critical situations.

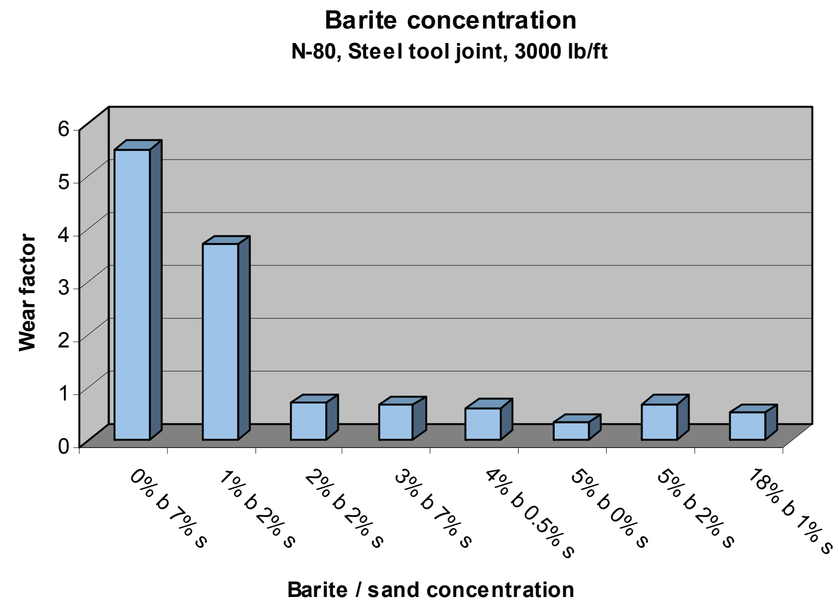

Figure 31: Effect of barite concentration – wear factor

The reduction in friction factor with barite is less than the reduction in wear.

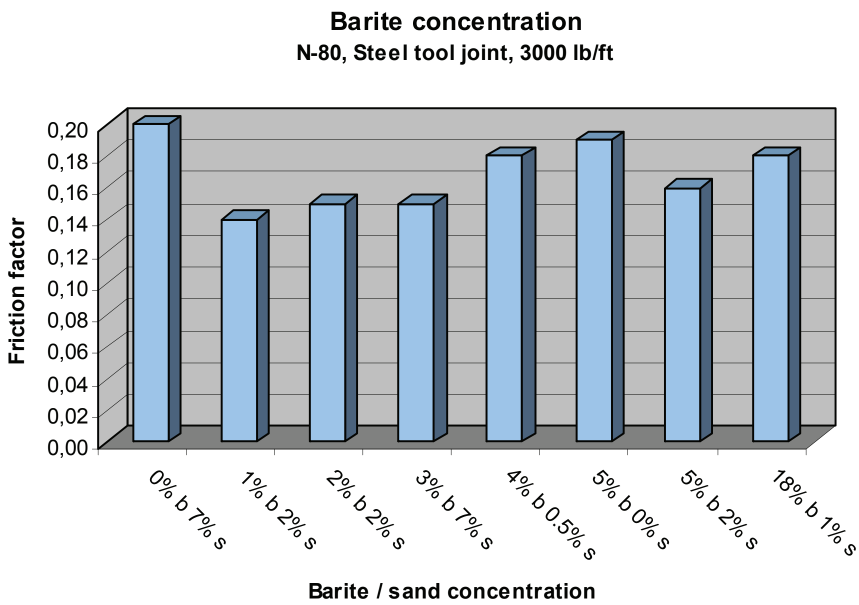

Figure 32: Effect of barite concentration – friction factor

2.4.1.3 *Effect of mud weight*

There is no direct correlation between casing wear and mud weight since properties of the various weighting materials differs (e.g.: sand is much more abrasive than barite). Wear is therefore determined by what materials are used to weight the mud.

Mud type	Mud weight		Barite vol.	Sand vol.	Wear depth		Wear factor	Friction factor
	[ppg]	[sg]	[%]	[%]	[in]	[%]	[10^{-10} psi^{-1}]	
Water	8.3	1,00	0	0	0.270	57.2	29.60	0.32
Wb + s	10.0	1,20	0	7	0.084	18.0	5.50	0.20
Wb + iron oxide 4%	10.0	1,20	0	0	0.064	14.0	3.70	0.19
Wb + b	10.0	1,20	5	0	0.012	2.5	0.30	0.19
Wb + s + b	11.2	1,34	3	7	0.020	4.2	0.66	0.15
Wb + s + b	14.0	1,68	18	1	0.017	3.6	0.51	0.18
Wb + s + b	16.0	1,92	23	7	0.023	4.9	0.79	0.18

Table 6: Effect of mud weight

Wear with 10 ppg, 1,2 sg, mud was 2.5% when weighted with barite and 18% when weighted with sand. This is shown in the figure below.

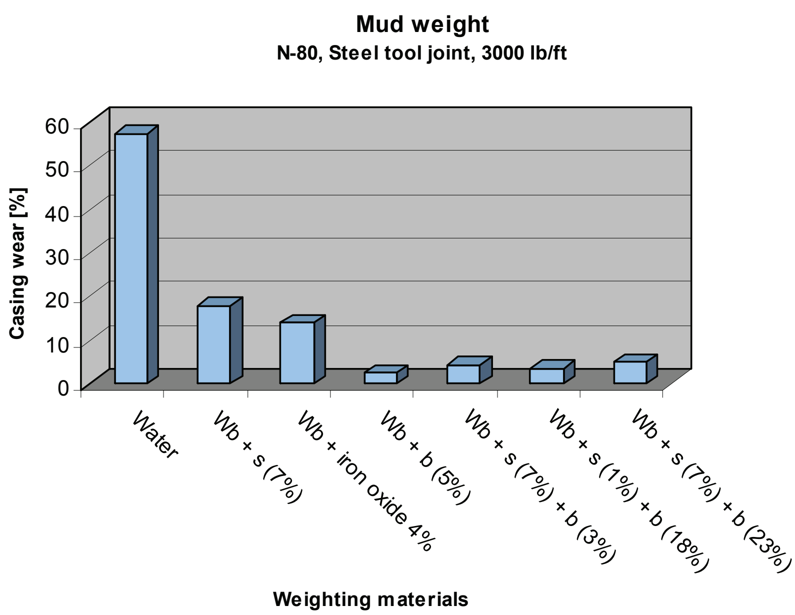

Figure 33: Effect of mud weight – casing wear

The figure below shows that the wear factor was much lower for weighted mud containing barite.

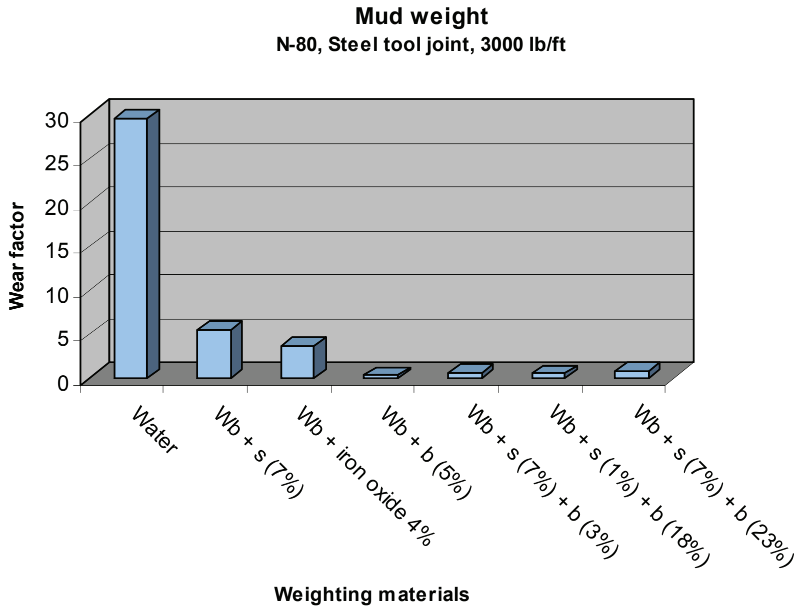

Figure 34: Effect of mud weight – wear factor

The friction factors for all weighted muds were similar and less than the friction factor for water.

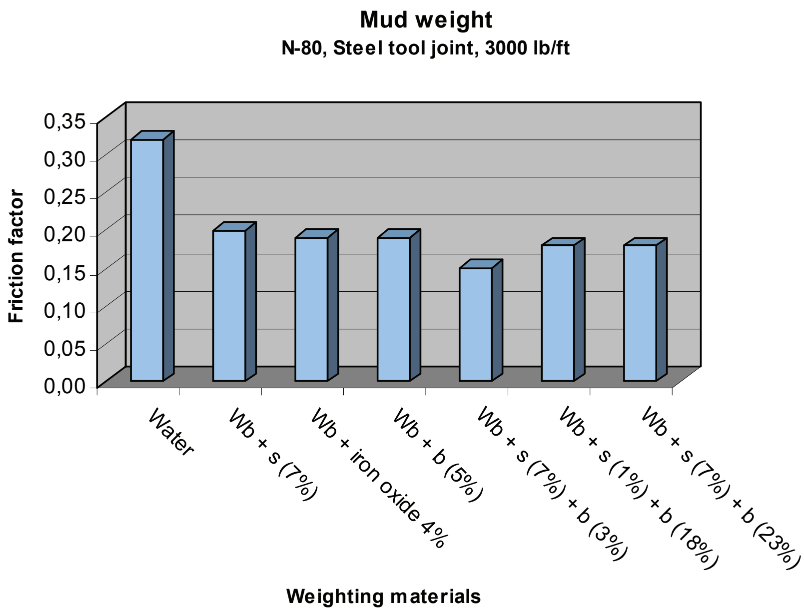

Figure 35: Effect of mud weight – friction factor

2.4.2 Lubricants

A large number of tests were conducted to determine the effects of lubricants on casing wear.

The tables and figures in this chapter compare the performance of 5 lubricants and rubber drill pipe protector in water based mud (7% sand, 10 ppg / 1,20 sg and 3000lbf/ft) with N-80 casing.

Lubricant type	Lub.		Sand vol.	Wear depth		Wear factor	Friction factor
	[lb/bbl]	[kg/m^3]	[%]	[in]	[%]	[10^{-10} psi^{-1}]	
None	0	0	7	0.084	18.0	5.50	0.20
Drill beads	4	11,41	7	0.061	13.0	3.50	0.19
Torq Tim	2	5,71	7	0.044	9.0	2.20	0.15
DL100	2	5,71	7	0.044	9.0	2.20	0.09
EP lube	2	5,71	7	0.014	3.0	0.40	0.01
Enviro-lube	(4%)	(4%)	7	0.035	7.0	1.50	0.07
Protector	-	-	7	0.002	0.4	0.04	0.01

Table 7: Effect of lubricants

The addition of drill beads reduced casing wear from 18% to 13%. Torq Trim, a miscible lubricant, and DL100, a dispersible lubricant, both reduced casing wear to 9%. EP lube, a dispersible lubricant, reduced casing wear to 3% compared to 0.4% for rubber drill pipe protectors.

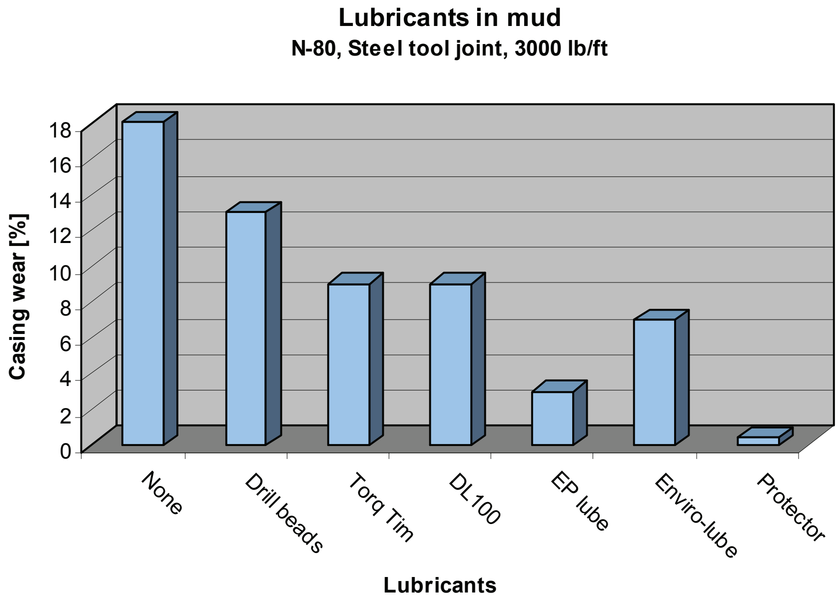

Figure 36: Effect of lubricants – casing wear

Wear factors for the different lubricants ranged from 0.4 to 3.5 compared to 5.5 for water and 0.04 for drill pipe protectors.

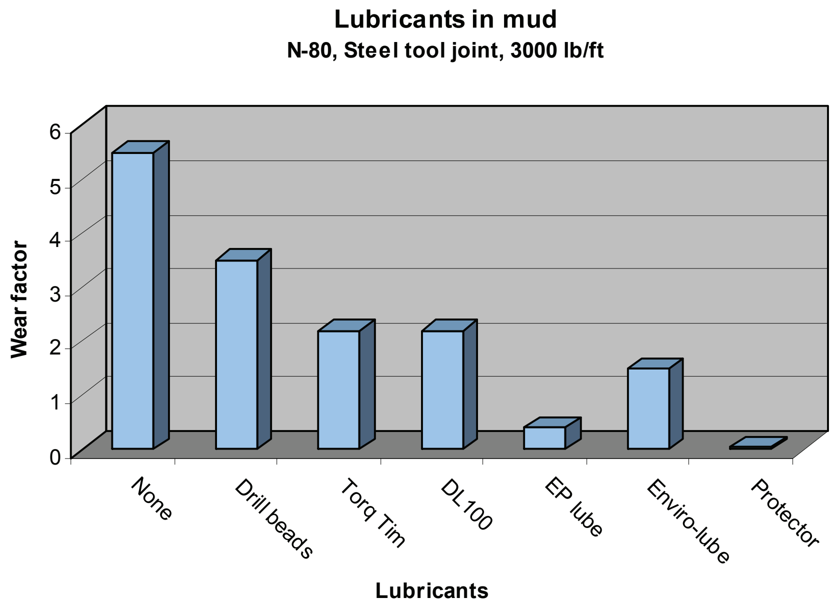

Figure 37: Effect of lubricants – wear factor

The friction coefficient varied widely for the different lubricants, ranging from 0.01 for EP lube and drill pipe protectors to 0.19 for drill beads. This compares to 0.2 for water based mud with no lubricants.

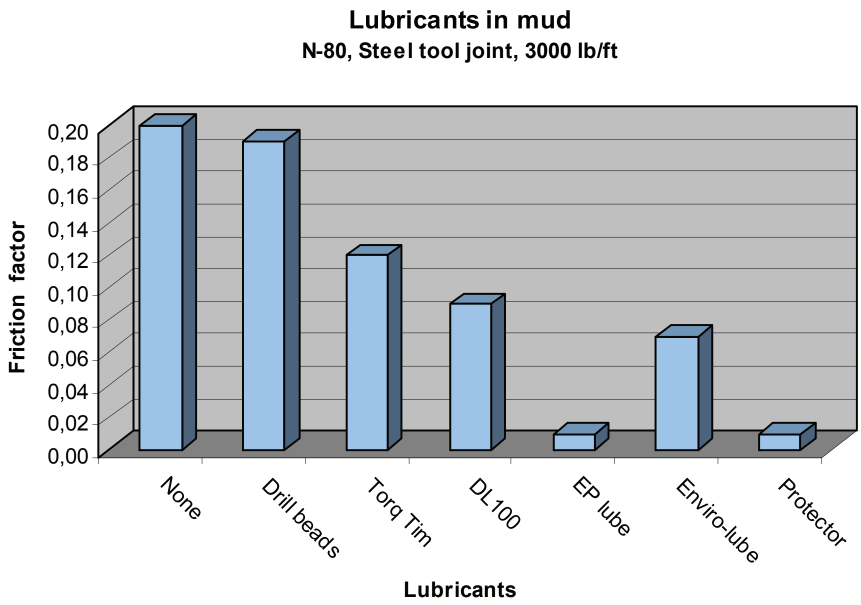

Figure 38: Effect of lubricants – friction factor

2.4.3 Casing properties

Extensive tests were conducted to determine the effect of casing properties on casing wear.

2.4.3.1 Effect of casing material in water based mud

The table and figures below compare casing wear in different casing grades and materials in 10ppg, 1,2 sg, water based mud containing 7% sand.

Casing Grade	Mud weight	Sand vol.	Wear depth		Wear factor	Friction factor
	[ppg	[%]	[in]	[%]	[10^{-10} psi^{-1}]	
K55	10	7	0.152	32	13.0	0.24
C75	10	7	0.094	20	6.4	0.17
N80	10	7	0.084	18	5.5	0.20
C90	10	7	0.105	22	7.5	0.17
C95	10	7	0.133	28	10.9	0.24
P110	10	7	0.131	28	10.8	0.26
Q125	10	7	0.151	31	13.1	0.19
V150	10	7	0.120	25	9.5	0.22

Table 8: Effect of casing material in WBM

The figure below shows that casing wear in N80 casing (18%) was lower than any other casing material tested.

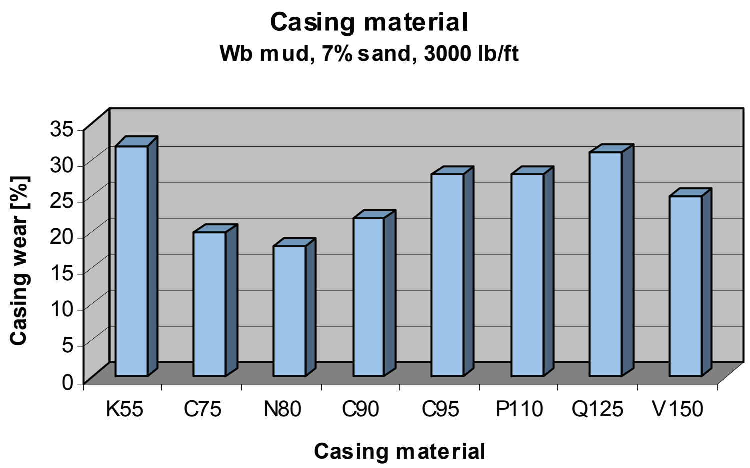

Figure 39: Casing material in WBM – casing wear

Wear factors for metal casing range from 5.5 for N80 to 13.1 for Q125 as shown in the figure below. These results demonstrate that the casing material has a major effect on wear factor.

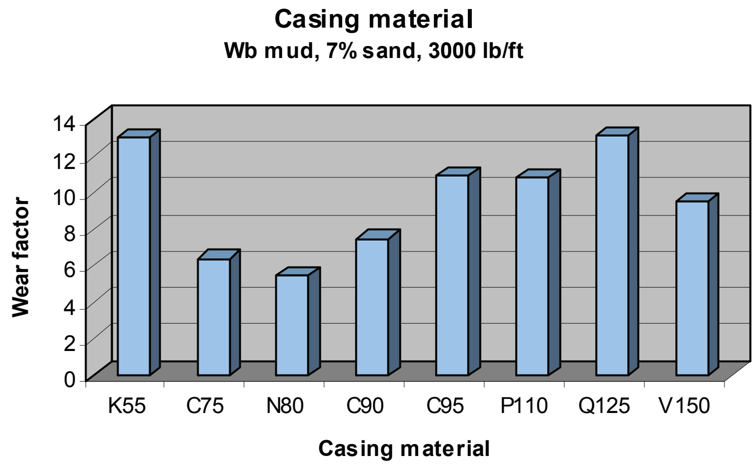

Figure 40: Casing material in WBM – wear factor

Friction factors for the various casing grades range from 0.17 to 0.26.

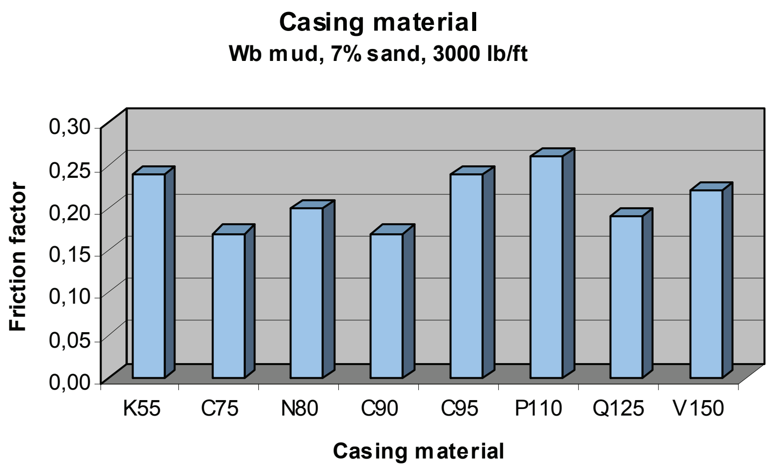

Figure 41: Casing material in WBM – friction factor

2.4.3.2 Effect of casing material in oil based mud

In this chapter different casing grades in oil based mud, containing 7% sand and weighting 9.7ppg, 1.16 sg, are compared.

Casing Grade	Mud weight	Sand vol.	Wear depth		Wear factor	Friction factor
	[ppg	[%]	[in]	[%]	[10^{-10} psi^{-1}]	
N80	9.7	7	0.039	8	1.8	0.10
P110	9.7	7	0.053	11	2.8	0.10
K55	9.7	7	0.071	15	4.2	0.09

Table 9: Effect of casing material in OBM

The wear rate for N80 casing (8%) in oil based mud was lower than for P110 (11%) and K55 (15%) as shown in the figure below. The casing wear trend for these casing materials in oil based mud was similar to that shown in the previous section for water based mud except that the wear rates in oil based mud are reduced by more than 50%.

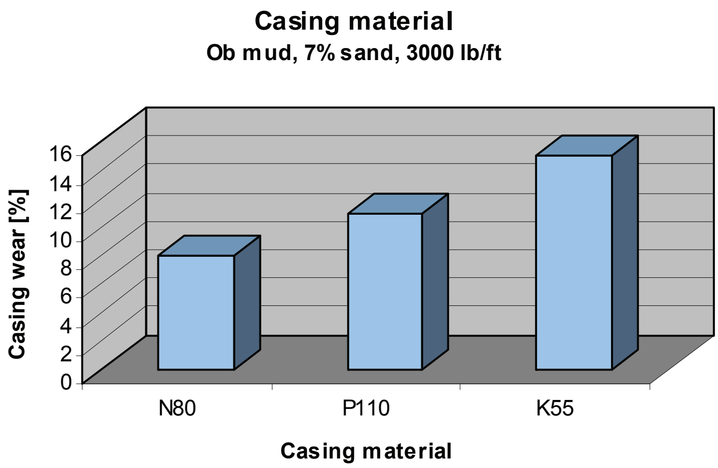

Figure 42: Casing material in OBM – casing wear

The wear factors in oil based mud are very low, ranging from 1.8 in N80 casing and 4.2 in K55 casing. These wear factors are considerably lower than those in water based mud.

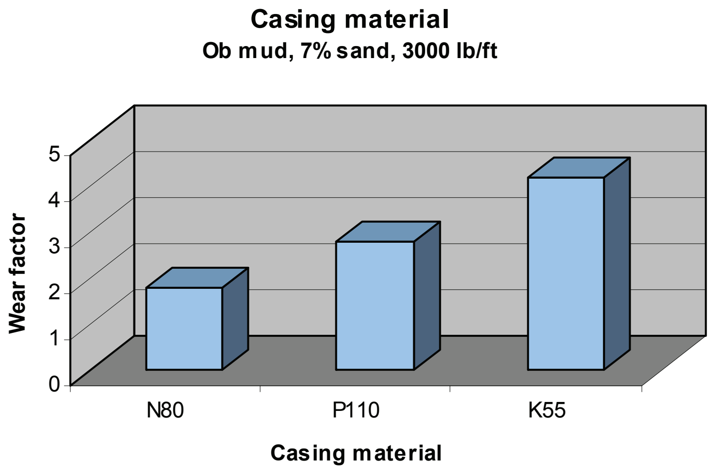

Figure 43: Casing material in OBM – wear factor

The friction factors with the casing grades in oil based mud range from 0.09 to 0.10 as shown in the figure below. These factors are about half those in water based mud.

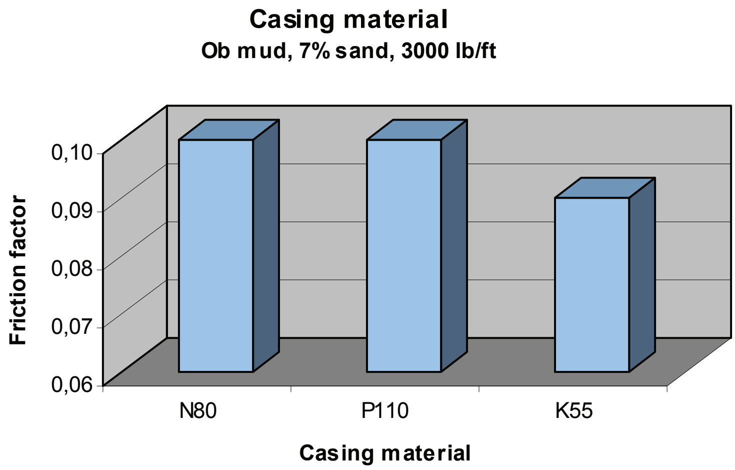

Figure 44: Casing material in OBM – friction factor

2.4.4 Tool joint material

Shell and Texas A&M conducted studies of the effect of hardbanding materials and finishes on casing wear.

The tests focused on four basic types of tool joints:

- Smooth steel
- Tungsten-carbide hardfacing
- Two phase hardfacing
- Non-tungsten-carbide hardfacing

2.4.4.1 Smooth steel

Hardfacing can cause excessive wear under some field conditions. Because of that many companies allow only the use of steel joint when drilling in casing. The two advantages of steel joints are that they become smooth after a few hours of operation and they have longer contact areas with the casing, resulting in reduced contact pressure between tool joint and casing.

Significant tool joint wear and galling wear when drilling with water and high contact pressures are the major limitations of steel tool joints.

The use of steel tool joints in abrasive open hole section should be avoided due to excessive wear.

2.4.4.2 Tungsten-carbide hardbanding

The hardfacing is initially welded onto the tool joint boxes, close to the elevator shoulder and flush with the tool joint outer diameter. Hardmetal is not applied to the pin in order to protect the tong dies. The hardmetal is about 0.1 inch thick and 3 to 4 inches long. The size, shape and application method and the experience of the welder governs the wear rate of the hardmetals. The size of the tungsten-carbide particles ranges from fine to coarse. Care must be taken to produce a smooth, flush surface. Raised edges are often produced on one side of the tool joints and can increase wear. Tool joints with new hardmetal should initially be run in open hole until the hardmetal is worn smooth.

2.4.4.3 Non-tungsten-carbide hardfacing

Various types of non-tungsten-carbide hardfacing have been used including special steel alloys, chrome and nickel. These materials typically have twice the hardness of the tool joint steel (~30-36 Rc)

Tool joint material	Mud type	Wear depth		Wear factor	Friction factor
		[in]	[%]	[10^{-10} psi^{-1}]	
Steel	WB + 7% sand	0.084	18	5.5	0.20
Armacor-M	WB + 7% sand	0.028	6	1.1	0.15
Arnco-200XT	WB + 7% sand	0.033	7	1.4	0.14
Stellite	WB + 7% sand	0.046	10	2.2	0.17
Colmony 5	WB + 7% sand	0.021	4	0.7	0.16

Table 10: Non-tungsten carbide hardfacing

Wear with all four hardmetals was considerably less than with steel tool joints or tungsten carbide hardfacing. Initial results with these new hardmetals showed that there is potential for significantly reducing casing wear by implementation of these hardmetals.

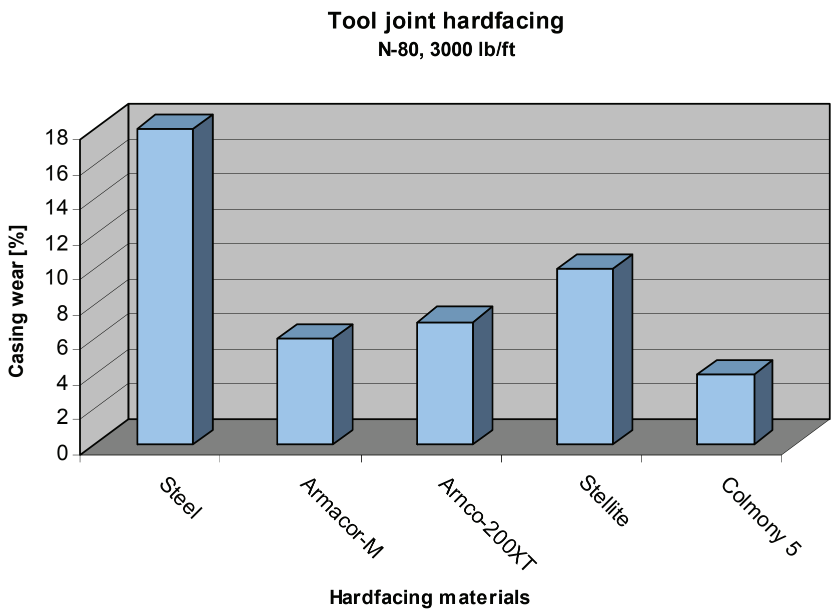

Figure 45: Tooljoint hardfacing – casing wear

The wear factor for Armacor-M hardmetal was only 1.1, only 20% of that for steel tool joints. Arnco-200XT wear factor was 1.4. Stellite and Colomony 5 had wear factors of 2.2 and 0.7, respectively as shown in the figure above.

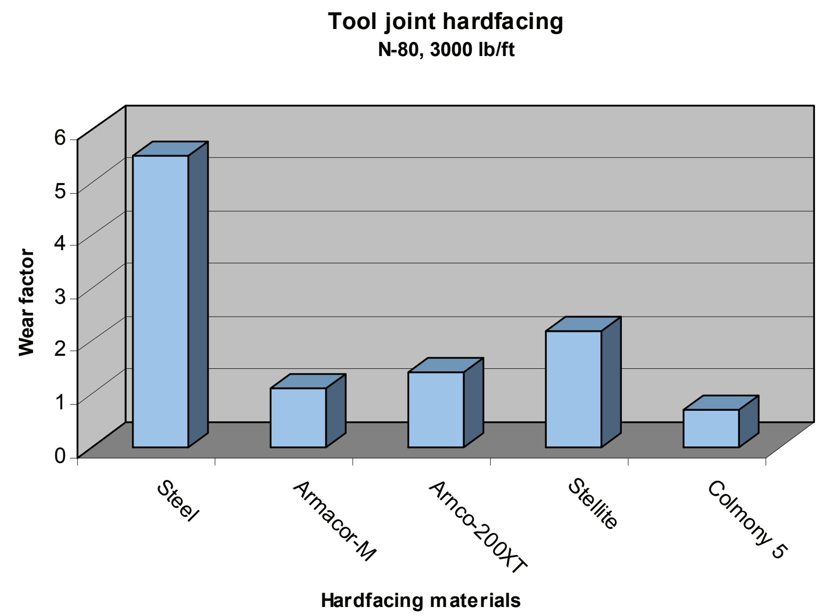

Figure 46: Tooljoint hardfacing – wear factor

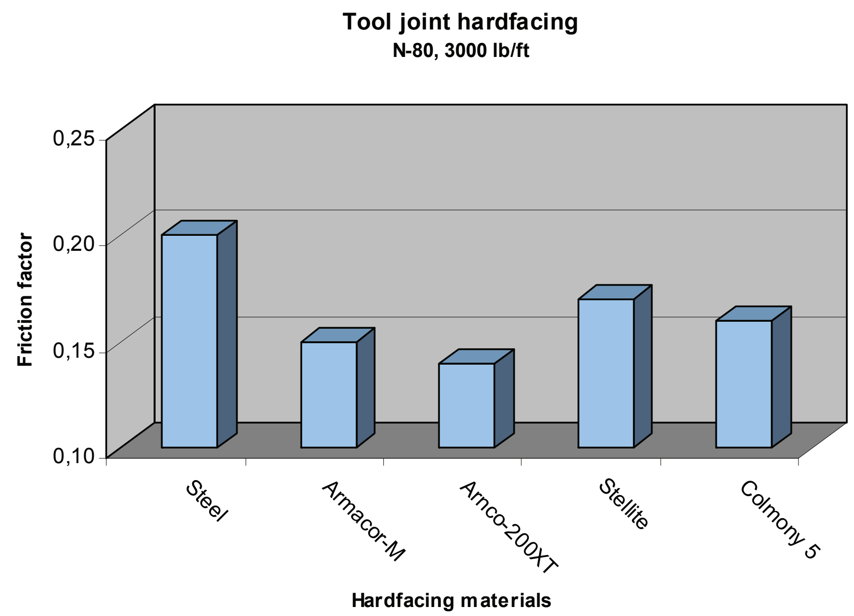

Figure 47: Tooljoint hardfacing – friction factor

2.4.5 Buckling

Casing buckling can cause increased casing wear due to doglegs produced by the buckled casing

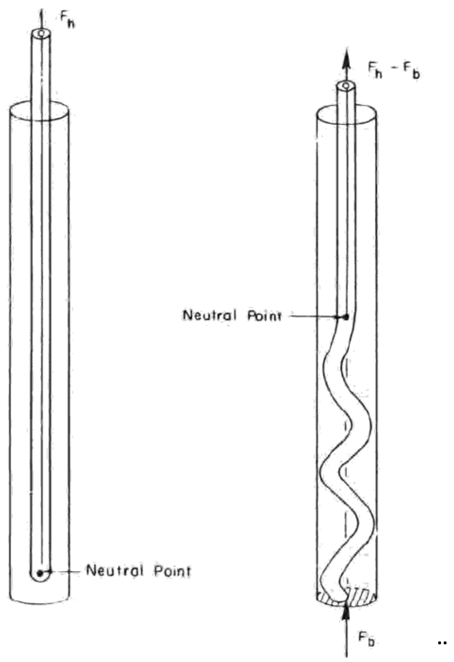

Figure 48: Effect of buckling I [9]

Severe casing wear often occurs at buckled points in the casing because

- The lateral loads are very high at these points
- All wear is concentrated at these points instead of being uniformly distributed.

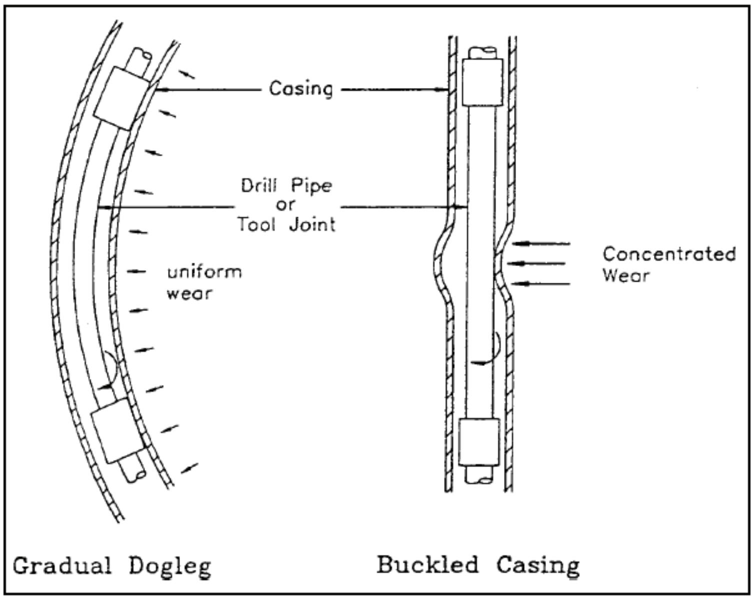

Figure 49: Effect of buckling II [9]

For example, if the rotating drillpipe or tool joint contacts the buckled zone over a 5 feet length (abrupt doglegs), wear will be approximately 6 times higher than if the wear is distributed uniformly over a 30 feet section gradual dogleg. This is one reason why high wear is often observed near the bottom of casing strings in an area where low wear is expected (due to the low tension in the drillstring). A detailed review of the mechanics of casing buckling is beyond the scope of this study and the reader is referred to the references.

2.4.6 Doglegs

Most casing wear problems exist at doglegs because wear is accelerated at these points, especially when the doglegs are high up in the well where drill string tension is highest.

A simplified vertical example well is used to demonstrate the effects of doglegs on casing:

2.4.6.1 Effect of dogleg location

The table below show how casing wear varies with depth of the 6°/100ft (30m) dogleg in this example well.

Dogleg depth	Average lateral	Wear volume	Wear depth	
[ft]	[lbs]	[in^3/ft]	[in]	[%]
0	280,000	17.9	0.40	85
2,000	240,000	15.3	0.36	76
4,000	200,000	12.8	0.32	68
6,000	160,000	10.2	0.19	57
9,000	100,000	6.4	0.19	40

Table 11: Effect of dogleg location

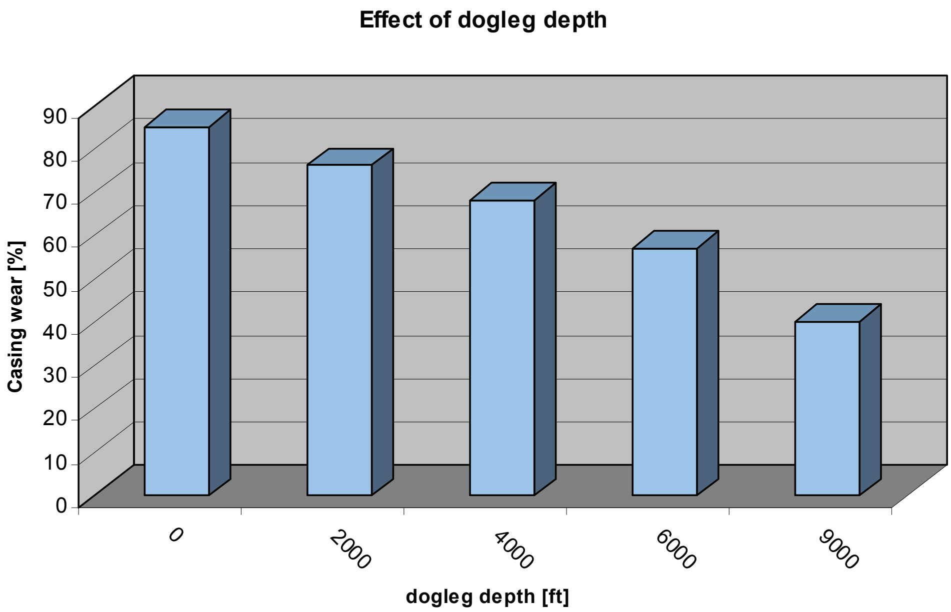

Figure 50: Effect of dogleg depth – casing wear

The figure above shows that the dogleg will create 85% wear at the surface compared to 40% at 9,000 ft. This wear corresponds to the 500 rotating hours required to drill from 10,000ft, 3,048m, to 20,000 ft, 6,096m, in the example well.

This example clearly demonstrates that doglegs cause more wear when they are located high up in the hole and why special care should be taken to avoid doglegs in the upper section.

2.4.6.2 Effect of dogleg magnitude

The following table shows how wear varies with doglegs at the surface and at 9,000 ft with several dogleg severities.

Dogleg severity	Dogleg depth	Average lateral	Wear volume	Wear depth	
[°/100 ft]	[ft]	[lbs]	[in^3/ft]	[in]	[%]
0	0	280,000	0.0	0.00	0
2	0	280,000	6.0	0.18	38
4	0	280,000	11.9	0.30	64
6	0	280,000	17.9	0.40	85
8	0	280,000	Worn through		100
10	0	280,000	Worn through		100
0	9,000	100,000	0.0	0.00	0
2	9,000	100,000	2.1	0.09	19
4	9,000	100,000	4.3	0.15	32
6	9,000	100,000	6.4	0.19	40
8	9,000	100,000	8.5	0.24	51
10	9,000	100,000	10.6	0.28	59

Table 12: Effect of dogleg severity

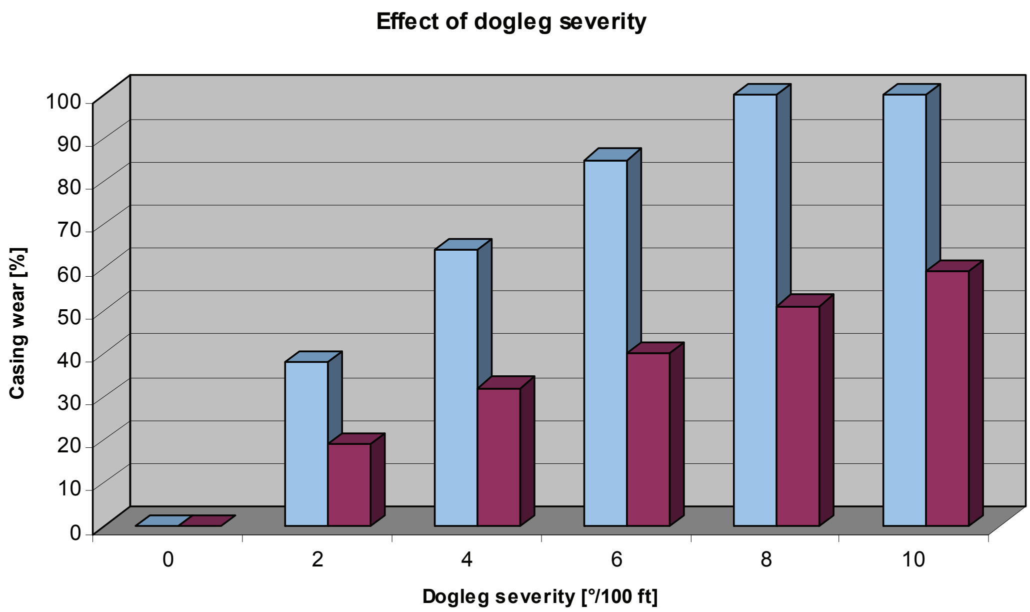

Figure 51: Effect of dogleg severity – casing wear

2.4.6.3 Type of dogleg

The existence of two types of doglegs has been established. The first are abrupt doglegs by finding drillpipe wear in doglegs where the drilling pipe would not contact the hole if the dogleg was gradual. With gradual doglegs only the tool joints contact the casing and wear is uniformly distributed along the dogleg as drilling progresses. Wear can therefore be greatly accelerated in abrupt doglegs. [10]

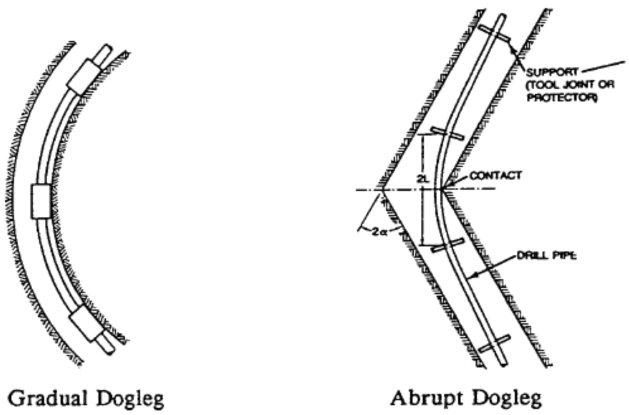

Figure 52: Types of doglegs [10]

2.4.7 Lateral loads

Extensive tests were conducted in the DEA 42 project to determine the effect of lateral loads on casing wear.

The table below shows the effect of lateral loads in ranges from 3,000 to 7,000 lbf/ft with several drilling fluids.

Lateral load	Mud type	Wear depth		Wear factor	Friction factor
[lbs/ft]		[in]	[%]	[10^{-10} psi^{-1}]	
3,000	water	0.091	19	33.7	0.31
5,000	water	0.173	37	50.9	0.36
7,000	water	0.195	41	43.5	0.42
3,000	wb + 7% sand	0.107	23	7.9	0.23
5,000	wb + 7% sand	0.130	28	6.3	0.22
7,000	wb + 7% sand	0.201	43	8.4	0.19
3,000	wb + 5% barite	0.012	3	0.3	0.19
5,000	wb + 5% barite	0.034	7	0.9	0.21

Table 13: Effect of lateral loads

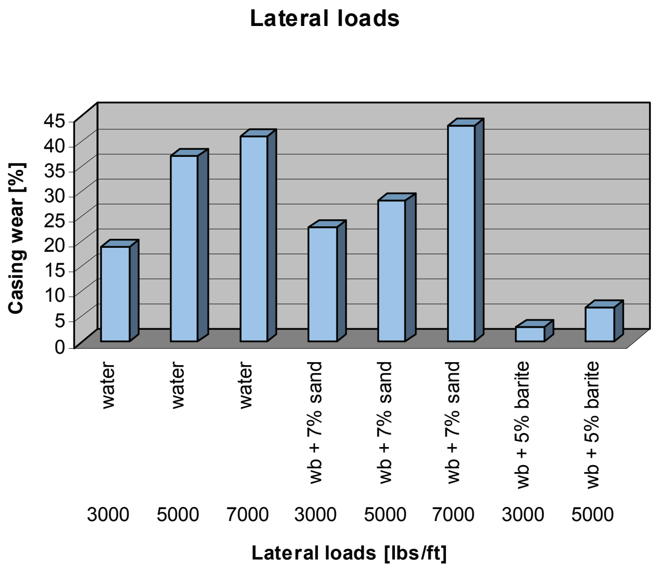

Figure 53: Effect of lateral loads – casing wear

The wear definitely increases with increase of lateral loads. The high wear is caused by galling or adhesive wear, where particles of steel are cold welded to the tool joint and torn from the casing. The wear ranges from 3 to 43 % indicating the aggressive nature of galling wear in water.

The wear in the water based mud with 7% sand increases almost constantly. This confirms the wear assumption that wear is proportional to the lateral load.

Water based mud with barite will produce significantly less wear.

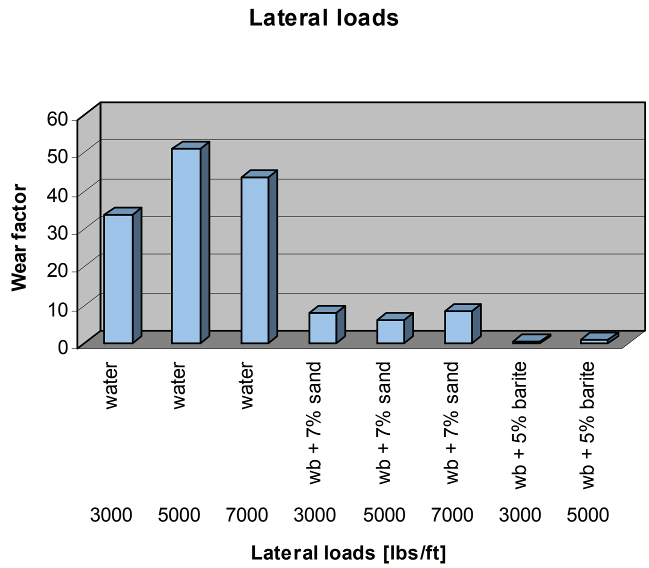

Figure 54: Effect of lateral loads – wear factor

The wear factors also differ widely from 0.3 with barite to 50.9 with only water.

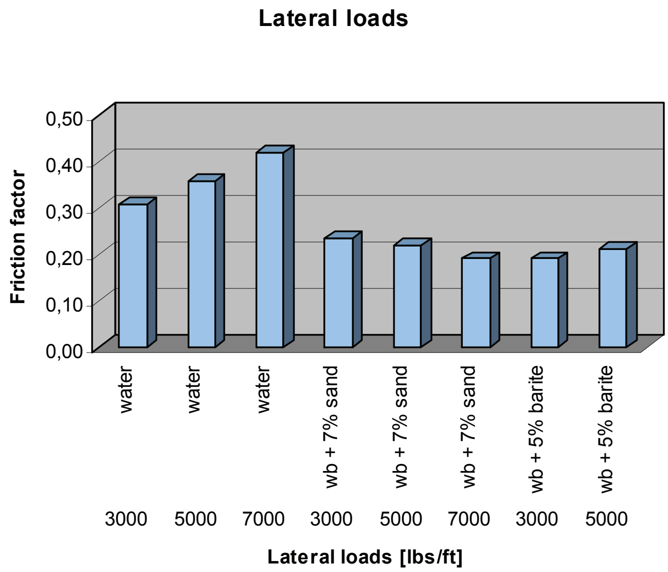

Figure 55: Effect of lateral loads – friction factor

High friction factors in water indicate the stick / slip nature of the wear progress taking place. Although wear was significantly reduced with barite weighted mud, the friction factor was not decreased. That indicates that there is no reduction of mechanical work input into the system and that only a small portion of mechanical work is being used to wear casing.

2.4.8 Tripping

Shell carried out several tests of casing wear during tripping the drillstring. Unfortunately data from these tests were not accessible. The conclusions of these tests were:

- Casing wear is primarily caused by drillstring rotation, not by tripping
- More galling wear was observed with P-110 casing than with K-55, apparently due to the closer similarity in hardness between the drillpipe and the P-110 casing.
- Wear rate due to reciprocation does not vary linearly with lateral load.
- But if considering tripping wear, it is much greater in water than in mud containing sand, apparently due to galling and seizing
- The addition of barite or ground limestone reduce tripping wear nearly to zero
- Five foot long, tapered tool joints produce the same wear as short, one foot long, tapered tool joints. The consequence of this is, that tripping wear is not dependent on tool joint lengths.[11]

2.5 Effects of wear on casing strength

Engineers that are studying the effect of casing wear on casing strength must be aware that there can be a significant variation in casing dimensions and properties as shown in the figure below.

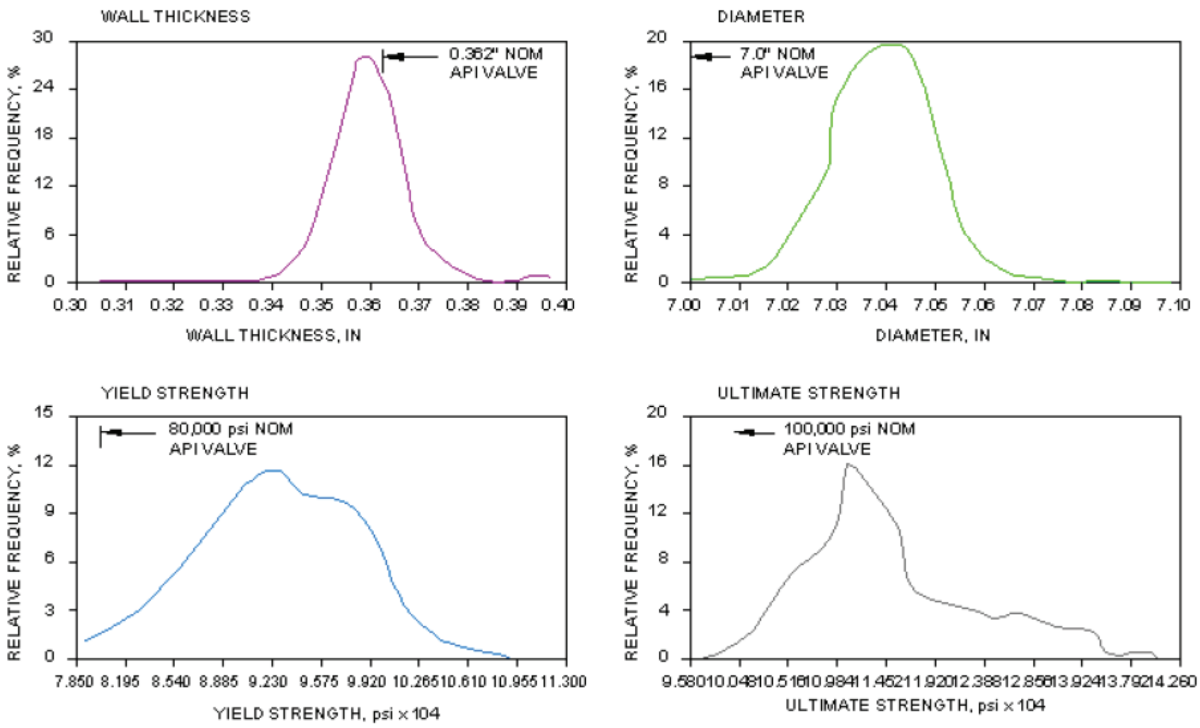

Figure 56: Variation of casing dimensions [12]

The thickness in the 7 inch casing varied from 0.34 to 0.38 in. compared to the nominal value of 0.362 in. The mean yield strength was about 93,000 psi compared to 80,000 psi nominal and the mean ultimate strength was about 110,000 psi compared to 100,000 psi nominal ultimate strength [12]

2.5.1 Types of casing failures

There are four types of casing failure that occur due to excessive fluid pressure.

- Burst (internal pressure)
- Joint thread leakage (internal pressure)
- Collapse (external pressure)
- Joint thread leakage (external pressure)

Internal casing wear reduces the pressures at which they occur, except for joint leakage due to external pressure.

2.5.2 Failure due to internal pressure

2.5.2.1 Failure modes

If the internal pressure in the casing is increased beyond the failure limit, the casing will fail due to the fluid pressure expanding the coupling to the point where fluid leaks through the joint or the pressure yielding and bursting the casing.

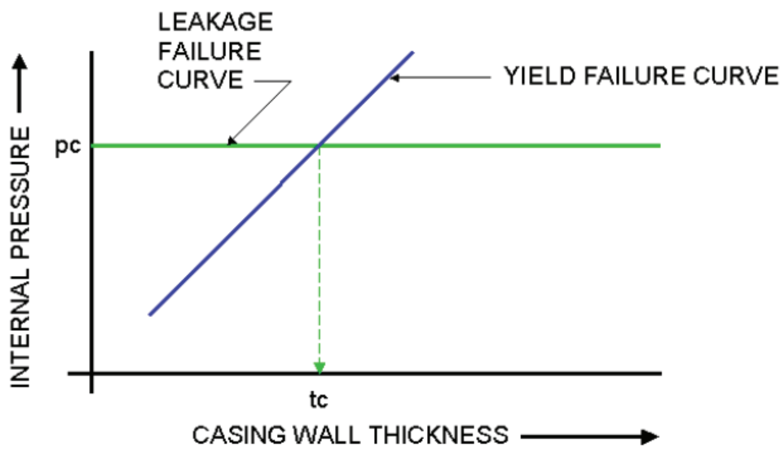

Figure 57: Internal pressure failure tc [7]

For a given size casing, thread leakage due to internal pressure is independent of wall thickness whereas the burst yield strength is proportional to the wall thickness. Therefore the two lines cross at the critical wall thickness tc. Below the critical wall thickness the casing will fail due to elastic yield of the steel whereas above the critical thickness, the joint will fail due to leakage through the coupling.

2.5.2.2 Internal pressure thread leakage

The internal pressure pi at which leakage occurs equals

$$p_i = \frac{U_D \cdot E \cdot \left(W^2 - d_i^{\,2}\right)}{2 \cdot d_1 \cdot W^2} + p_o \quad [psi]$$

Equation 27

where

p_i	= internal casing leak pressure [psi]
p_o	= external casing pressure [psi]
U_D	= diametral interference [in]
E	= elastic modulus [psi]
W	= outside diameter of coupling [in]
d_1	= diameter at first sealing point [in]

The internal pressure at which thread leakage occurs is independent of the inside diameter of the pin, therefore casing wear will not reduce the internal leak pressure unless the wear cuts all the way through the pin at the first sealing point.

The leak pressure p_i increases as the pressure outside the coupling p_o increases since differential pressure across the coupling (p_i-p_o) controls leakage. The leak pressure of the couplings increases as they are made up tighter, because of the increased diametral interference. The figure below shows the effect of wear on internal leak pressure.

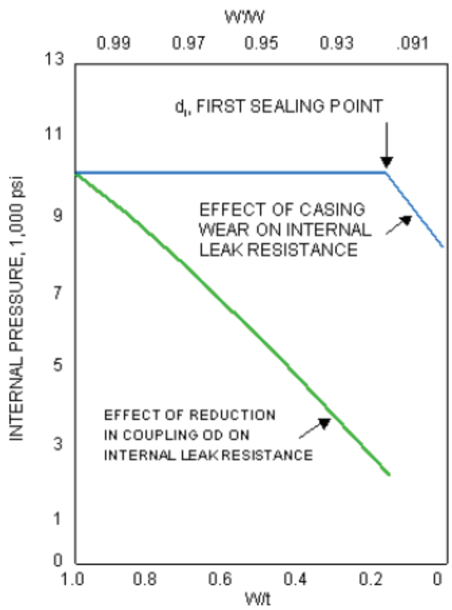

Figure 58: Internal pressure leakage [7]

The upper curve shows that internal wear does not affect leak pressure until the wear exceeds 86 %. This is the point where the wear is reaching the first thread seal point. The lower curve shows that reducing the coupling OD due to external corrosion or other factors decrease the leak pressure nearly linearly. [7] [12]

2.5.2.3 Burst failure

Several equations are used to calculate the pressure at which yielding and failure occur.

Yielding:

$$p_i = \frac{2 \cdot t}{D} \cdot Y_P \quad [psi]$$

Equation 28

API yielding:

$$p_i = \frac{2 \cdot t}{D} \cdot Y_P \cdot 0.875 \quad [psi]$$

Equation 29

API failure:

$$p_i = \frac{2 \cdot t}{D} \cdot U_{LT} \quad [psi]$$

Equation 30

ASME failure:

$$p_i = \frac{2 \cdot t}{D - 0.8 \cdot t} \cdot U_{LT} \quad [psi]$$

Equation 31

where

p_i = internal casing leak pressure [psi]

t = wall thickness [in]

D = casing diameter [in]

Y_p = minimum yield strength [psi]

U_{LT} = ultimate strength [psi]

The yield equations calculate when the steel begins to yield but has not failed, whereas failure equations predict the internal pressure at which the casing will burst. The failure (ultimate) pressure is typically 20 to 30% higher than the yield pressure. [7] [12]

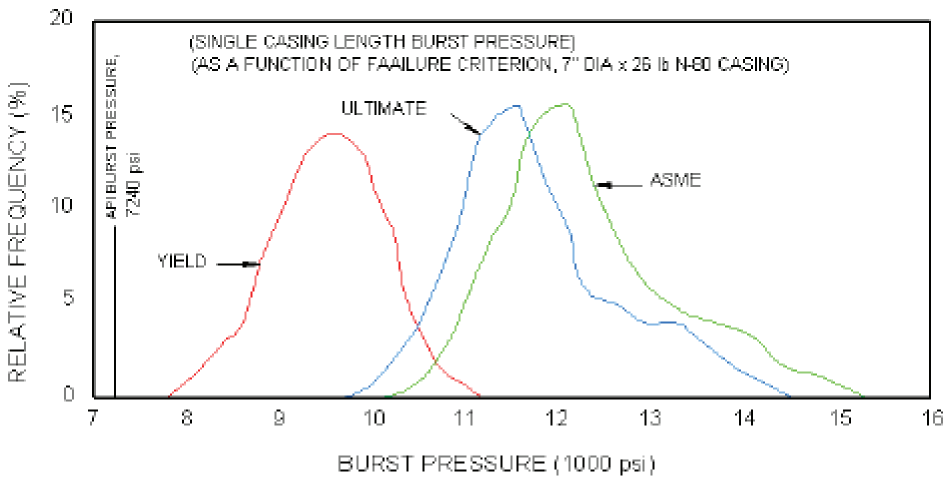

Figure 59: Burst pressure comparison [7]

2.5.3 Failure due to external pressure

2.5.3.1 External pressure thread leakage

As the external pressure in casing is increased, the casing will either yield and collapse or leak inward through the joint. The external pressure at which the joint will leak equals to:

$$p_o = \frac{U_D \cdot E \cdot (d_2^{\ 2} - D_i^{\ 2})}{2 \cdot d_2 \cdot D_i^{\ 2}} + p_i \quad [psi]$$

Equation 32

where

p_i = internal casing pressure [psi]

p_o = external casing leak pressure [psi]

U_D = diametral interference (from point of hand tight make up) [in]

E = elastic modulus [psi]

d_2 = diameter of first sealing [in]

D_i = internal diameter of the pin [in]

This equation shows that the external leak pressure will decrease as the inside diameter of the pin is worn away. The external leak pressure increases with increased internal pressure since the differential pressure across the joint controls the leakage.

2.5.3.2 Collapse failure

Collapse calculations in casing are quite extensive, but will be simplified in the following chapter as follows:

As the external pressure is increased, yielding will occur when the external pressure equals:

$$p_{YP} = 2 \cdot Y_P \cdot \left[\frac{\left(D/t \right) - 1}{\left(D/t \right)^2} \right] \quad [psi]$$

Equation 33

For most casing D/t ranges from 12 to 24 so D/t>>1. Therefore the collapse yield pressure equals:

$$p_{YP} = Y_P \cdot \left(\frac{2 \cdot t}{D} \right) \quad [psi]$$

Equation 34

The collapse failure pressure therefore equals:

$$p_{UL} = U_{LT} \cdot \left(\frac{2 \cdot t}{D} \right) \quad [psi]$$

Equation 35

where

D = casing diameter [in]

t = casing thickness [in]

Y_P = minimum yield strength [psi]

U_{LT} = ultimate strength [psi]

p_{UL} = collapse failure pressure [psi]

p_{YP} = collapse yield pressure [psi]

The equation above shows that the collapse failure pressure is proportional to casing thickness and therefore will decrease linearly as the casing wall is worn away. [7] [12]

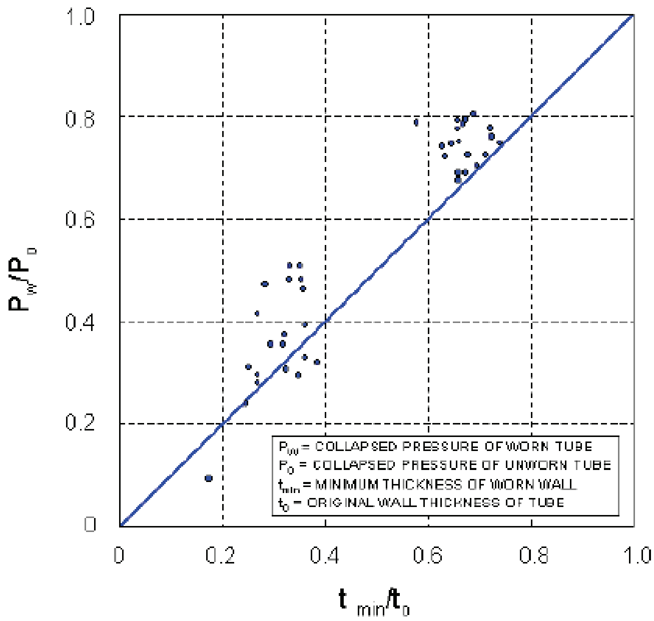

Figure 60: Collapse failure [7]

2.6 Casing wear logging

As part of the DEA-42 program, extensive logging tests on a 1,600 ft, 487m, water filled and centralised vertical casing test well in Houston were carried out.

The objectives of these logging tests were to:

- Determine what instruments are available on the market
- Determine the accuracy of the measurement systems under ideal condition
- Determine the best procedures to obtain accurate measurements
- Identify tool improvements

2.6.1 Logging principles

Ten companies provided several tools of six basic measurement principles:

- Electromagnetic (phase shift)
- Acoustic (fixed)
- Acoustic scanning
- Electromagnetic (Flux Leakage)
- Multifinger calliper
- Video Camera

All of the tested equipment was less accurate than indicated by the companies and the variation of results was huge under these optimum conditions. Acoustic tools were second to multifinger calliper tools but their performance was not up to expectations. Electro magnetic tools were not suitable for this application. The multifinger calliper tools were the most accurate logging methods tested. The borehole television camera performed well in water but can only operate in clear fluids.

There is no further discussion on the different logging methods, because Statoil is running USIT logs to identify casing wear. Ultra sonic imaging will be covered in detail in the following chapter.

3 Ultra-sonic-imaging

The USIT tool is an acoustic borehole imager. Cased hole applications for the USIT tool include cement evaluation and casing inspection with a 360 degree angle. Precise acoustic measurements ensure a map like presentation of the casing condition. These measurements include external and internal damage and deformation. The casing maximum and minimum thicknesses are evaluated by a low resolution transducer.

3.1 Tool principle

It is necessary to include a rotating transducer subassembly in different sizes to measure all casing sizes. The distance travelled by the ultrasonic sound pulse in the borehole fluid is optimized by selecting the most suitable transducer subassembly to reduce attenuation in heavy fluids and to maintain a low signal-to-noise-ratio. The transducer is both a receiver and a transmitter, transmitting an ultrasonic pulse between 195 and 650 KHz and receiving the deflected pulse. In a cased hole the actual frequency is controlled by a software package according to the casing thickness and fluid type. [13] [14]

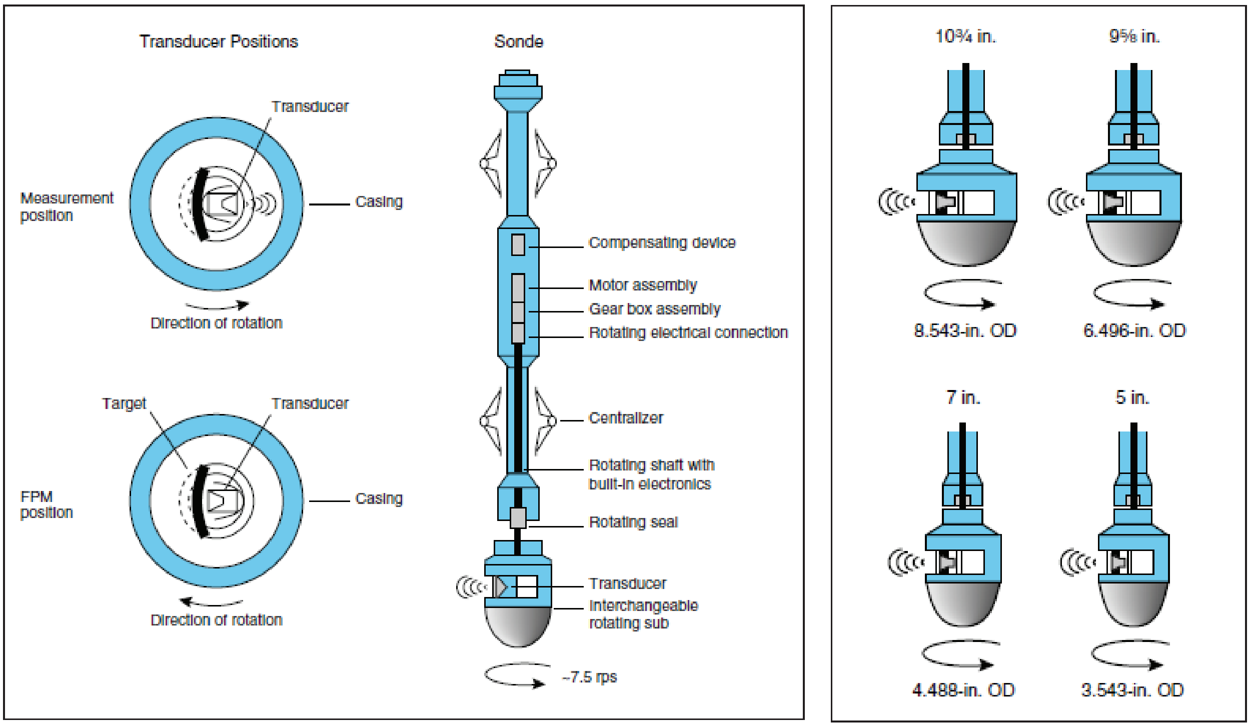

Figure 61: USIT tool description [13]

3.2 USIT measurement

The ultrasonic imaging tool is used to carry out following measurements:

- Annular acoustic impedance (T3 processing)
- Casing wall thickness (T3 processing)
- Amplitude of primary reflection (roughness of internal casing surface)
- Internal Radius (travel time)

Since the most accurate of these parameters is the casing wall thickness, which was used for the simulations, the other measurements will not be discussed.

A technique called T3 processing derives very reliable information from the USI (Ultra Sonic Imaging) acquisition measurements. The acoustic impedance, calculated from fundamental resonance, is used to measure the casing thickness. This is the difference between the CET (Cement Evaluation Tool) and the T3 processing of USI data. The natural resonance frequencies of the casing wall are approximately inversely proportional to the wall thickness. [15]

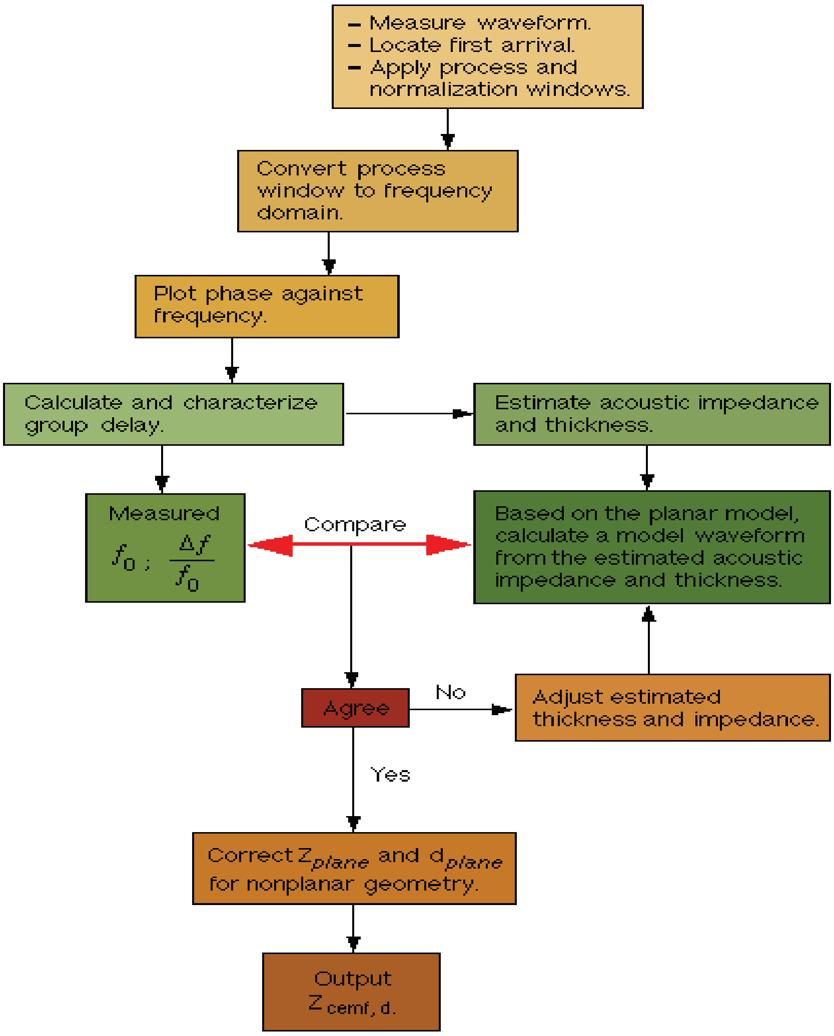

Figure 62: USIT processing[13]

After the T3 processing is completed a data file is created and the results are graphically displayed. The image is divided into four major parts: one casing and one cementing part, enclosed by two quality control parts. [13] [14]

The casing streams include:

- Amplitude (no rugosity or eccentering)
- Casing cross section (derived from travel time)
- Image of casing cross section
- Minimum, average and maximum casing thickness (derived from T3 processing)

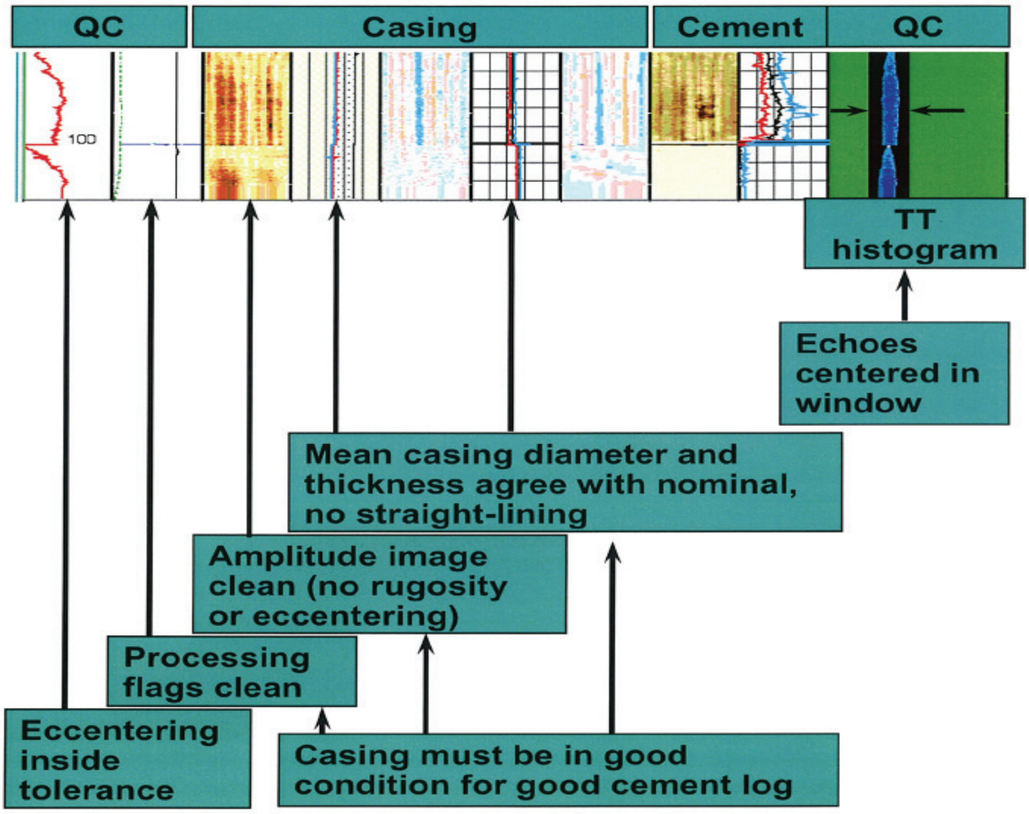

Figure 63: Output description [13]

4 Introduction to Cwear

Cwear is a software package to calculate casing and riser casing wear for onshore and offshore operations including drilling, redrilling, reaming upward, and rotating off bottom. It accurately predicts extent, magnitude and location of tubular wear as well as flex-joint wear. Impacts of wear on burst and collapse pressures are also indicated. The program was originally developed by Maurer Technologies under sponsorship of the joint-industry project DEA-42 – Casing Wear Technology.

4.1 Theoretical Background

The model accurately predicts the location and magnitude of wear in casing/riser strings for both onshore and offshore geometries. It predicts volumetric casing wear by calculating the energy imparted by the rotating tool joint to the casing at multiple positions along the casing and dividing this by the amount of energy required to wear away a unit volume of the casing.

Lateral forces press the tool joint against the casing, and are a combination of gravity, buoyancy, tension in the drill string, and hole trajectory geometry. Wear depth at each point along the casing is calculated from volumetric wear. Dynamic effects, such as resonant vibration of the drill string, are not considered in this model. A critical element in the mathematical model that evolved from theoretical development of casing-wear analysis is the "wear factor." This empirically-derived quantity represents the energy required to remove a unit volume of casing material for a given set of conditions (casing/tool-joint geometry, drilling fluid, solids content, etc.).

Wear-factor data are incorporated into the program from an extensive range of laboratory tests conducted as part of the DEA-42 project. Evaluation and application of these wear factors is the crucial element in the transition of the model from a theoretical exercise to a practical engineering tool. [16]

4.1.1 Nonlinear correction factor

Experimental results from a large number of laboratory riser/casing wear tests have shown that wear factors are not constant for a given set of test conditions, but decrease with increasing wear depth and approach an asymptotic value as wear exceeds about 40%. Wear factors reported and used in most calculations are the asymptotic values.

Summary data from several laboratory tests were compared in the figure below and show that variation of the wear factor as casing wear increases is similar for different casing loads. These tests were performed under the DEA-42 project's standard conditions with N-80 casing, steel tool joints, and water-base mud with 7% sand.

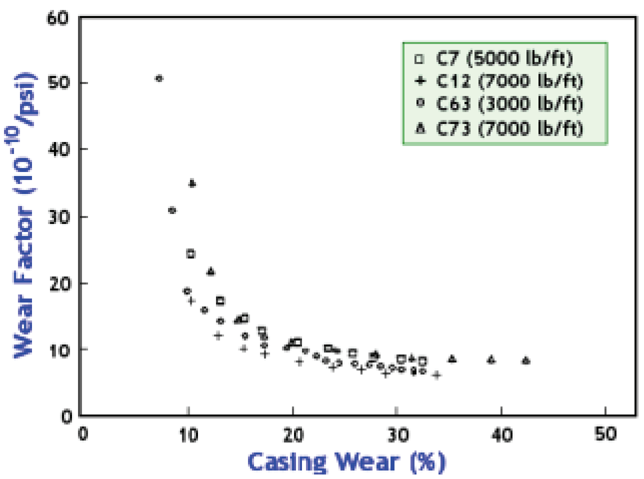

Figure 64: Wear factor vs. casing wear [16]

Based on this body of laboratory tests, an empirical casing-wear correction factor was developed to account for the observed wear-factor/wear-depth relationship. The non-linear correction factor is used in Cwear calculations and increases casing-wear values below about 40% penetration depth to a value greater than would be calculated using the asymptotic wear factor.

Standard correction factors for casing wear ranging from 0 to 50% are plotted below. The correction factor for casing wear above 50% is taken as unity (that is, the data are not corrected).

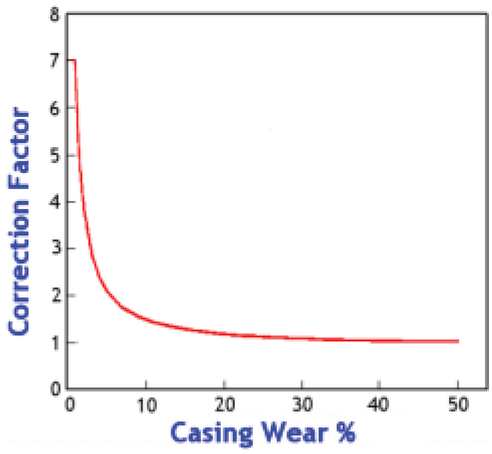

Figure 65: Nonlinear correction factor [16]

To obtain corrected or adjusted casing-wear percentages, casing wear calculated using the asymptotic value of wear factor is multiplied by the correction factor shown in the graph. Note that non-linear correction is applied only to the final casing-wear results. Internal computations use the constant value of wear factor and are not affected by the non-linear correction. [16]

4.1.2 Drag and lateral loads

Calculation of drag and lateral loads in a drill string is based on a mathematical model developed by Exxon Production Research. The model is based on the assumption that loads on tubular result solely from effects of gravity, tension, and compression acting through curvatures in the wellbore. Axial friction force and the effect of drill-pipe bending are ignored in the calculation.

The model considers tubing to be made up of short segments joined by connections that transmit tension and compression. Basic equations are applied to each segment with calculations starting at the bottom of the tubing and proceeding upward to the surface. Each short element thus contributes small increments of axial drag and weight. These forces are summed to produce total loads on the tubing.

In the simple free-body diagram of a single element of tubing shown:

T = axial tension force

N = normal force

W = tubing weight

θ = inclination angle

α = azimuth angle

Δ = incremental values

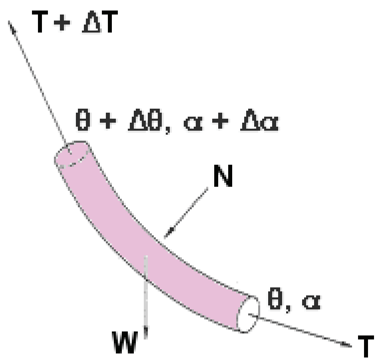

Figure 66: Drag and lateral loads [17]

Normal force and lateral load can be calculated from the bottom of the drilling string to the surface in a step-wise fashion. [17]

4.1.3 Burst and collapse of worn casing

Wear reduces pressure capacity of riser/casing strings. Crescent-shaped wear grooves complicate the assessment of pressure capacity of worn riser. Three methods are included in the program to estimate burst and collapse limits of grooved riser/casing.

4.1.3.1 Biaxial equations

Casing burst pressure, Pi, and collapse pressure, Po, can be calculated according to Lame's equation for thick cylinders and the von Mises equation. Note that this model assumes no axial stress in the casing. [18]

4.1.3.2 API equations

API Bulletin 5C3, 1989, "Formulas and Calculations for Casing, Tubing, Drill Pipe and Line Pipe Properties" lists all API standard equations for burst pressure limits, and four collapse pressure range limits. This approach also uses minimum casing wall thickness to estimate pressure capacity. [19]

4.1.3.3 OTS equations

Both biaxial and API equations use minimum wall thickness instead of considering the specific non-uniform wall for calculating burst and collapse pressures. The former approach results in an underestimation or overestimation of internal and external pressure capacities, depending on the conditions.

Oil Technology Services Inc. proposed a new method to calculate hoop stress of crescent-shaped worn casing using bipolar coordinates and a complex mathematical approach. Their equations account for the reinforcing nature of the remaining casing wall. It is reported that OTS's predictions agreed with experimental results.

Note that for crescent-shaped worn casing, a higher hoop stress can occur at either the inside or outside surface. Therefore, the von Mises equivalent stress must also be evaluated for both surfaces to obtain pressure capacities. [20]

4.2 Input parameters

This chapter will discuss the software structure of Cwear, which will help to understand the workflow and some of the challenges.

4.2.1 Tool bar

Tool-bar icons can be used to quickly access commonly used functions. The icons are short-cuts for menu options. The functions of the icons are:

 New project: Clears all input data.

 Open project: Activates the open Cwear file window.

Save: Saves all input data to current file name. If the project is new, the save as window is activated automatically.

Print: Prints the current window (input or output). To change printers, open the "Page Setup" window under the file menu.

View input: Used to return to the Input window for reviewing and modifying input data after the output window has been accessed.

View output: Launches the calculations based on the current input data and automatically displays the results in the Output window.

Wellbore schematic: Shows a multi-option schematic of the current wellbore geometry.

Units: Opens the units selection window.

Help: opens the Cwear help system directly to a description of the current page. Same as [F1]. Alternatively, select "help topics" from the help menu to open the Help system from the introduction.

Calculator: Activates the windows utility calculator for quick arithmetic.

4.2.2 Units

A mix between SI and field units is usually found in the reports. Therefore Cwear provides a unit selection tool. If the “custom” units are selected, the user has the possibility to set every type of unit. A custom mix of SI and field units can be chosen.

4.2.3 Project page

These data provide specific information about the project as well name, field, comments and so on.

Below the drilling operational mode, from the four options provided, has to be selected. Input parameters and labels on other input pages will change to reflect each selected operation.

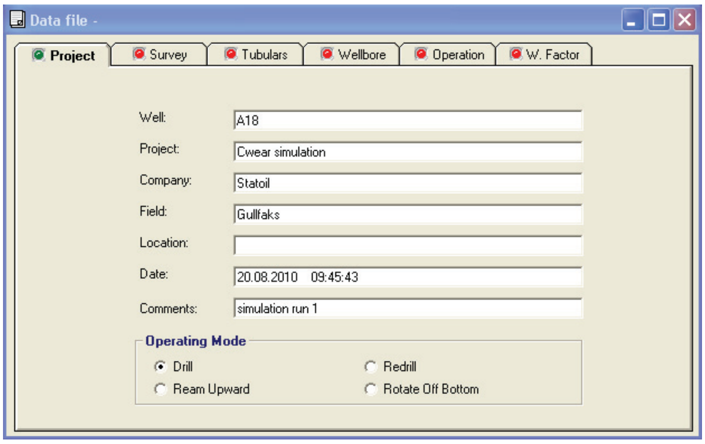

Figure 67: Cwear project page

4.2.3.1 Drill

For this case, initial casing wear is zero (i.e., the casing is new). Wear will be accumulated as the specified interval is drilled. Note that the Wear History page is hidden for drilling operations, since no previous wear is assumed to exist for this case. If previous wear exists, select "Redrill" and enter the existing data on the Wear History page.

4.2.3.2 Redrill

This case includes previous casing wear, i.e., wear accumulated during previous drilling or redrilling operations.

4.2.3.3 Ream Upward

Here the initial wear is wear accumulated during previous drilling or redrilling operations. Practically speaking, reaming upwards is redrilling with negative bit weight.

4.2.3.4 Rotate Off Bottom

This is reciprocation of the drill string over a specified stroke length without weight on bit.

4.2.4 Survey page

Wellbore survey data are entered into the first three columns of the table. Column 1 is Measured Depth of the survey point. Column 2 is Inclination Angle at that depth. Column 3 is Azimuth Angle at that depth.

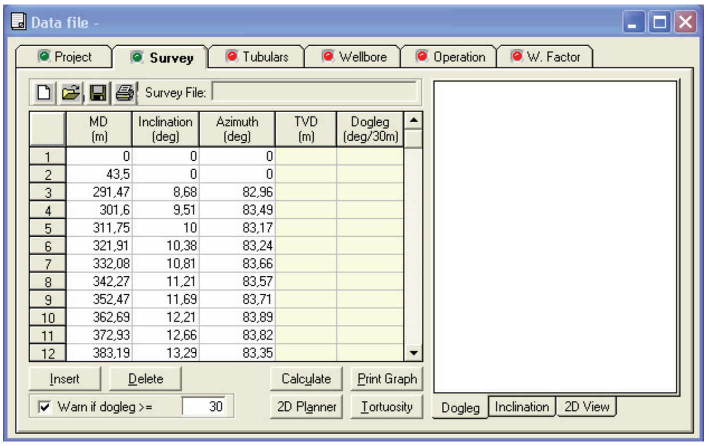

Figure 68: Cwear survey page

There are two possibilities of entering data into the table. The most straightforward technique for data entry is to type the number and then press <Enter>. This will automatically shift the cursor position to the next cell. The standard Windows key combinations can be used to copy, paste or move individual entries or blocks of cells in the survey table. Control+C will copy the selected entry (ies); control+V will paste. Note that you can copy individual entries only to individual cells, not to a block of cells.

To copy from a spreadsheet application (e.g., Excel), assemble the data in the spreadsheet in three columns in the correct order. Select the range of interest and copy to the clipboard <Control+c>. Go back to Cwear, click on the upper left cell to position the cursor, and press <Control+v>.

4.2.5 Tubular page

The drillstring being run into the well must be specified in detail. If "starting from bottom" is selected the description has to start with the BHA (not including the bit). Other sections of pipe should be entered in order proceeding up the string.

In the tool joint specification fields all tool joint parameters in the DP section have to be defined. Since Statoil did not use pipe protectors, this part of the sheet stays empty.

An extensive database of drillpipe dimensions and properties is provided. Dimensions and strengths for a wide variety of drill pipes can be directly imported into the Drillstring data table. Before accessing the tubular database, position the cursor anywhere on the row into which data are to be imported. Note that column 1 (description) and column 2 (length) will not be affected by the import. Any information entered in those columns will remain after importing data from the database.

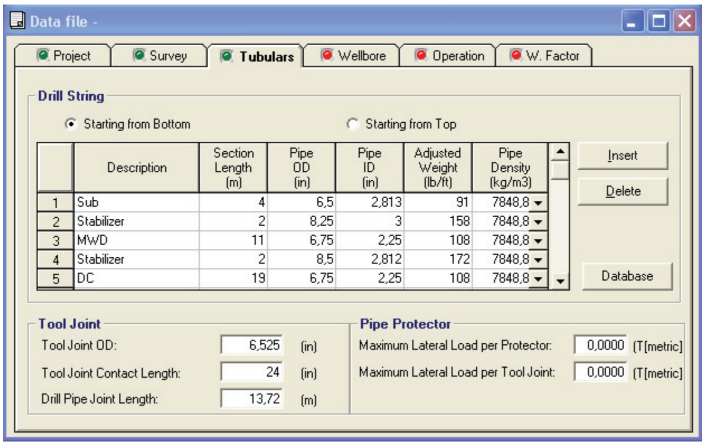

Figure 69: Cwear tubular page

4.2.6 Wellbore page

Specify the casing geometry starting from the surface and proceeding in order toward the bottom. Select a wellbore type from the drop-down list in column 1. Required parameters and wear algorithms differ depending on the type selected. Geometric and materials data may be typed in or imported from the lookup table. The total length of casing and other components should not exceed the survey depth (plus riser length).

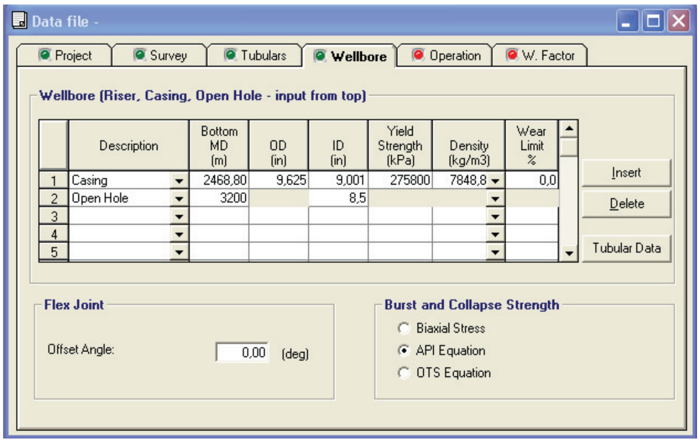

Figure 70: Cwear wellbore page

If a riser wear simulation is not intended, the casing strings can start directly from 0 depths.

Three models are provided to calculate the burst and collapse strength of the casing. The biaxial stress model is set as standard. The three models are discussed in a previous chapter.

4.2.7 Operation page

Depending on the type of operation chosen in the project page the operation page will look a little bit different.

4.2.7.1 Drill / Redrill

Operations start and end depths are specifying the starting and ending position of the bit during the selected operation.

The drilling parameter data table must be filled with the different operational stages. ROP, rpm and weight on bit control the volume and magnitude of content between the tool joint and the casing. The bottom of interval specifies the depth until these parameters apply.

Mud weights are also listed with corresponding bit depth.

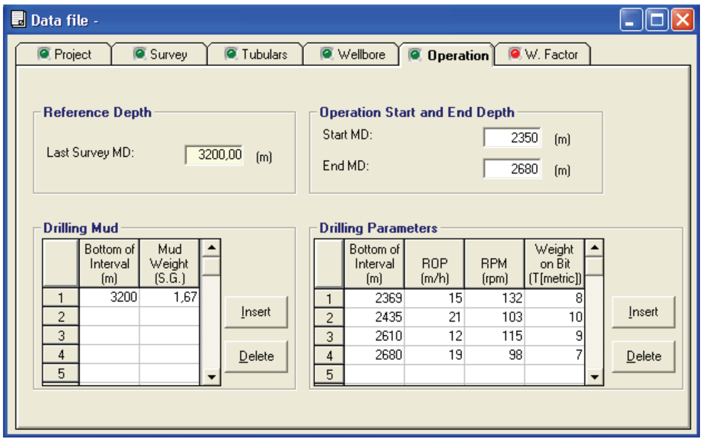

Figure 71: Cwear operation page – drilling

4.2.7.2 Ream upwards

This input page looks exactly the same as in the drilling / redrilling phase. The information has to be entered as this section would be drilled, and not backreamed! Since the ream upwards operation is chosen, the software converts this to backreaming.

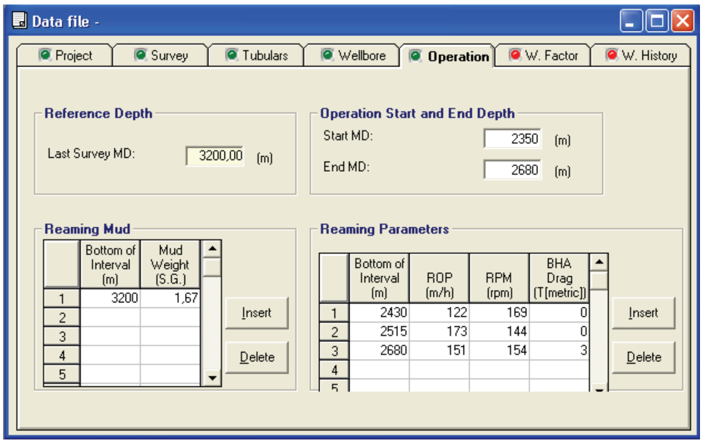

Figure 72: Cwear operation page – backreaming

4.2.7.3 Rotate off bottom

In this mode of operation the input page looks slightly different. All rotating or reciprocating parameters have to be filled in. The stroke has to be set to 0.1 if the string is purely rotating with no reciprocating movement.

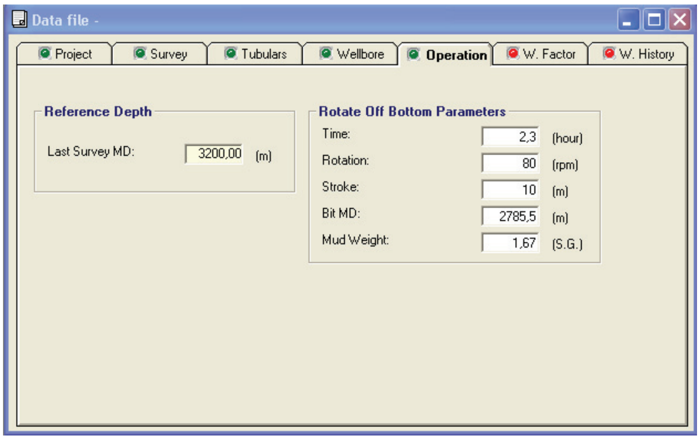

Figure 73: Cwear operation page – rotating off bottom

4.2.8 Wear factor page

The number of wear factors to be used for each wear analysis can be set based on the preferences. Depending on the information describing the wellbore conditions and which (if any) field measurements are available, the analysis can be simple (a single wear factor for the entire well) or more complicated (a specified range of wear factors for various sections of the well).

It is suggested to take a single wear factor if multiple simulations in a row are performed, since the following simulation only takes into account one base case based on one wear factor.

The engineering sense of these wear factors is that, if no appreciable wear is predicted with the high wear factor, the operation is most likely safely designed. If, on the other hand, significant wear is predicted with the low wear factor, steps must be taken to modify the operation prior to undertaking field operations.

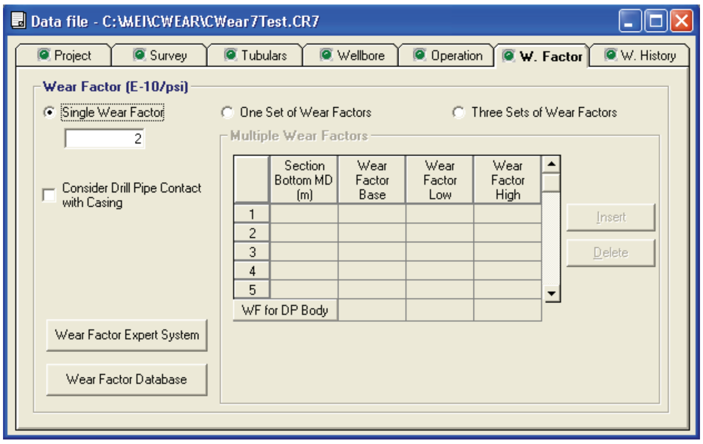

Figure 74: Cwear wear factor page

4.2.8.1 Wear Factor Expert System

As an aid in the selection of the best wear factor(s), an Expert System is incorporated into Cwear. The Expert System captures a large portion of laboratory test results conducted during the DEA-42 project. Within the Expert System window, select the tool-joint material, drilling fluids, additives, lubricants and other pertinent parameters. A range of wear factors and a suggested value from laboratory tests are displayed for every combination of drilling conditions listed.

4.2.8.2 Wear Factor Database

The Wear Factor Database provides more comprehensive results from DEA-42 laboratory testing. The extensive database covers a broad range of drilling conditions and casing/tool-joint combinations.

The database is also fully editable by the user. New data may be added easily and the results saved for future reference.

Best suitable wear factors for Gullfaks will be found the following chapter.

4.2.9 Wear history page

This page is not displayed if “drill” is selected in the project page and the previous wear is assumed as zero.

Wear history data with depth are shown for review. Two sets of wear history are now stored for "before and after" comparison. These are referred to as "Previous History" and "Current History."

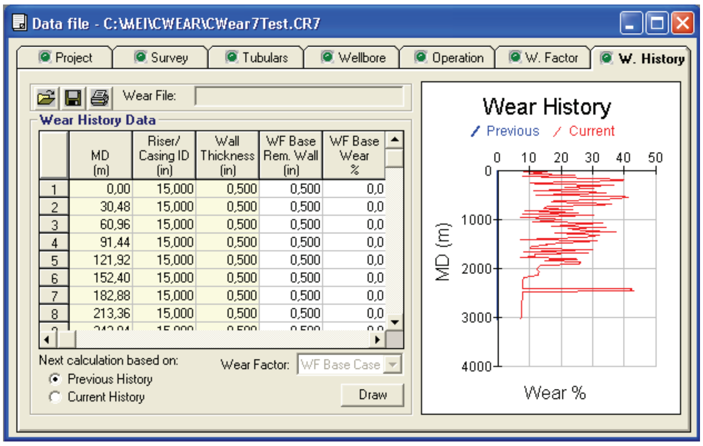

Figure 75: Cwear wear history page

Click "Current History" to display data based on the most recent calculations. For example, if you enter input parameters, select "Drill" and calculate wear results, the predicted wear condition after your specified drilling operation is now stored in this table and can be reviewed by returning to the input window . To move to the next drilling operation while accounting for the previous wear, change the input parameters as required and select "Redrill" on the Operation page. For redrilling, reaming upward, and rotating off bottom, wear will accumulate, with the total wear from all operations shown in the table as Current history.

4.3 Result output

Output presentations include graphs, wear logs and tables. Options are provided to view the graphs individually or in groups, exporting them to Microsoft Word, Excel or Power Point, as well as several other features.

4.3.1.1 Main output window

The main output window is loaded automatically after the simulation is executed by pressing the [view output] button. The now displayed graphs can be enlarged by double clicking their title bar. Output presentations include:

- Wear Schematic: This multifunction window displays wear along the wellbore. Zoom into any area of interest for detailed analysis. Specific depths can be selected to be displayed in the table.
- Wear %: An X-Y graph of casing/riser wear is displayed for the entire well (that is, all well sections inside casing). Three curves will be displayed if you have selected three sets of wear factors.
- Riser/Casing Remaining Thickness: This graph is similar to Wear %. Remaining thickness of the casing wall is shown with depth.
- Axial Load: This is a snapshot of the axial load experienced by each section along the drill string from the BHA to the surface.
- Normal Force: Normal force (in units of force per unit length) is shown along cased sections of the well. This is the force that presses the tool joint against the casing wall. Areas with high normal forces are normally associated with doglegs.
- Riser/Casing Burst Pressure: An X-Y graph shows casing/riser burst strength with measured depth. Performance results are based on the model you selected for worn casing on the wellbore page.
- Riser/Casing Collapse Pressure: An X-Y graph shows casing/riser collapse strength with measured depth. Results are based on the model you selected for worn casing selected on the wellbore page.
- Wall Plot Preview: A detailed log of wear and casing strength with depth is presented. If an analysis based on three sets of wear factors was performed, you can select the wear factor of interest prior to printing the log.
- Tabulated Results: Results summarizing casing/riser wear predictions are presented in a tabular format for rapid review, printout, or copying/exporting to other software applications. The output data are organized under five tabs:

- Wear Results
- Drag Force
- Burst and Collapse
- Summary
- Wear Volume

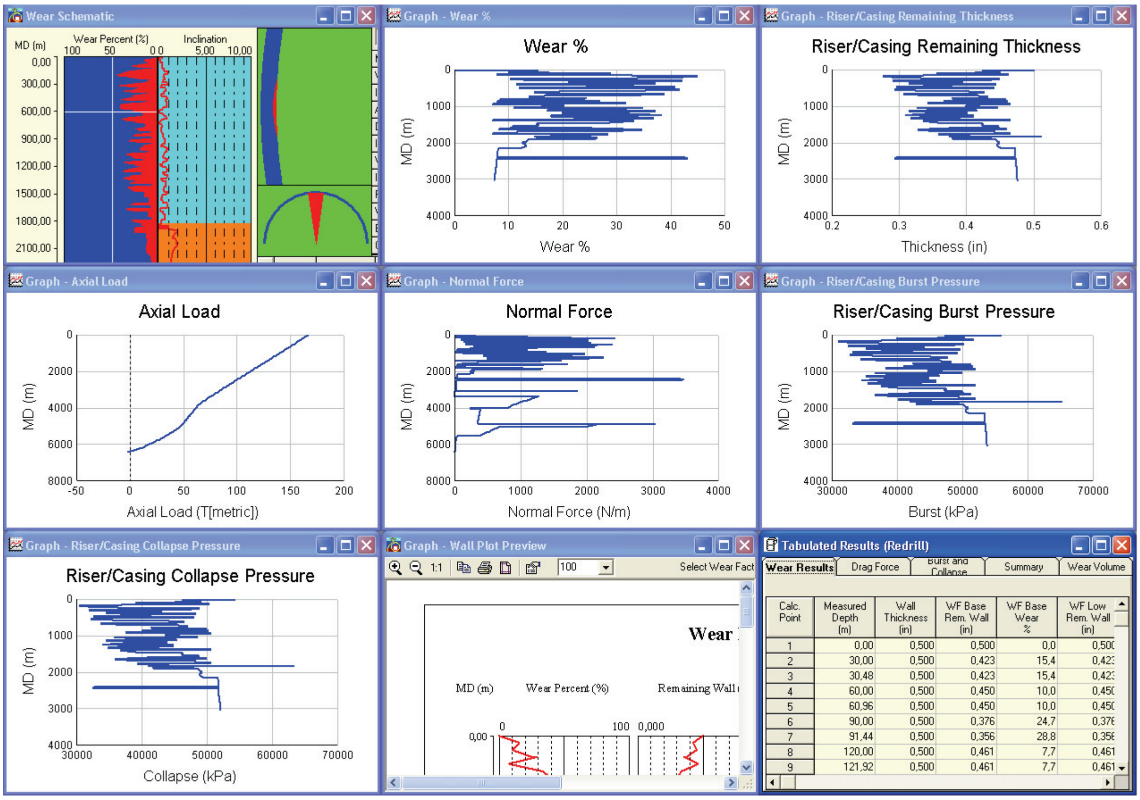

Figure 76: Cwear result ouput

A complete generated result report can be found in the Appendix.

4.3.2 Casing wear schematic graph

The Casing Wear Schematic is one of the nine graph/table windows displayed in the main output window. This multi-function graph includes several important options and therefore is discussed in detail.

Wear graph: A scaled plot of the wear %with depth is presented. Since wear often correlates with doglegs in the wellpath, inclination with depth is also displayed.

Cross sectional view: A cross sectional view is presented to the corresponding depth of interest. The upper half of the graph is a zoomed view of the wear groove and the remaining wall thickness. The lower part is a view which emphasizes the relative width of the wear groove compared to the casing OD.

Parameters at selected depth: Parameters associated with the chosen depth are also shown on the right part of the window.

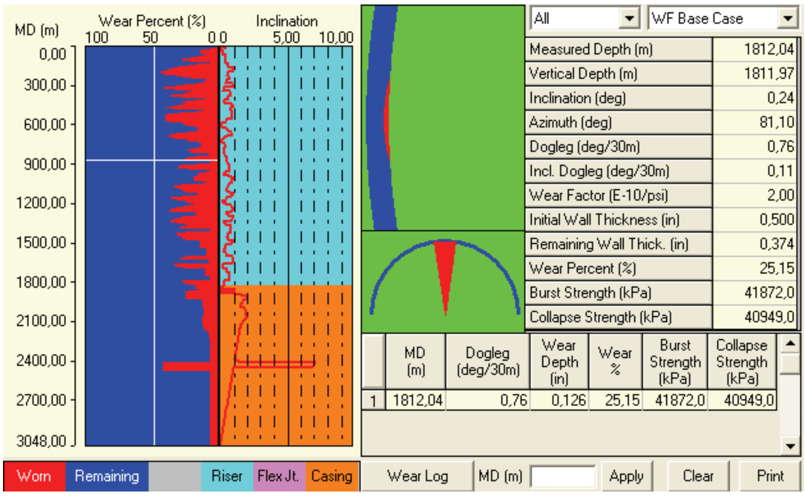

Figure 77: Cwear schematic graph

5 Gullfaks wear model

The main task of this thesis was to derive an accurate casing wear simulation model for all the wells in the Gullfaks field. This is quite a challenge, since the wells were drilled over almost 25 years from 3 platforms. Wear simulations on all wells, which have been logged for casing wear, have been done. The procedures, results and challenges are described in the following chapters.

The Gullfaks platforms have the same difficult situations like most mature North Sea platforms. All available slots are already in use. So it is necessary to sidetrack these wells to reach new areas of the reservoir. Because every new sidetrack has to be drilled through an existing casing, the condition of the pipe has to be known. The easiest and most cost efficient way to get an idea about the casing state is to do wear simulations.

Important properties for future operations can be estimated with the help of the results of these simulations. These include burst pressures, collapse pressures, the need of drillpipe protectors and many more.

5.1 Data acquisition

Gathering good data is vital for running an accurate simulation on casing wear and to get high quality results. It is probable, that gathering and processing all the information takes more time than the actual simulation.

5.1.1 Well information

All the needed data can be divided into following groups:

- Wellbore survey
- Casing sizes and depths
- Information about operations
- Drill string composition

An Excel file was created to bundle all the necessary data from different sources.

5.1.1.1 Wellbore survey data

The survey, describing the wellbore inclination and azimuth are required input parameters. A very practicable way of getting a Gullfaks wells wellpath is to copy or export it from the database “EDM Landmark”.

Some investigations, if the survey export resolution can take influence on the quality of the wear simulation, were carried out. Whereas the export resolution has no impact on the simulation quality, the actual logging resolution definitely has. Due to low logging resolution real doglegs can be missed out, which will cause high wear in the casing string. On the other hand, so called artificial doglegs, which occur due to bad logging quality and resolution, can be observed.

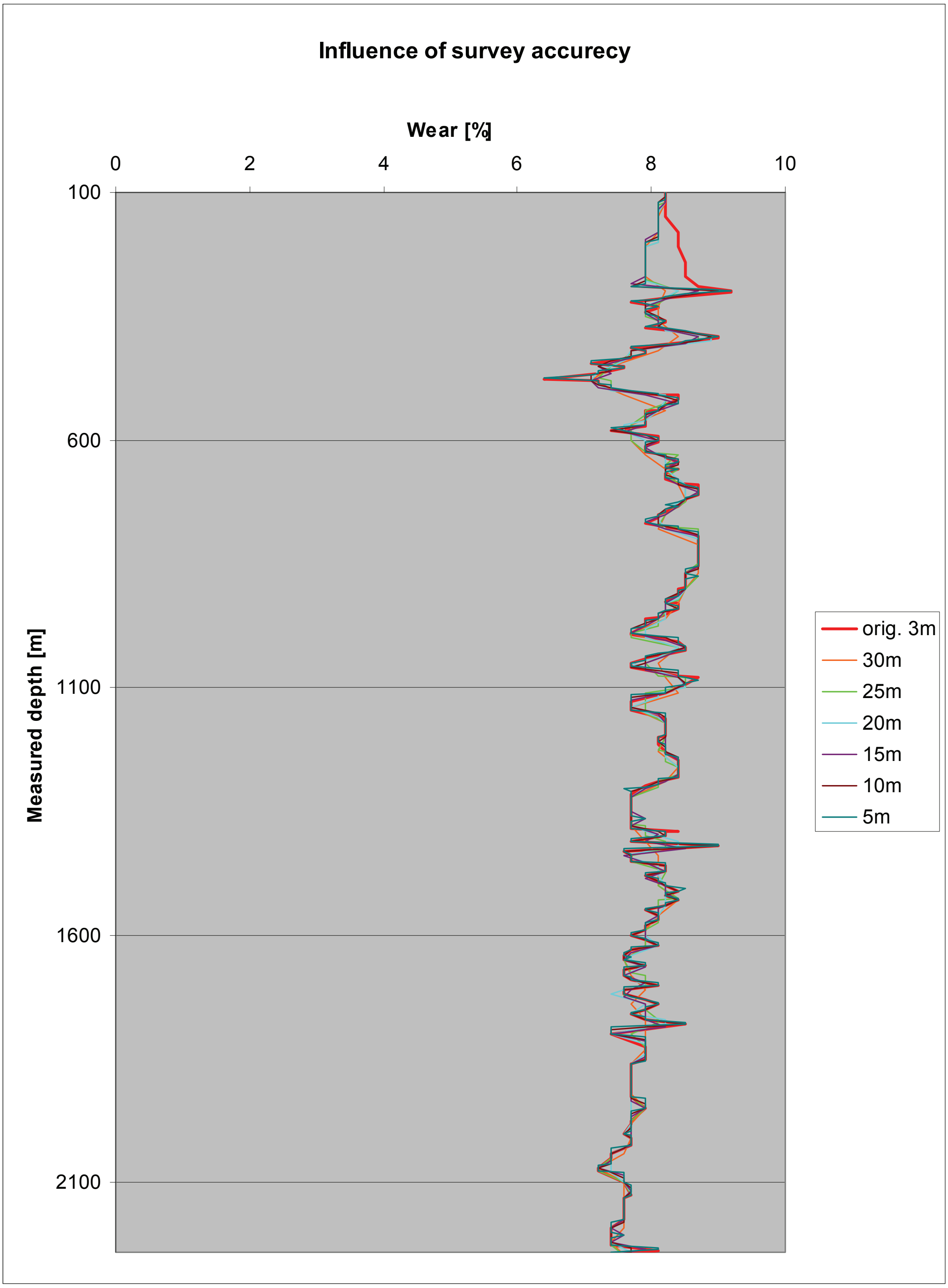

Figure 78: Influence of survey resolution

The comparison of different export resolutions on a test well can be seen in the figure above. As discussed before, there are almost no differences between the different resolutions.

5.1.1.2 Casing sizes and depths

The software simulates all operations which are run through a specific casing. A well sketch is always helpful on complicated or unfamiliar wells. Casing properties and setting depths can be found in “EDM Landmark” and in the daily drilling reports. A crosscheck is advisable.

Necessary casing properties are:

- Setting depth
- OD
- ID
- Yield strength
- Density

If the casing grade and coupling type is known, a casing database can be used to provide the necessary data.

5.1.1.3 Operations data

Although a very detailed splitting of operations would give a really accurate simulation, it is necessary to group comparable operations in order to reduce the simulation runs. A table including following operations:

- Drilling / reaming (start and end MD, duration, ROP, rpm, WOB)
- Backreaming (start and end MD, duration, ROP, rpm, BHA drag)
- Circulating / reciprocating (bit depth, rpm, stroke length, duration)

and following additional data:

- Mud weights and types
- Changes in BHA

should be prepared in advance. All information can be found in the daily drilling reports.

Date	Operation	Start MD	End MD	Duration	ROP	rpm	WOB
31.03.1991	MU BHA						
	RIH						
	Reaming	3018	3079,5	2	31	130	0
	Drilling	3079,5	3098	3	6	120	8
	Drilling	3098	3153	6	9	120	8
	Drilling	3153	3200	5	9	120	8
	Circulation	3180	3180	1,5	0	80	0
	Backreaming	3180	200	11,5	-259	130	0

Figure 79: Operation data

5.1.1.4 Drill string composition data

Every drill string geometry has to be defined for every operations run in the specific casing. It might get very difficult to get all the parameters from a well drilled 20 years ago, but the more accurate the drillstring data is, the more accurate the simulation gets. BHA assemblies can be found in the Statoil daily morning reporting system.

String component	Supplier	OD inch	ID inch	Length m	Acclength m
BIT, PDC/DIAM		12,250		0,47	0,47
BIT SUB		8,000	3,000	0,91	1,38
XO SUB		8,880	2,875	0,53	1,91
MWD TOOL,HIGH FLOW		8,125		12,88	14,79
STABILIZER, NM		12,250	2,750	2,65	17,44
DRIL COL, NM		8,000	3,000	9,46	26,90
STABILIZER		12,250	2,750	2,20	29,10
DRIL COL		8,000	3,000	9,46	38,56
STABILIZER		12,250	2,750	1,72	40,28
DRIL COL		8,000	3,000	37,80	78,08
JAR		7,750	2,875	11,03	89,11
DRIL COL		8,000	3,000	18,90	108,01
XO SUB		7,875	2,875	1,09	109,10

Figure 80: Drillstring composition

5.1.2 Log data

The USIT log raw data is delivered as data file (*.dlis) from the various logging companies. These files consist of various data channels which have to be separated from each other. Schlumberger offers a free software tool, “Toolbox”, to execute that. This can be downloaded from their homepage.

As discussed in a previous chapter, the most accurate value, to compare the simulation with the measurements, is the minimum thickness measured by the resonance (T3 processing). Since the T3 processing can crosscheck if the measurement point is an obvious failure, so-called unflagged values should be chosen for comparison. This data channel is most probably named THMN_RF. The software will create a *.las file, which can be imported into Microsoft Excel for further processing.

It is advisable to calculate the percentage of wear for every measured data point to have a better comparison and evaluation.

$$W = 100 - \left(\frac{t_m}{t_n} \cdot 100 \right) \quad [\%]$$

Equation 36

where

W = wear [%]

t_m = measured remaining wall thickness [in]

t_n = nominal wall thickness [in]

The next step is to remove the high data peaks, generated by the casing couplings to smoothen the log a little. This can be done manually in short distance logs, or with a Microsoft Excel routine.

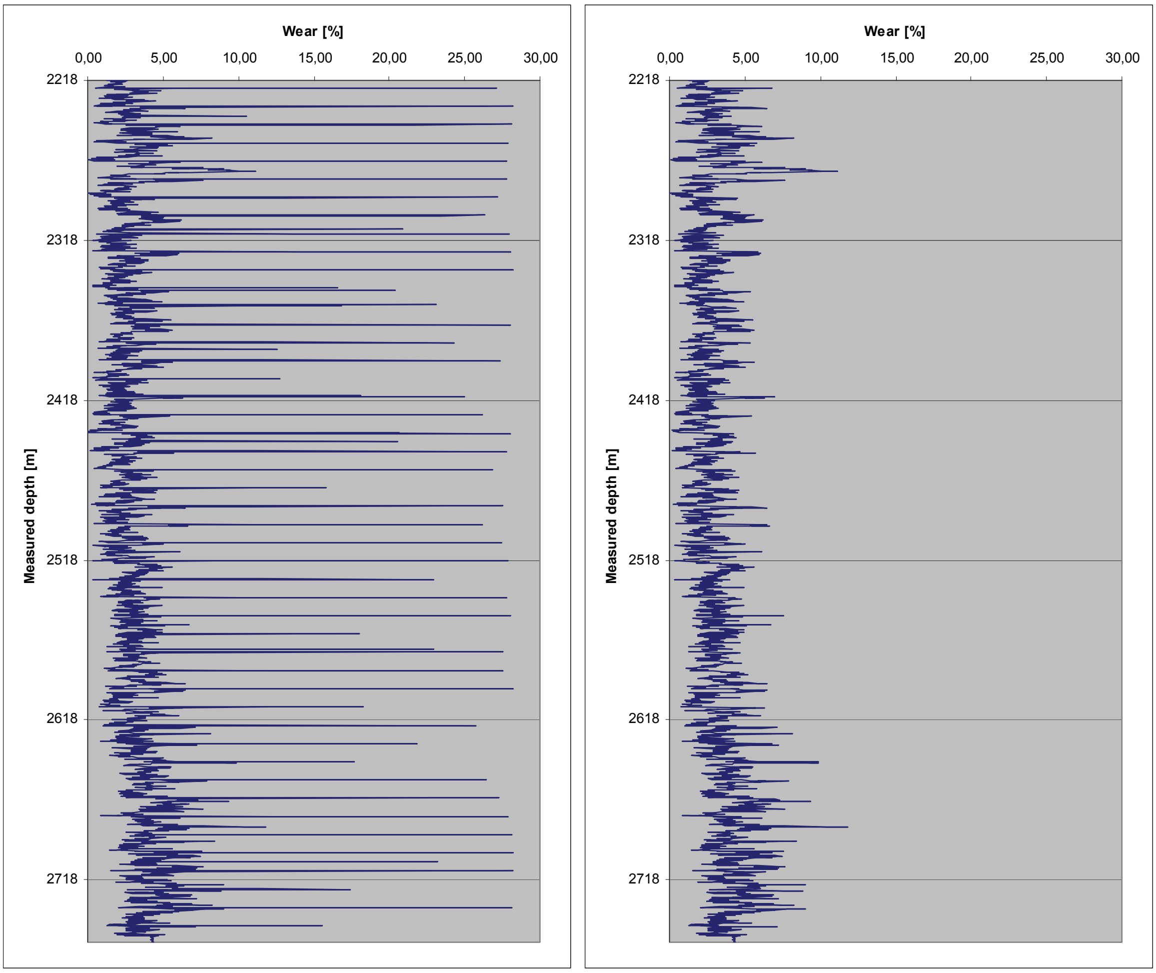

Figure 81: USIT data of C-38 original and removed connections

After removing the high peaks caused by the casing couplings, it is necessary to smooth the log curve even more in order to get a good match for the simulation.

The first attempt was to do a Fast Fourier Transform to filter all high frequencies. The Fourier transform converts a time representation (samples) into a frequency representation (i.e. the frequency spectrum of these samples) and vice versa. Commonly it splits a number of samples into a corresponding number of sine waves of different frequencies, so that you know the amplitude and the frequency for each sine. Although this procedure looked very promising a lot of data loss occurred and the FFT approach was abolished.

The next attempt was to apply a moving average at the data set. A moving average is the unweighted mean of the previous n data points. For example, a 10 depth increment moving average of log values is the mean of the previous 5 and following 5 log values. After tests and simulations on the magnitude of the moving average and discussions with Statoil and

Schlumberger log specialists, a MA with the magnitude of 6 was chosen. 6 depth increments give a total distance of 90 cm, which means, that if a worn segment is longer than 90 cm it is displayed in the log with its original wear percentage. If it is smaller (i.e. just one high peak) it is most likely a measurement failure and thereby flattened out by the moving average.

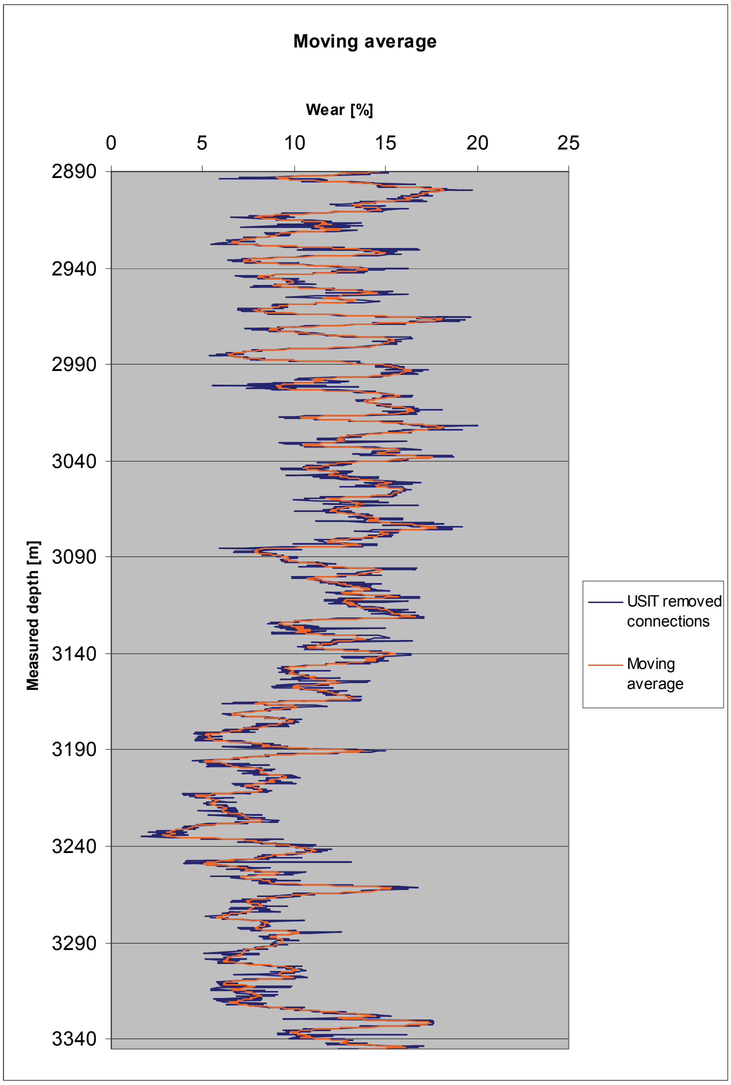

Figure 82: USIT data of B-28 removed connections and moving average

To make sure, that the decrease in wall thickness is due to wear and not due to example corrosion, two possibilities of confirmation can be chosen.

The first one is the visual confirmation, which can be done with the help of the Schlumberger wear reports. One Example can be found in the following chapter. Although this method gives a quite good overview, it gives no numerical or statistical analysis.

The second, and much more time consuming method is to use the USIT log raw data value for the thickness for every increment of rotation. That gives 72 values for every depth interval spread over 360 degrees.

The figure below shows a wall thickness cross section plot of a sample well. The wear groove can be clearly seen in the left upper corner. Since the other wall thickness is almost equal to nominal it is proven that there was no corrosion and only wear.

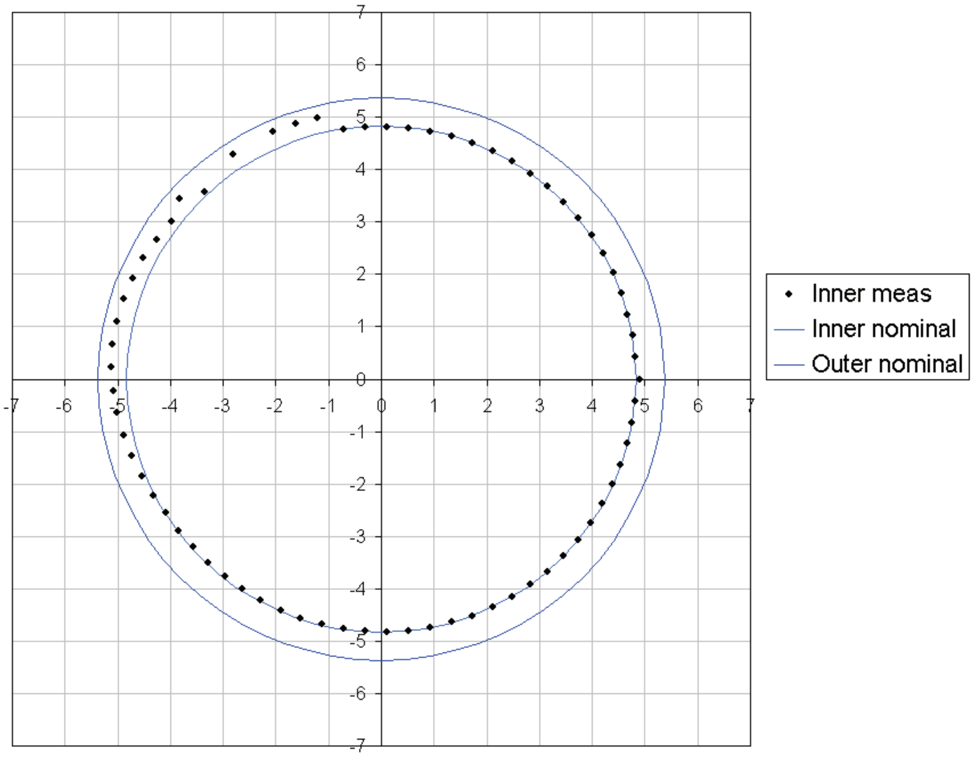

Figure 83: Wall thickness cross section

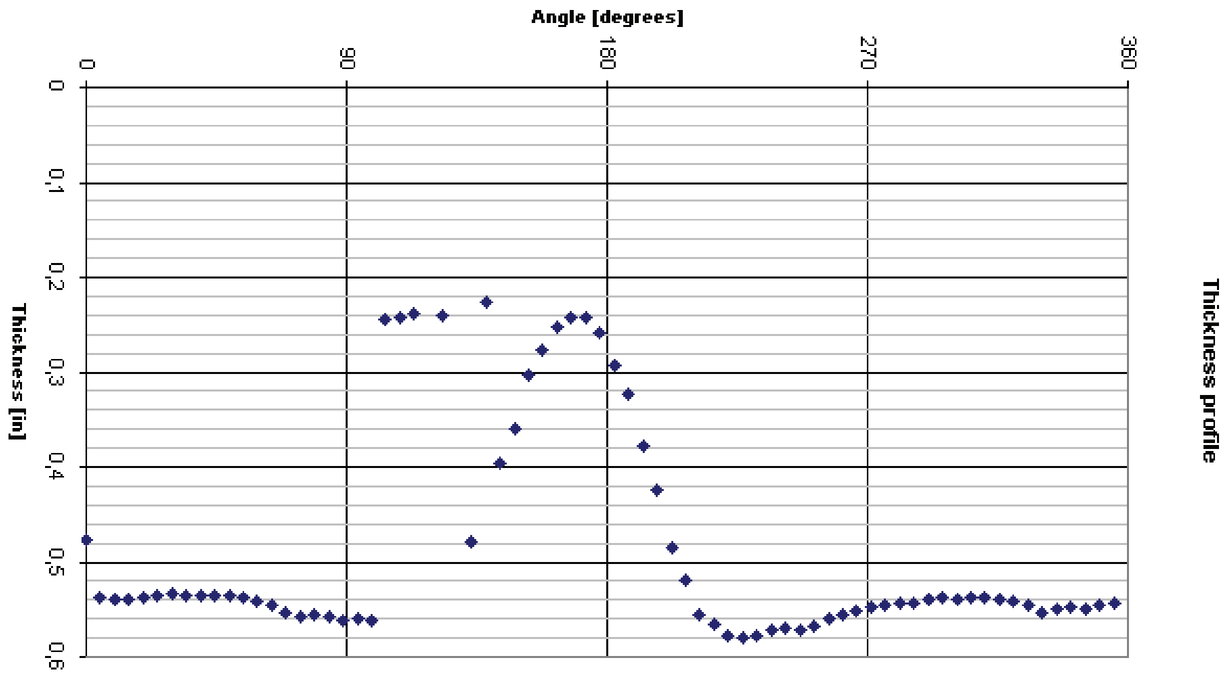

Figure 84: Wall thickness vs. angle

The figure above shows the thickness value for every circle increment. Here the groove can be seen even better. The five high peaks left of the groove are a good example of wrong measurement values. At this side of the groove the sonic waves are deflected and not brought back to the measurement tool correctly. This causes wrong thickness values, which normally have to be filtered before using the log for comparison. In this case, when using the minimum thickness for simulation matching it does not make any difference because the wrong values have the same magnitude than the right thicknesses.

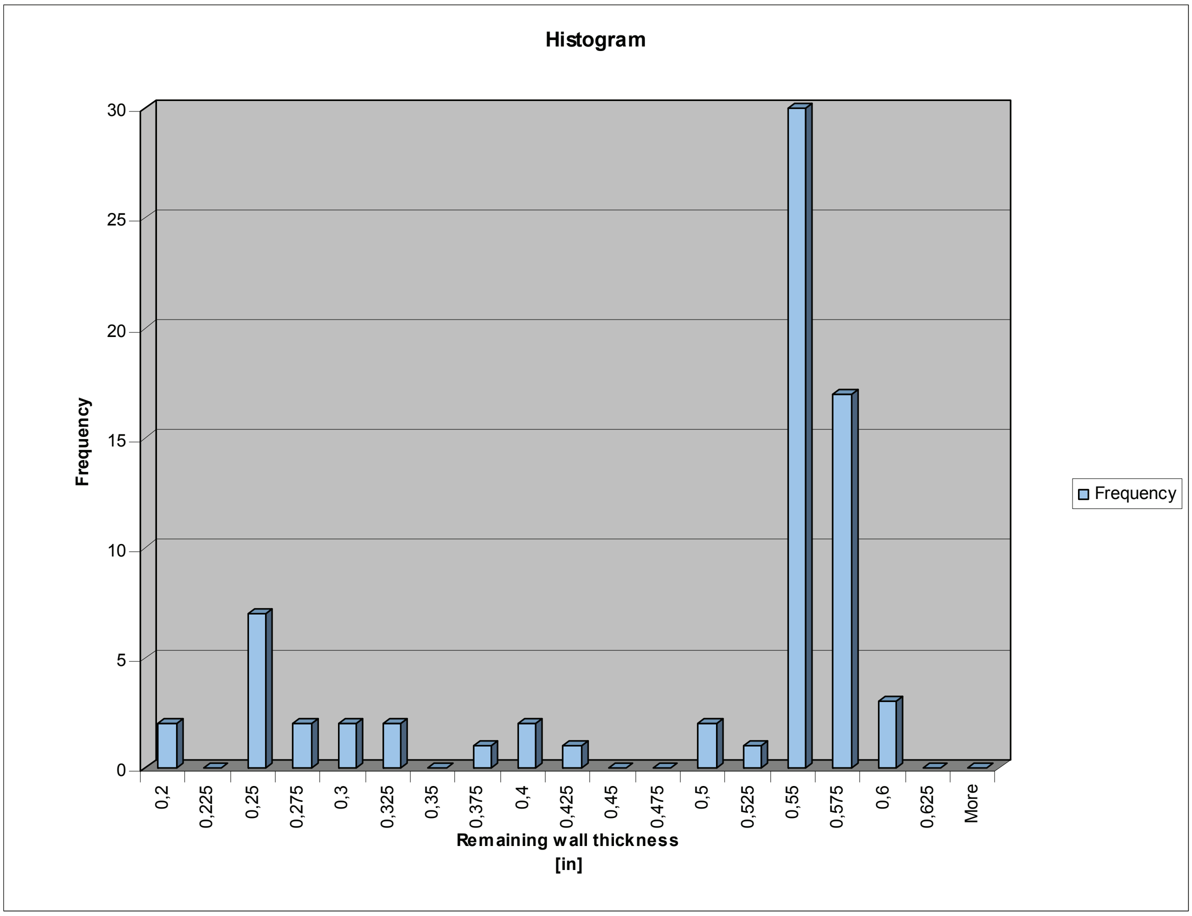

Figure 85: Cross section histogram

The histogram shown above is another clear indication of wear. The two concentrations of frequencies around 0.25 and 0.55 inch exclude the possibility of corrosion.

5.1.2.1 Simulation matching

How and where to match the simulation runs to the USIT measurements was one of the greatest challenges during this thesis.

The first approach was to make the simulation following the overall trend of the log, which was working really well. After many discussions with well logging experts the decision was made to change this approach.

For planning new sidetracks it is important to simulate the maximum occurred wear, to be sure that future operations will not damage the existing casing. This might be a conservative approach but it would be easier to plan a new section for oversized wear, as to set expensive repair activities because of a leak. So the decision was made to match the simulation to the maximum occurred casing wear. This is shown at the example well in the Appendix.

5.1.2.2 Comparison with Schlumberger wear report

Schlumberger produces a USIT log report for every log they run for Statoil. In this report the cement bond and the casing condition are discussed based on human visual interpretation.

In addition to the USIT raw data curve this interpretation was used to verify, that the simulated wear curve was aligning with the maximum wear according to the Schlumberger report.

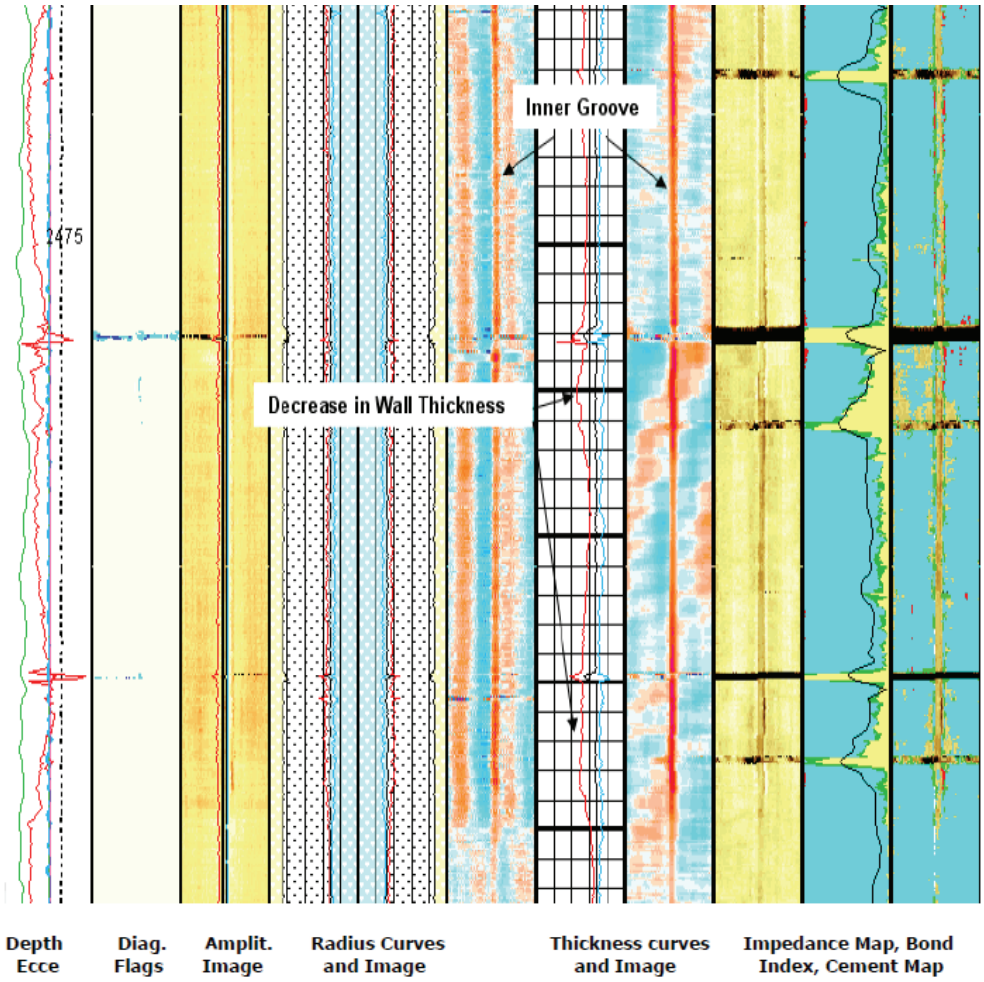

Figure 86: Schlumberger visual USIT log interpretation [21]

This Schlumberger report verification can be seen in the example well in the Appendix. It is indicated with a green dot in the wear curve.

5.1.3 Operation simplification

Complicated wellpaths or difficult geological formations can often result in a lot of different BHA runs and operation in a specific casing section. This would result in a very large numbers of single simulations in the initial operation configuration which will end up in quite some simulation time for the engineer. In order to reduce the necessary simulation time it is necessary to connect single operations.

Drilling: It can be assumed that a certain distance is only drilled once. This results in the possibility to connect all the drilling operations and exclude the circulating, reciprocating and backreaming between. This will end up with only one simulation for the whole drilling process.

Backreaming: Simplifying and combining this operations is a little bit more complicated because some distances are often reamed twice or more. These procedures need to be combined into more simulations. But it is still possible to divide the necessary simulations by three, when grouping them.

Rotate off bottom: All the different rotate off bottom activities can be brought down to number of rotations. These numbers can be summed up and recalculated into a total time of rotating with a specific rpm. The bit position should be set to TD because it can be assumed that nearly 100% of the rotating activities take place in the open hole, which is not wear simulated.

This simplification method can be only applied if all the drillstrings in the model have the same dimensions. If the diameters differ, no simplification can be applied, since the sequence of the operations have an influence on the wear groove.

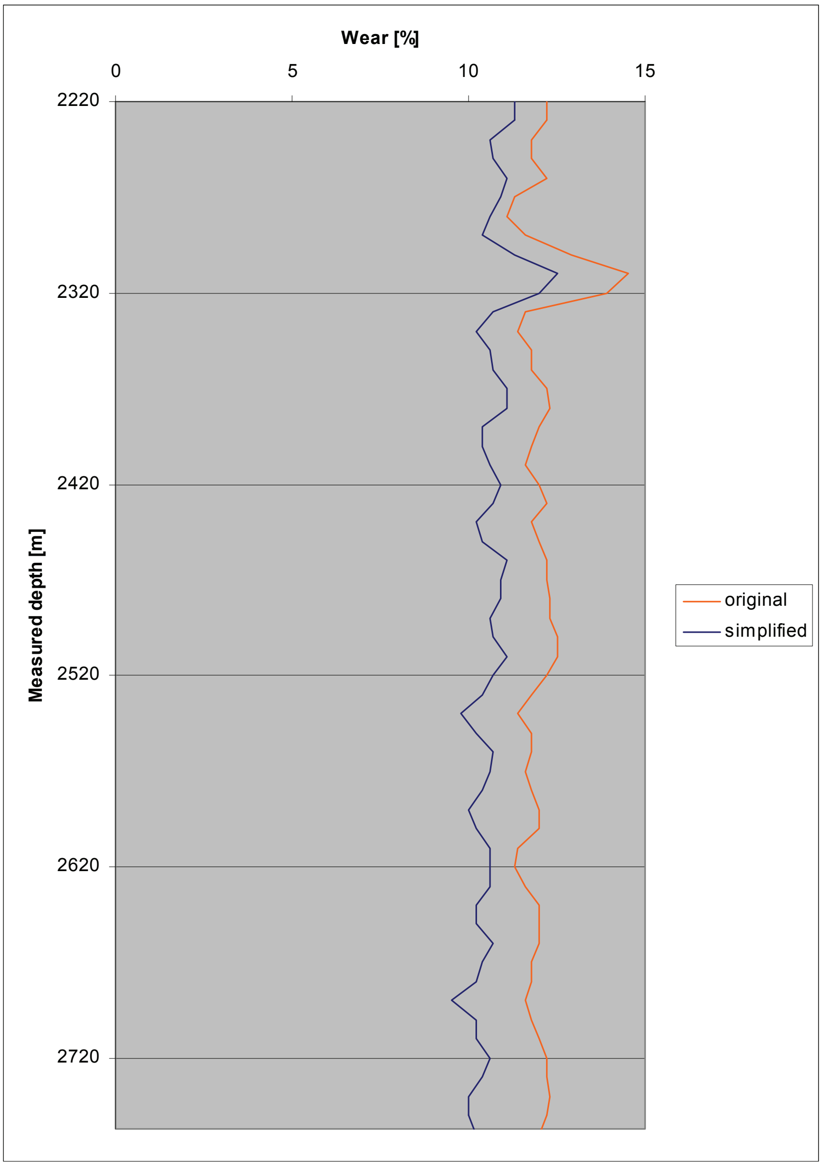

Figure 87: Original vs. simplified operations

The figure above shows the Well C-38 T2, which needed originally 51 runs to simulate the 10 3/4'' liner section. After the simplification the number of simulation runs came down to 12. As it can be seen the two wear curves differ only in about 1% wear.

This is a timesaving method for engineers carrying out Cwear simulations. All the results in this thesis are based on precise simulations.

5.2 Simulations

5.2.1 Uncertainties

Most of the investigated wells were drilled in the late eighties, where data collecting and drilling parameter monitoring was not very important. For most of the wells it is not possible to specify which drillpipes exactly were used for that particular well. In order to discover the impact of these uncertainties on the results, simulations of these effects have been carried out. The following chapter should give a guideline of values, which are applicable for Gullfaks A, B and C.

5.2.1.1 Tool joint outside diameter

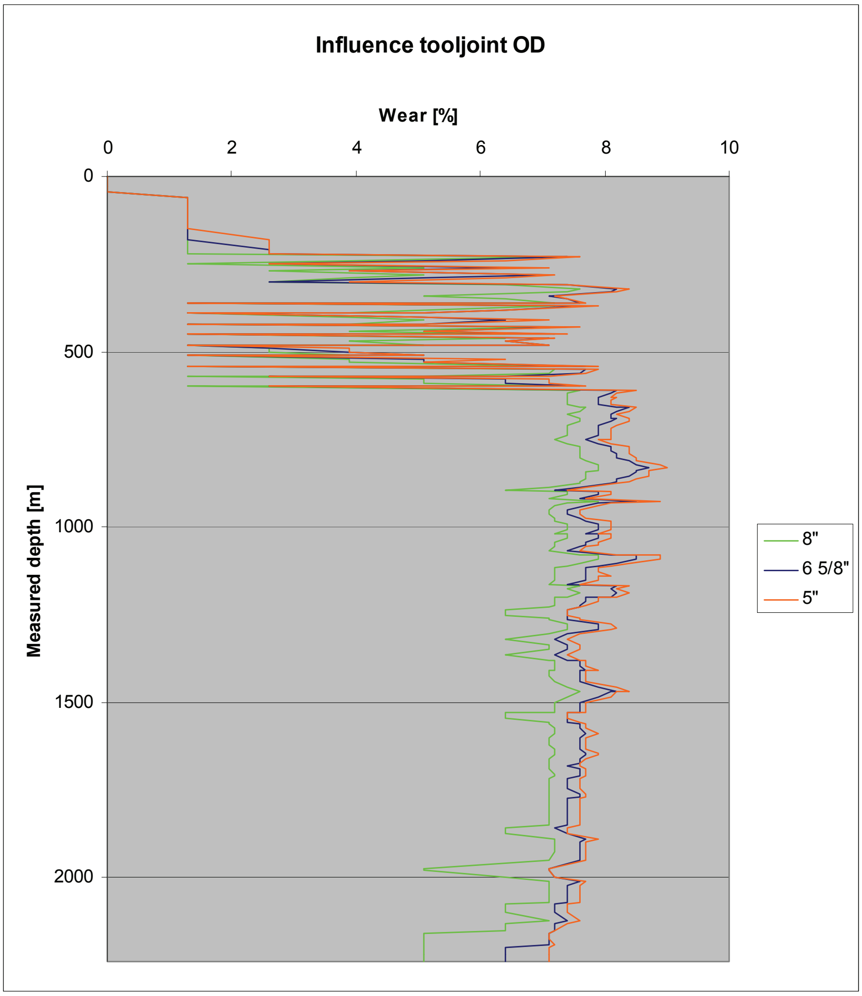

Figure 88: Influence of tool joint OD

The simulation of the tool joint outer diameter on a test well showed differences in wear [%] of up to 2%. This can be easily explained with the help of the casing wear simulation model. Since the Volume of the wear groove is calculated and from that volume the depth is derived it is obvious that with increasing diameter but constant drillstring weight the wear depth is decreasing. The wear groove in this case will be wider but less deep. A trend can be seen in the figure below, where some possible tool joint ODs are compared.

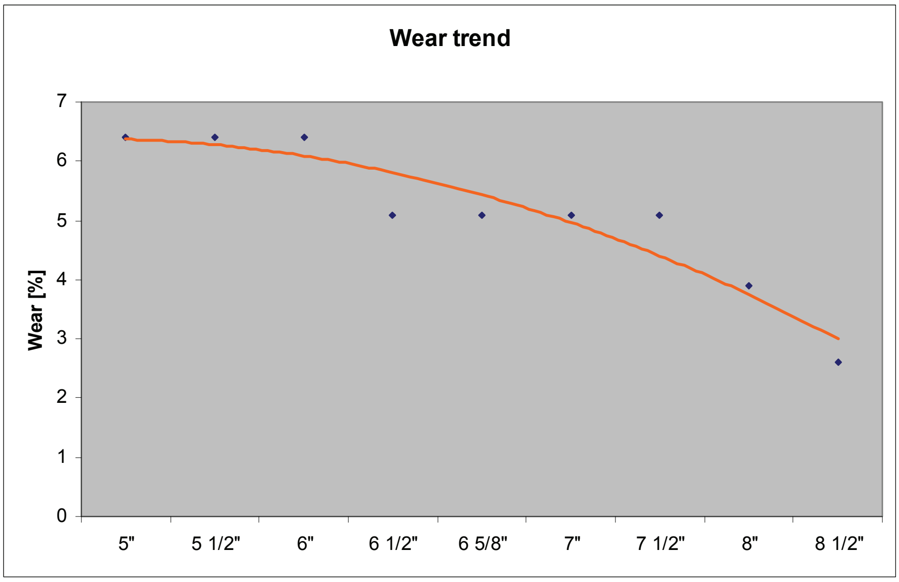

Figure 89: Wear trend for tool joint OD

In general the connection between the tooljoint OD and the wear can be described as followed. The smaller the tooljoint OD the deeper the produced wear groove. The reason for that is the impact of the diameter on the wear depth, which is discussed in a previous chapter.

5.2.1.2 Tool joint length

The tool joint length of the used drillpipe had absolutely no influence on the casing wear in the test well simulation. Since the wear depth is not dependent on the tool joint length these results are no surprise. Only very small variations can occur when the drillstring is rotated for a long time on one position. In reality, when the drillpipe is rotating, it is reciprocated a few meters to avoid exactly this effect.

Figure 90: Influence of tool joint length

5.2.1.3 Drillpipe outside diameter

The drillpipe outer diameter has compared to the tool joint length a little bit more influence on the casing wear.

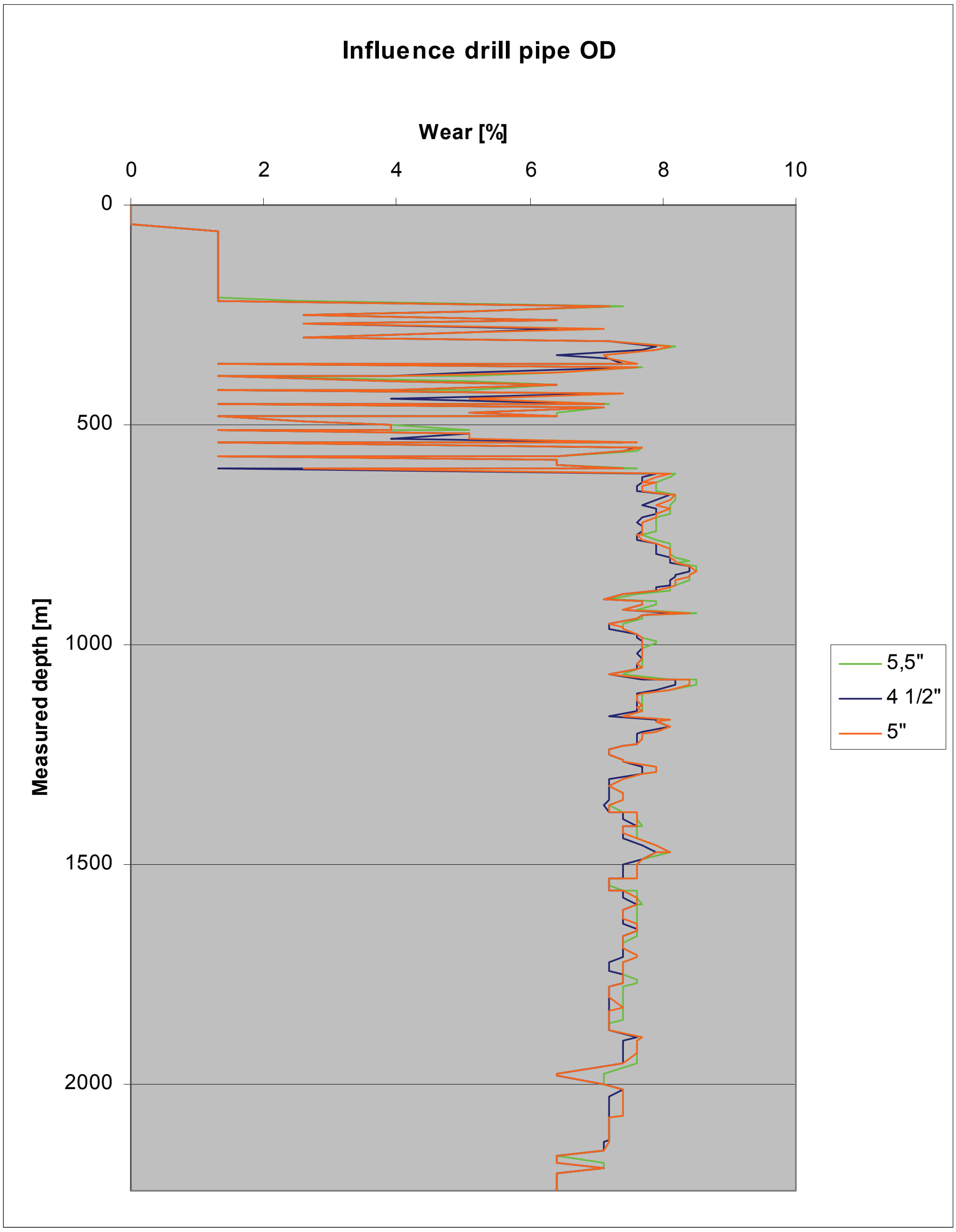

Figure 91: Influence of drillpipe OD

It can be observed that bigger drillpipe outer diameters result in slightly more wear, which seems to disagree with the explanation for the tool joint outer diameters. But the model assumes that the drillpipe is not in contact with the casing. That means the only contact point between the drillstring and the inner wall of the casing is the tool joint. The only thing the drillpipe contributes to the casing wear is the weight. That means that bigger drillpipes add more weight to the tool joint which will result in more normal forces at the casing. The trend of different drillpipe ODs can be seen in the figure below.

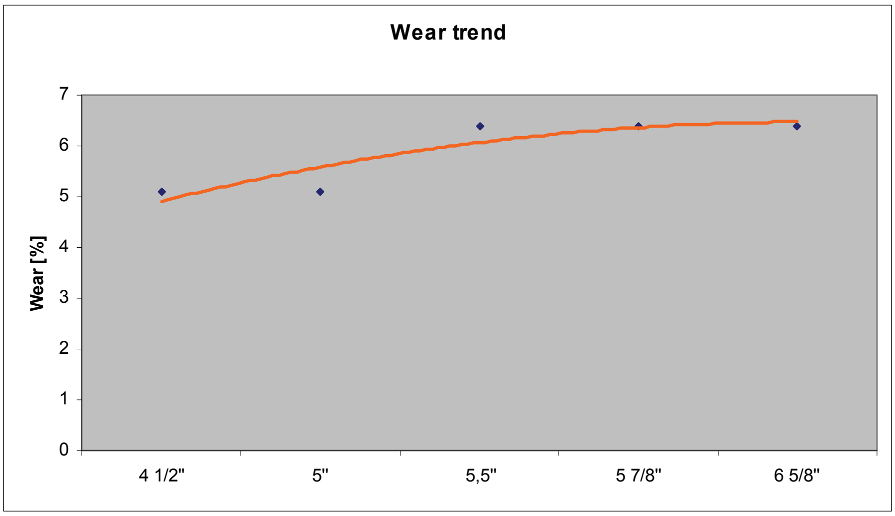

Figure 92: Wear trend for drillpipe OD

5.2.1.4 Hardbanding material

Two types of hardbanding materials were used in Gullfaks A, B and C wells over the years. When Statoil started developing the field drillpipes with tungsten carbide hardbanding were in use. These were quite robust against abrasion but this resulted in a very bad casing wear performance.

Approximately 1993 the drillpipes were gradually changed and replaced by pipes with tool joint made of pure steel. Of course this was good for the casing wear performance but unfortunately they were worn quite fast.

The next progress was taken in 1997 were drillpipes with an ARNCO 300 XT hardbanding were established. This improvement reduced the wear significantly while the tool joints are protected from abrasion in the open hole. This type of hardbanding material is still in use on every three Gullfaks platforms.

1987 – 1993	tungsten carbide hardbanding
1993 – 1997	no hardbanding (steel joints)
1997 – now	ARNCO 300 XT hardbanding

Based on their different wear attributes these three types of drillpipe have different wear factors, which will be shown in the following chapters.

ARNCO 300 XT

The ARNCO 300 XT is a chrome-free hardbanding. It is a ferrous-based alloy containing Nickel, Boron and Niobium, creates minimum casing wear and maintains significantly more open hole wear resistance needed to protect the drill pipe tool joints from rapid wear found in highly abrasive drilling conditions. An Rc micro-hardness of about 60 ensures an optimum balance of tool joint protection and casing wear reduction.

Figure 93: Hardbanding ARNCO 300 XT [22]

5.2.1.5 Operational parameters

When running a simulation, all operational parameters have to be derived from the daily drilling reports. Depending on the accuracy these reports were written, they contain more or less accurate information. When no information of rpms and WOBs are available probable values from offset wells have to be chosen.

A case study and comparison of daily drilling reports resulted in the following table of most likely operational parameters for 8 1/2” BHA in a 9 5/8” casing.

Operation	rpm	WOB
	[rpm]	[t]
Drilling	120	8
Drilling casing shoe	100	8
Coring	100	10
Backreaming	160	0
Circulating	70	0
Reciprocating	80	0

Table 14: Operational parameters

5.2.2 Workflow

The first thing, that had to be done, was to get familiar with the topic casing wear in theory and practically. With the help of different books, papers and several articles it is possible to get a good overview of the problem. Good fundamentals in physics help to work on the theoretically side. The first introductory steps in Cwear were rather elementary but when it comes to complex simulations a lot of practise and knowledge is vital.

Simultaneously, all the Gullfaks wells had to be looked through to spot those, which were logged with USIT. To understand the USIT logs measurement technique and to get an idea of how to interpret the raw data a lot of instructions, time and practise were necessary.

After all the wells were gathered and those, suitable for the comparison were chosen, the next step could start. All the operation, survey, drillstring and casing data and the USIT log analysis was collected and brought together in one Excel based database. This task was really challenging since every piece of data is stored within different software packages and has different file standards and units.

Then the simulation process on the more simple wells could start. This simulation methodology can be described as followed:

- Define project data
- Integrate survey, tubular and casing data into the software
- Specify a single operation
- Specify a wear factor
- Load a wear history

- Run simulation

This methodology had to be adjusted and repeated for every single part of operations during the drilling process.

When the simulation progress included all the operation in a specific casing section, which was logged with USIT, a report had to be made and the tabulated results had to be included into the MS Excel database. A comparison between the simulated results and the USIT log data can now be executed and the wear factor can be adjusted.

With this adjusted wear factor a new simulation run is started and the whole process is repeated until the simulated wear matches the measured as close as possible.

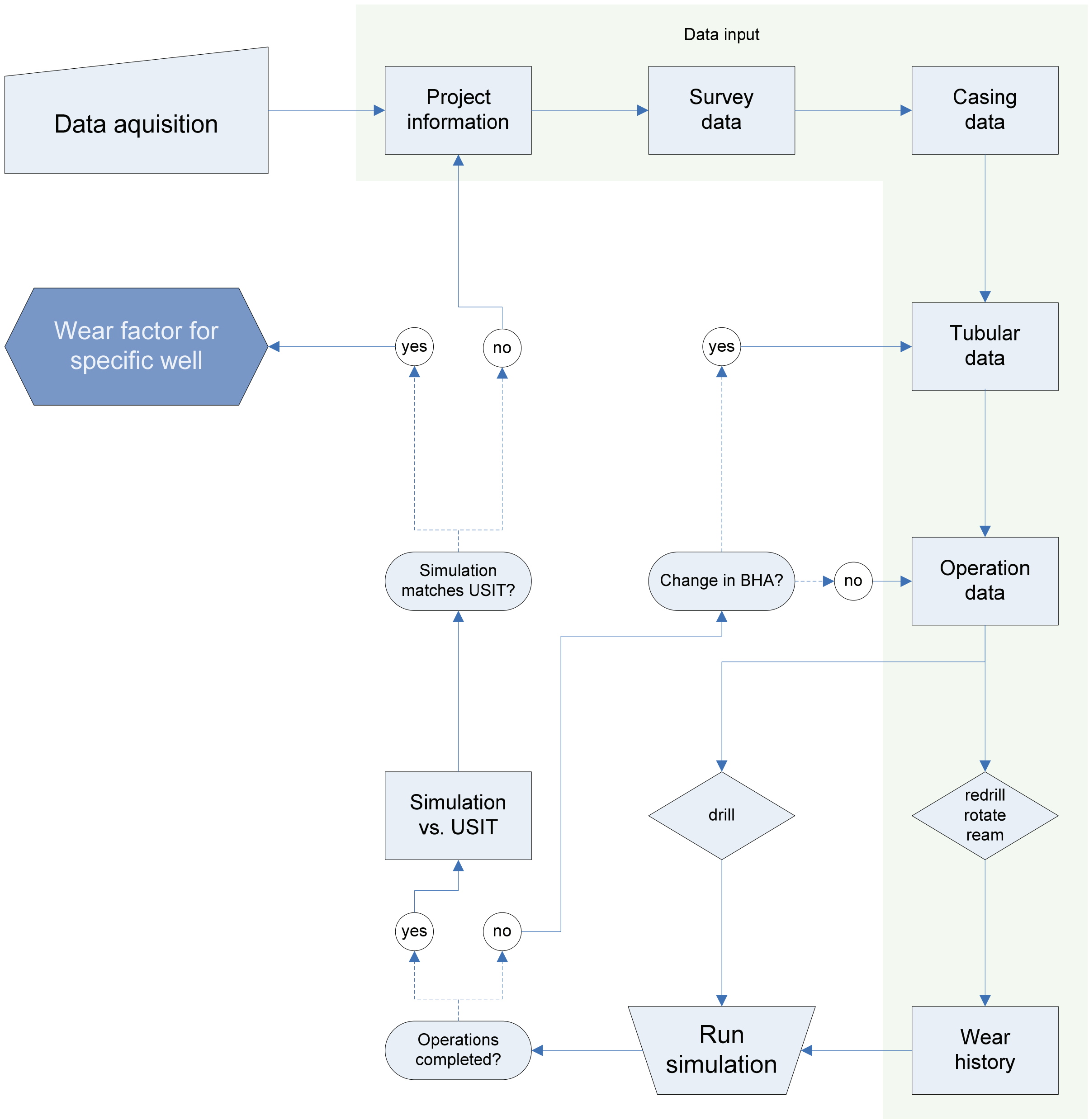

Figure 94: Simulation workflow

5.3 Results

After carrying out over 580 simulations on Gullfaks wells and matching them to existing USIT log curves and Schlumberger visual interpretation reports, a trend in the results can be clearly seen. As shown in the table below 15 Gullfaks wells have been USIT logged with a total of nearly 11,000 meters of usable log data.

Well	Comment	Logged section	Drilled	Logged
34/10 A-18	standard	9 5/8''	1988	18.03.2010
34/10 A-36C	production casing logged	7''	2009	05.01.2010
34/10 B-04B	production casing logged	4 1/2''	2007	03.06.2007
34/10 B-08	standard	9 5/8''	1989	15.01.2010
34/10 B-12	technical sidetrack	9 5/8''	1989	19.12.2007
34/10 B-14A T2	lateral	9 5/8''	1991	15.02.2009
34/10 B-24	standard	9 5/8''	1992	01.08.2010
34/10 B-28	standard	9 5/8''	1993	12.12.2009
34/10 B-35	production casing logged	9 5/8'' x 7''	1995	29.04.2010
34/10 B-37	production casing logged	7''	1997	08.04.2006
34/10 B-42B	production casing logged	7''	2002	27.02.2002
34/10 C-06A	logging directly after casing installation	10 3/4'' x 9 5/8''	2010	05.03.2010
34/10 C-06 T2	technical sidetrack	13 3/8''	1991	23.11.2009
34/10 C-10	production casing logged	7''	1992	18.09.2007
34/10 C-38 T2	technical sidetrack	10 3/4''	1999	10.02.2010

Table 15: Well overview

The resume of all this simulations can be found in the table below. Although these results are based on Gullfaks log data, it is possible to use this data as guideline values for wear simulations in other fields.

General wellpath	Drilling period	Mud type	Wear factor
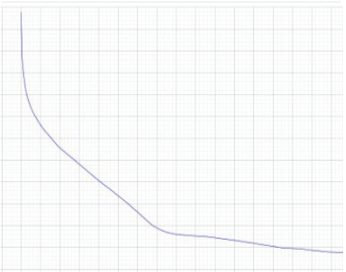	1987 - 1993	water based oil based	30 30
	1993 - 1997	water based oil based	13 5
	1997 - now	water based oil based	2 2
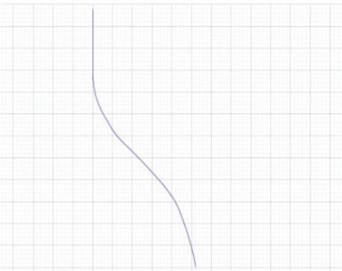	1987 - 1993	water based oil based	30 30
	1993 - 1997	water based oil based	13 5
	1997 - now	water based oil based	2 2

Table 16: Simulation results

As it can be clearly seen in the table above, the wear factor is not dependent on the general wellpath at all. Since most of the wear is accumulated in doglegs, it is more important to have a smooth trajectory than a specific shape.

This table also shows that the wear differs dramatically between three time periods. These represent the different hardbanding material used in Gullfaks over the years. Since not all drillpipes on all three platforms were replaced at once, this time period border can differ a little bit from platform to platform.

The green colour indicates that sufficient data material was available to make a high quality prediction. Unfortunately, only one well was available in the time period from 1993 to 1997. The results for this time span are based on this single simulation and on the laboratory test, which were carried out in the DEA-42 project.

In general these values are rather conservative, because it is necessary to be on the absolute safe side when results of wear simulations are used to calculate future maximum burst and collapse pressures.

5.4 Discussion on the analysis

This chapter deals with the problem and possible improvements, which came up during working on this thesis. Special attention is turned on the software package Cwear itself and its input data.

It has to be considered that this was a field analysis and that the qualities of the results are dependent on available data quality and quantity.

5.4.1 Cwear

5.4.1.1 Operation Limitations

To simplify the simulation process, the software Cwear has four predefined types of in hole operations.

- Drill
- Redrill
- Ream upwards
- Rotate off bottom

Modern drilling processes and complicated well paths often require more complex operations. Sometimes other operations can be expressed as one of the predefined four (e.g.: reaming downwards) but not all operations comply with this possibility.

In order to fit the software to complex simulations it would be necessary to eliminate the operation types completely and work with the initial raw data itself. The software could decide which operation is carried out, if the input data is accurate enough and compatible with the software.

5.4.1.2 Cwear workflow

To run a Cwear simulation it is necessary to run several little simulation steps one after another, depending on the predefined operations. This results in a total of up to 100 runs per casing section.

As discussed in previous chapters Cwear uses a value called wear factor to establish a connection between the wear and the material properties. If changing this property, drillpipe configuration or any other detail, this will mean that all the simulations have to be repeated.

A possible advancement would be to combine all the little simulations into one, which can be adapted as required. This would save a lot of time, and allow doing various simulations even with a small variation of input parameters to plan for every uncertainty.

5.4.1.3 Input data

A simulation can only be as good as the initial data. Most of the simulations input data is based on hand-written daily drilling reports. Depending on how accurate the drilling supervisor recorded ongoing operations, the accurate is the simulation. Although the source data is not very exact, it would not make sense to split the initial data into a finer resolution, because the software could not handle it.

The computer program needs various sets of data (measured depth, ROP, rmp, WOB) to calculate the casing wear. If it is possible to feed the software with input files, coming from real time data recording, it would be possible to calculate wear directly from this file. Using the information about bit position, WOB, rpm and time, very accurate wear computation can be done.

This will approach will lead to the next level in wear simulation and monitoring.

5.4.1.4 Wear history

Cwear has the function to use three different wear factors for one single simulation, which is very practicable to simulate a high, low and base case. But when a second simulation is run after the first one, that should take the previous wear into account, only one case can be chosen as initial values.

It would be necessary to succeed the following base case simulation on the base case, the following low case on the low case and the following high case on the high case, to simulate a well with three different wear factors

5.4.2 USIT logs

In general the USIT log data were of good quality, although some problems with tool eccentricity occurred. This had no big impact on the actual comparison itself because the measurement of the wall thickness is not dependent on tool centralisation. This is discussed in a previous chapter.

Never the less the confirmation, whether it is wear or corrosion, would be easier if the tool is accurately centralized.

5.4.3 Uncertain drilling parameters

As discussed in a previous chapter it is difficult to collect all the drilling related data from a well, drilled in the eighties. With the help of experienced drilling engineers and old drilling reports most of the uncertainties were uncovered.

5.4.3.1 Comparison measured and reported operations

Basically wear is directly proportional to one major influence factor, the number of rotations of the drillstring in the casing. As discussed in previous chapters, this number is calculated from duration and rpm data, read from the daily drilling report.

From	To	Duration [h]	Start Hole MD [m]	Code	Description
Oct-24 00:00	Oct-24 03:30	3.5	4099.5	DDDU	Drilled 8 3/8" x 9 1/4" hole from 4099,5 m to 4129 m with 1380 lpm/ 150 bar/ 150 rpm/ 15-17 kNm/ 0-3 Ton WOB . Back reamed single from 4129 m to 4119 m. ROP 9 -13 m/h. ECD 1-828 sg - 1,857 sg. MW out 1,74+ sg. Max gas 0,4%.
Oct-24 03:30	Oct-24 06:00	2.5	4129	DDDU	Drilled 8 3/8" x 9 1/4" hole from 4129 m to 4150 m with 1380 lpm/ 151 bar/ 150 rpm/ 15-17 kNm/ 0-3 Ton WOB . ROP 9 -13 m/h. ECD 1,82 sg - 1,853 sg. MW out 1,74+ sg. Max gas 0,4%.
Oct-24 06:00	Oct-25 00:00	18	4150	DDDU	Drilled 8 3/8" x 9 1/4" hole from 4150 m to 4299,5 m with 1380 lpm/ 152 bar/ 150 rpm/ 16-17 kNm/ 0-3 Ton WOB. ROP 11 m/h. ECD 1,833 sg-1,852 sg. MW out 1,75 sg. Max gas 0,3%.

Table 17: DBR report [23]

This typical DBR report shows that, although all information needed to calculate the necessary data is included, the event resolution is much too high. When 18 hours of drilling are put down in the daily report, nothing is mentioned about times of no string rotation (e.g.: connection times, RIH, POOH, …)

With modern data monitoring and analysing software it is possible to determine the number of rotations very exactly. For this purpose an, in 2009 drilled, example well, 34/10-A36 A, was chosen to compare the number of rotations calculated from DBR and the number of rotation from sensor data. The total sensor data set, containing time, rpm and WOB with a time resolution of 10 seconds, was provided by TDE.

In the figure below 24 hours of drilling, split up into the different operations, can be seen. Now it can be observed, what is described in DBR by 18 hours of drilling is in reality a bit less. But this can result in major differences in number of rotations when drilling, like in this example, with 150 rpm.

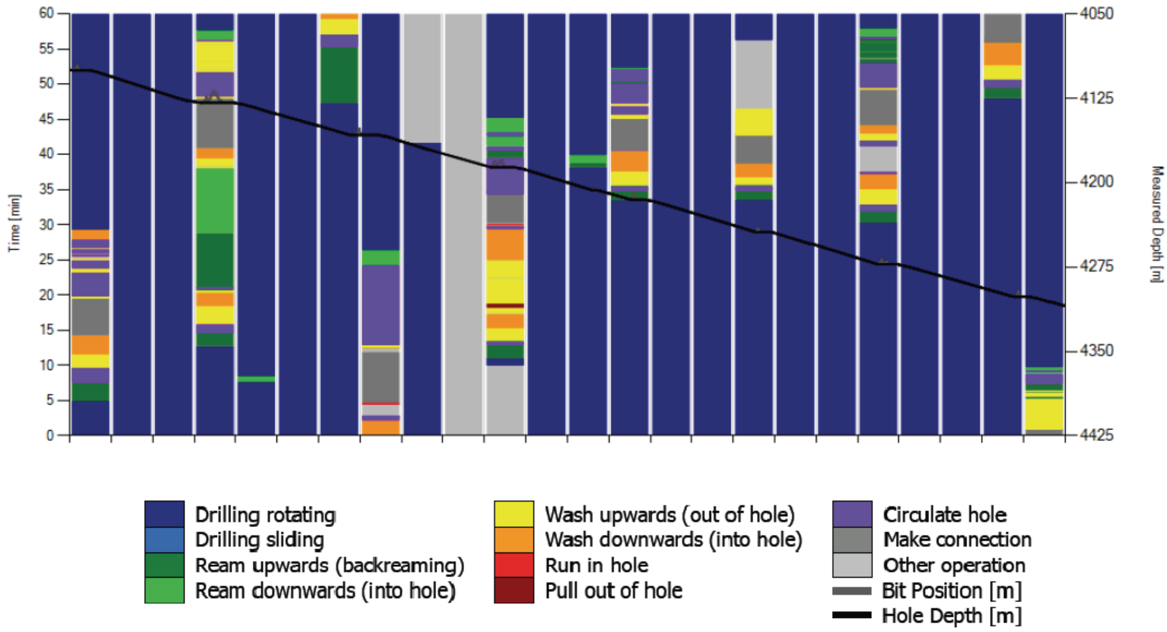

Figure 95: Equivalent proNova TxD – KPI – operation report [23]

By comparing the total drilling time of well 34/10-A36A a difference of 13 % from the DBR number of rotations to the sensor number of rotations occur. That means that the total number of rotations in the casing is just 87% of the assumed number. This would result in a necessary correction of the wear factors in the simulations if sensor data is used.

The figure below shows the 24 hours split up into different operations.

Color	Operation	[hh:mm]	[%]
	Drilling rotating	18:36	77.48%
	Drilling sliding	00:00	0.00%
	Ream upwards (backreaming)	00:35	2.43%
	Ream downwards (into hole)	00:20	1.38%
	Wash upwards (out of hole)	00:41	2.88%
	Wash downwards (into hole)	00:29	2.02%
	Run in hole	00:00	0.03%
	Pull out of hole	00:01	0.05%
	Circulate hole	00:51	3.55%
	Make connection	00:44	3.03%
	Other operation	01:43	7.16%
	Sum	**24:00**	**100.00%**

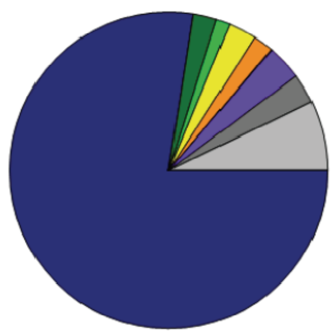

Figure 96: proNova time break down [23]

6 Conclusion

Casing wear is an often underestimated problem in modern planning and drilling of wells. Especially in offshore platform drilling, where limited slots on templates are available, it is necessary to use already existing casing sections to sidetrack new wells and reach new, productive areas of the reservoir.

To get a better understanding and a possible magnitude of this problem, software packages are often used to predict the abrasion.

The aim of this thesis was to give a general overview of the existing wear mechanisms, use of logging measurements and logged wells in the Gullfaks field, to come up with a relevant casing wear model for these boreholes.

This work proves, that it is possible to precisely simulate and predict wear if the raw data is of good quality. This prediction is vital for well integrity issues when an old casing (wellbore) is reused. A few interesting observations will be mentioned here:

- Adding ether sand or barite to a downhole system will reduce wear significantly. As a consequence of this drill cuttings in the mud may also reduce casing wear.
- For even better results it would be advisable to measure the initial casing thickness before the joints are installed to eliminate the possibility of taking manufacturing margins as real wear.
- Casing wear is not dependent on the tooljoint length but on the diameter.

The outcome is a set of simulation parameters which consider the special circumstances on Gullfaks. These parameters were developed with close consideration of the already conducted USIT log measurements in the wellbores. Further investigations showed that it might be possible to predict casing wear on analogical fields with similar well designs.

This thesis clearly showed the weaknesses and limitations of existing casing wear prediction software packages and resulted in the statement, that there is no accurate software for this purpose on the market. Since there is a need for precise monitoring and simulation of casing wear in the future, a simulator, fed by real-time data, would be the next logical step.

7 Nomenclature

BHA	Bottom hole assembly
CET	Cement evaluation tool
DC	Drillcollar
DP	Drillpipe
FFT	Fast Fourier transform
ID	Inside diameter
LWD	Logging while drilling
MA	Moving average
MD	Measured depth
MWD	Measuring while drilling
OBM	Oil based mud
OD	Outside diameter
POOH	Pull out of hole
Rc	Rockwell hardness
RIH	Run in hole
RPM	Rotations per minute
ROP	Rate of penetration
THMN_RF	Minimum unflagged casing thickness
TVD	Total vertical depth
USIT	Ultra sonic imaging tool
WBM	Water based mud
WF	wear factor
WOB	Weight on bit

Units:

[bbl]	Barrel
[ft]	Foot
[hr]	Hour
[Hz]	Hertz
[in]	Inch
[kg]	Kilogram
[lb]	Pound
[lbf]	Pound force
[m]	Meter
[min]	Minute
[ppg]	Pounds per gallon
[psi]	Pound per square inch
[sg]	Specific gravity
[t]	Metric ton

8 References

[1] Statoil ASA: **Facts about Gullfaks.**
http://www.statoil.com/en/OurOperations/ExplorationProd/ncs/Gullfaks/Pages/default.aspx - date: 28.09.2010

[2] Statoil ASA: **Gullfaks Blend.**
http://www.statoil.com/en/OurOperations/TradingProducts/CrudeOil/Crudeoilassays/Pages/GullfaksBlend.aspx - date: 28.09.2010

[3] Statoil ASA: **Reservoir management plan for the Gullfaks field ad Gullfaks satellites – reservoir description.** Bergen, 2007

[4] Russel, Hall; Garsaki, Ali; Deskins, Greg; Vozniak, John: **Recent Advances in Casing Wear Technology.** Maurer Engineering, Houston, Texas, 1994

[5] Russel, Hall: **Simplified wear groove calculations.** Maurer Engineering, Houston, Texas, 1998

[6] Williamson, J.S.: Casing wear: **The effect of contact pressure.** SPE 10236. Society of Petroleum Engineers Inc., Richardson, Texas, 1985.

[7] Maurer Engineering: **Casing Wear Technology DEA-42 Phase I to V.** Houston, Texas, 2000.

[8] Stachowiak, W. Gwidon; Batchelor, W. Andrew: **Engineering Tribology.** Department of Mechanical and Materials Engineering, University of Western Australia, Elsevier, 2005

[9] Bourgoyne, Adam T.; Millheim, Keith K.; Chenevert, Martin E.; Young F.S.: **Applied Drilling Engineering – Second Printing.** Society of Petroleum Engineers Inc., Richardson, Texas, 1991.

[10] Lubinsky, A.; Williamson, A.S.: **Usefulness of Steel or Rubber Drillpipe Protectors.** SPE 11381, Society of Petroleum Engineers Inc., Richardson, Texas, 1983.

[11] Fontenot, J.E; Mc Ever, J.W.: **Casing wear – 2. Tripping is not a key cause of casing wear.** Oil and Gas Journal, January, 1975.

[12] Bradley, W.B.: **Reducing casing wear – 2. How wear affects burst strength.** Oil and Gas Journal, January, 1976.

[13] Schlumberger: **USIT Log features – USIT Microdebonding.** JP Version 1. Houston, Texas, 2003

[14] Bettis, F.E.; Crane II, L.R.; Schwanitz, B.J.; Cook, M.R.: **Ultrasound Logging in Cased Boreholes Pipe Wear.** SPE 26318. Society of Petroleum Engineers Inc., Richardson, Texas, 1993.

[15] Schlumberger: **Ultrasonic Imaging handbook.** Houston, Texas, 1993

[16] Maurer Engineering: **Cwear help manual.** Texas

[17] Johancsik, C.A.: **Torque and Drag in Directional Wells – Prediction and Measurement.** SPE 11380, Society of Petroleum Engineers Inc., Richardson, Texas, 1984.

[18] Popov, E.P.: **Mechanics of Materials.** Prentice-Hall Inc., New York, NY, 1976.

[19] API Bulletin 5C3: **Formulas and Calculations for Casing, Drill Pipe and Line Pipe Properties.** API, Washington, 1989.

[20] Song, J.Z.: **The Internal Pressure Capacity of Crescent-Shaped Wear Casing.** IADC/SPE 23902, Society of Petroleum Engineers Inc., Richardson, Texas, 1992.

[21] Estrada P.: **Well integrity from USIT, CBL/VDL report of 34/10 B-28.** Schlumberger, 2009.

[22] Arnco Technology Trust LTD.: **Arnco Hardbanding Specification, Version 1.1.** Houston Texas, 2009.

[23] Thonhauser Data Engineering GmbH.: **ProNova TxD – KPI operation report 34/10-A-36 A**. Leoben, 2010.

[24] Formoso-Rafferty, R.: **Well integrity from USIT, CBL/VDL report of 34/10 B-14AT3.** Schlumberger, 2009.

Appendix A: Input for Example well 34/10 B-14A T3

In the following chapter, one of the simulated Gullfaks wells is presented as an example for the workflow.

The well 34/10 B-14A was kicked off and drilled from existent well 34/10 B-14 in the north shaft of Gullfaks B, through slot 15, just beneath 9 5/8’’ casing shoe. Many technical drilling problems occurred while drilling the 8 1/2’’ section. The problems started by loosing all three cones of the bit. A 100m cement plug was then set above and a technical sidetrack was drilled.

After continuing drilling the 8 1/2’’ section the lower part of the BHA was lost in the hole but could be recovered by fishing operations. But it was impossible to drill further due to an obstruction at 3649 m MD. A milling run was done, but without any success. Suspected that one or two casing joints were twisted off, the well was then plugged back again. And a new sidetrack was drilled.

The well name 34/10 B-14A T3 indicates that it is the second technical sidetrack of the well 34/10 B-14A, which is a sidetrack of the initial well 34/10 B-14.

The well was planned to be drilled in 33 days, including completion and plug back of the 6’’ hole. Actual drilling time was 69 days.

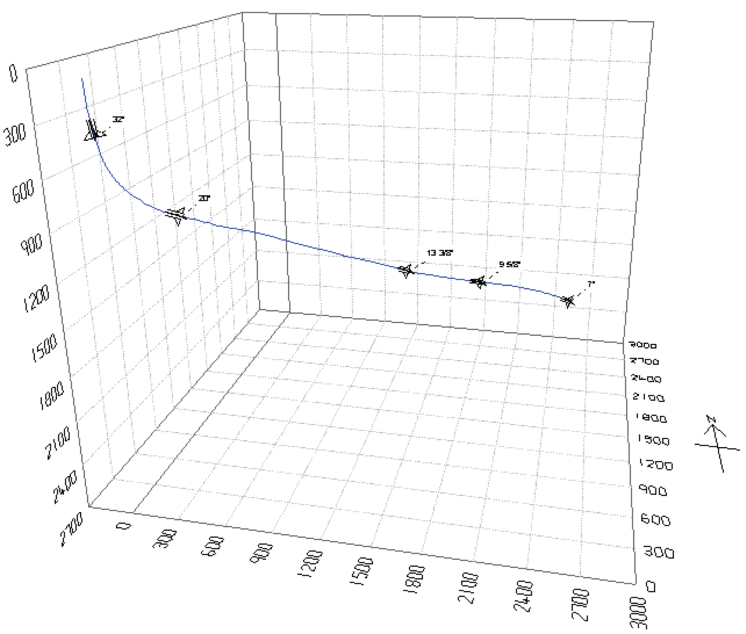

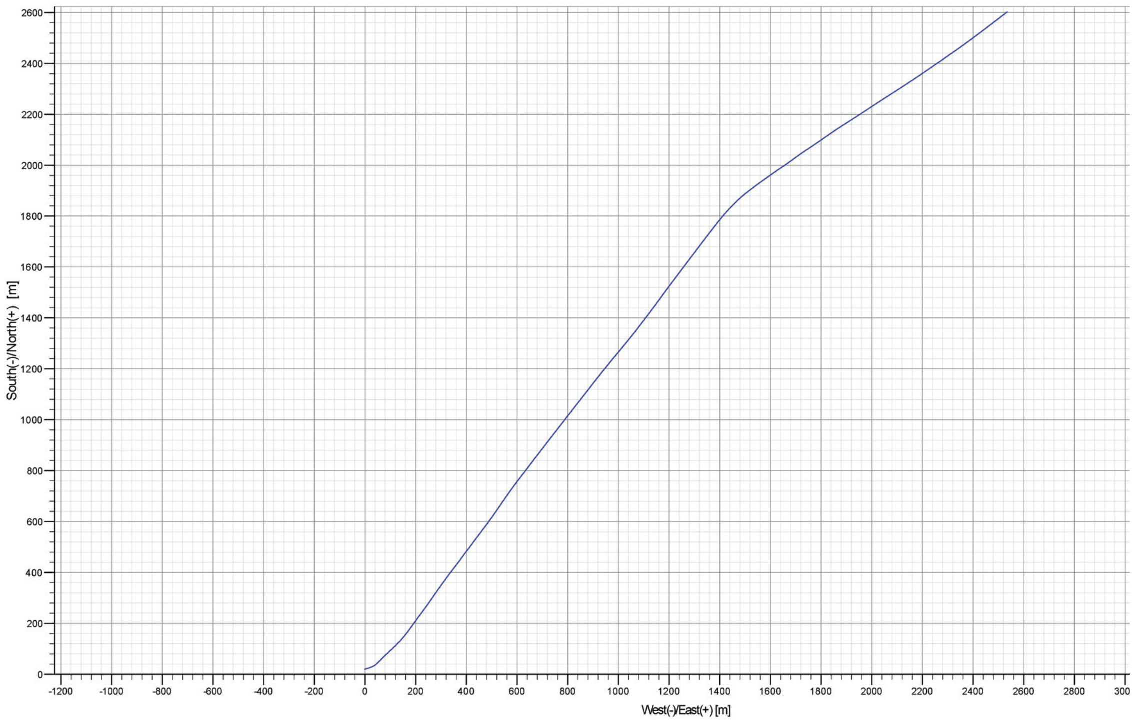

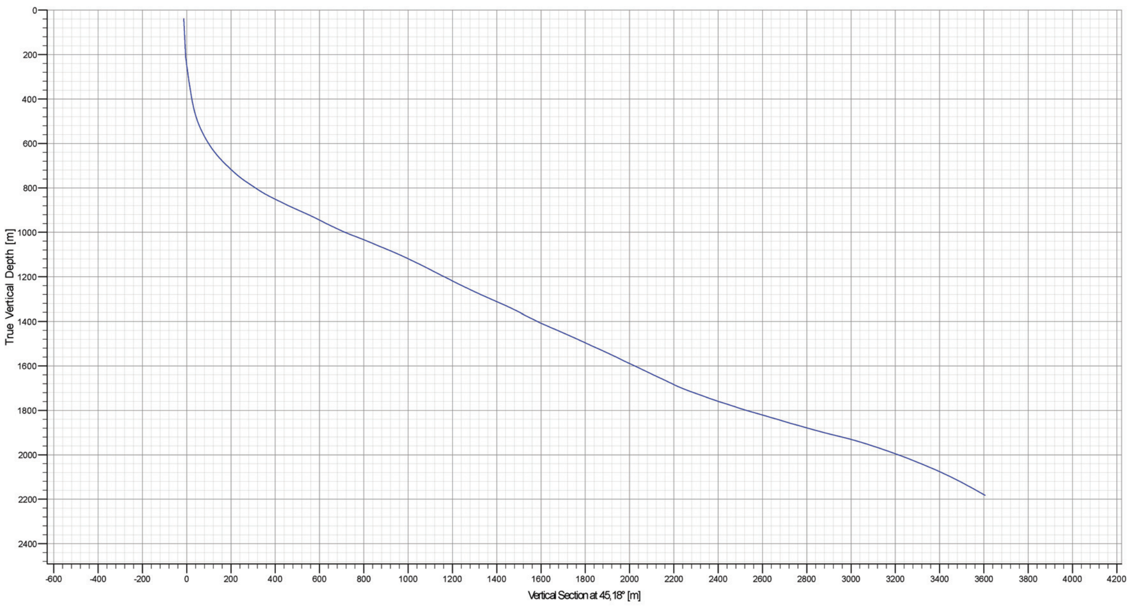

Figure 97: 30/10 B-14A T3 wellpath

Date	Operation	Starting depth	End depth	Duration	ROP	RPM	WOB	Rotations	Cumulative rotations
		[m]	[m]	[hr]	[m/hr]	[rpm]	[t]	[]	[]
WBM:1,68 SG									
19.02.1991	MU BHA 1								
	RIH								
	Drilling	3792	3828	4,5	8	100	8	27000	27000
	Circulation	3828	3828	1,5	0	80	0	7200	34200
Change to OMB: 1,64 SG									
	Circulation	3828	3828	1,5	0	80	0	7200	41400
	Drilling	3828	3832	1	4	120	8	7200	48600
	Drilling	3832	3835	1	3	120	8	7200	55800
	Drilling	3835	3868	4	8	120	8	28800	84600
	Circulation	3868	3868	1,5	0	80	0	7200	91800
	POOH								
21.02.1991	MU BHA 2								
	RIH								
	Drilling	3868	3913	4	11	120	8	28800	120600
	Drilling	3913	4201	18	16	120	8	129600	250200
	Drilling	4201	4303	5,5	19	120	8	39600	289800
	Circulation	4303	4303	1,5	0	80	0	7200	297000
	Drilling	4303	4450	9,5	15	120	8	68400	365400
	Circulation	4450	4450	2	0	80	0	9600	375000
	Backreaming	4450	3700	5,5	-136	170	0	56100	431100
	Circulation	3700	3700	1	0	80	0	4800	435900
	RIH								
	Drilling	4450	4532	3,5	23	120	8	25200	461100
	Circulation	4532	4532	2	0	80	0	9600	470700
	Backreaming	4532	3657	5	-175	170	0	51000	521700
	Circulation	3657	3657	2	0	80	0	9600	531300
	RIH								
	Circulation	4532	4532	2	0	80	0	9600	540900
	Backreaming	4532	3500	5,5	-188	170	0	56100	597000
	Backreaming	3500	1970	5	-306	170	0	51000	648000
	Circulation	1970	1970	2,5	0	80	0	12000	660000
	POOH								
28.02.1991	MU BHA 3								
	RIH								
	Reaming	3390	3714	4	81	80	0	19200	679200
	POOH								
01.03.1991	MU BHA 4								
	RIH								
	Reaming	3714	4474	6,5	117	80	0	31200	710400
	POOH								

Table 18: 30/10 B-14A T3 operational parameters

The table above shows the summary of operations through the 9 5/8'' casing. It is vital to know the BHA components as shown in the figures below to run adequate simulations.

String component	Supplier	OD inch	ID inch	Length m	Acclength m
BIT, PDC/DIAM		8,500		0,34	0,34
BIT SUB		6,750	2,750	0,50	0,84
STABILIZER, NM		8,500	2,750	2,61	3,45
DRIL COL, NM		6,750	2,750	4,59	8,04
STABILIZER, NM		8,375	2,750	2,01	10,05
OTHER		6,750		0,61	10,66
XO SUB		6,750	2,750	0,53	11,19
RLL MWD TOOL		6,750		9,48	20,67
MWD TOOL,LOW FLOW		6,750		6,25	26,92
FLOAT SUB		6,750	2,750	0,60	27,52
STABILIZER, NM		8,500	2,750	2,01	29,53
DRIL COL, NM		6,750	2,750	19,06	48,59
H W DRILL PIPE		5,000	3,000	54,32	102,91
JAR		6,250	2,250	10,17	113,08
H W DRILL PIPE		5,000	3,000	135,98	249,06

Figure 98: 30/10 B-14A T3 BHA I

String component	Supplier	OD inch	ID inch	Length m	Acclength m
BIT, PDC/DIAM		8,500		0,34	0,34
BIT SUB		6,750	2,750	0,50	0,84
STABILIZER, NM		8,500	2,750	2,61	3,45
DRIL COL, NM		6,750	2,750	4,59	8,04
STABILIZER, NM		8,375	2,750	2,01	10,05
OTHER		6,750		0,61	10,66
XO SUB		6,750	2,750	0,53	11,19
RLL MWD TOOL		6,750		9,48	20,67
MWD TOOL,LOW FLOW		6,750		6,25	26,92
FLOAT SUB		6,750	2,750	0,60	27,52
STABILIZER, NM		8,500	2,750	2,01	29,53
DRIL COL, NM		6,750	2,750	19,06	48,59
H W DRILL PIPE		5,000	3,000	54,32	102,91
JAR		6,250	2,250	10,17	113,08
H W DRILL PIPE		5,000	3,000	135,98	249,06

Figure 99: 30/10 B-14A T3 BHA II

String component	Supplier	OD inch	ID inch	Length m	Acc length m
BIT, CONVENTIONAL		6,000		0,18	0,18
SCRAPER		7,000	1,250	0,75	0,93
BIT SUB		4,750	2,250	0,91	1,84
STABILIZER		5,875	2,250	1,90	3,74
DRIL COL		4,750	2,250	112,44	116,18
DRILL PIPE		3,500	2,125	642,49	758,67
OTHER		6,250	2,625	2,15	760,82
BIT SUB				0,87	761,69
H W DRILL PIPE		5,000	3,000	18,34	780,03
JAR		6,250	2,250	10,17	790,20
H W DRILL PIPE		5,000	3,000	165,06	955,26

Figure 100: 30/10 B-14A T3 BHA III

The USIT log needs to be processed by removing the peaks resulted from the connections and smoothing the log curve itself by using a filter. The differences between the processed and the unprocessed USIT log curve can be clearly seen in the figure below.

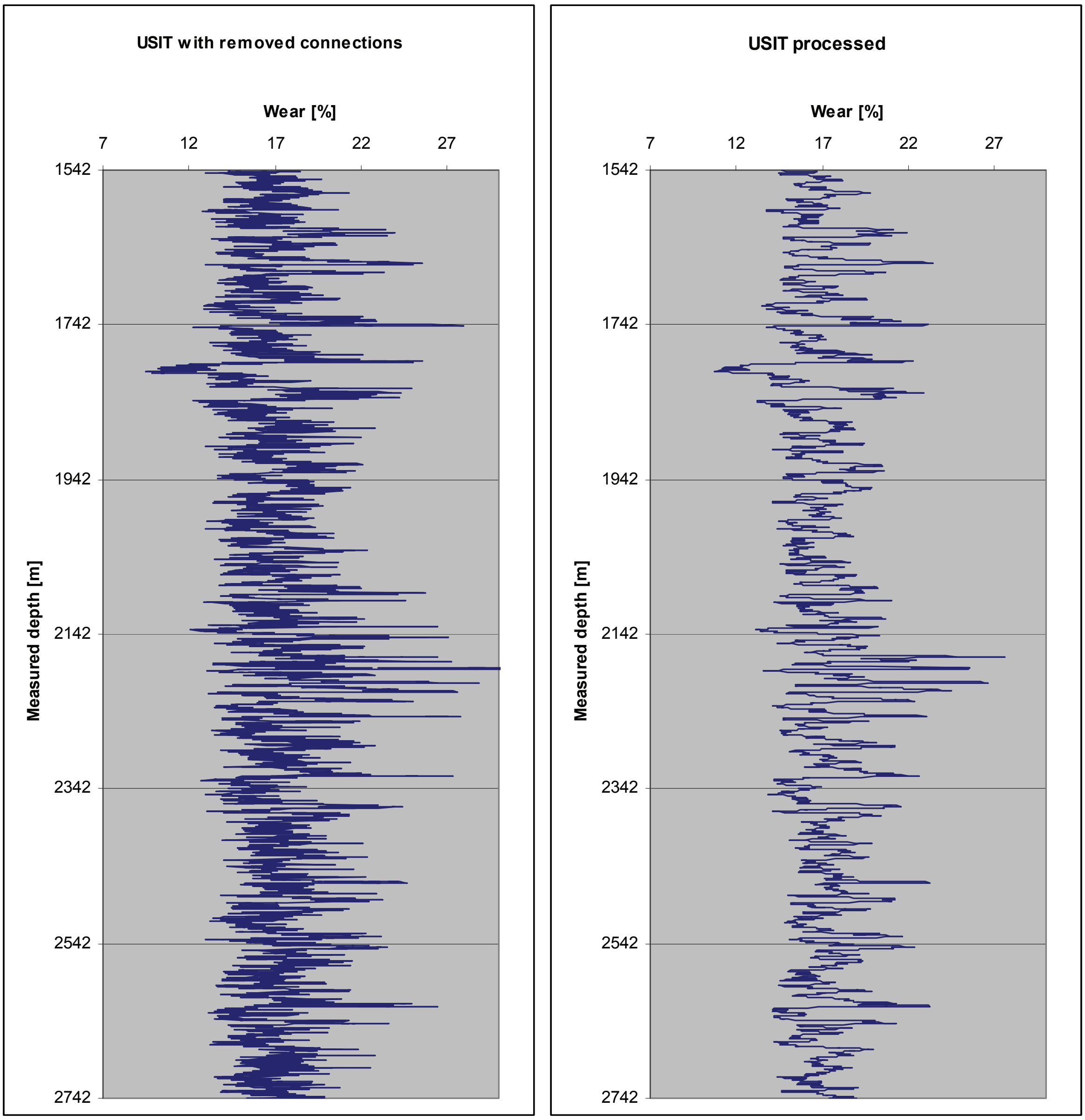

Figure 101: 30/10 B-14A T3 original and cleaned USIT log

Appendix B: Results for Example well 34/10 B-14A T3

The simulation matching is very time consuming at the beginning, because it is necessary to try different wear factors to find the best suitable. After starting with a wear factor of 9, other simulations with WF of 12, 20 and 30 were carried out. The results can be found in the figures below.

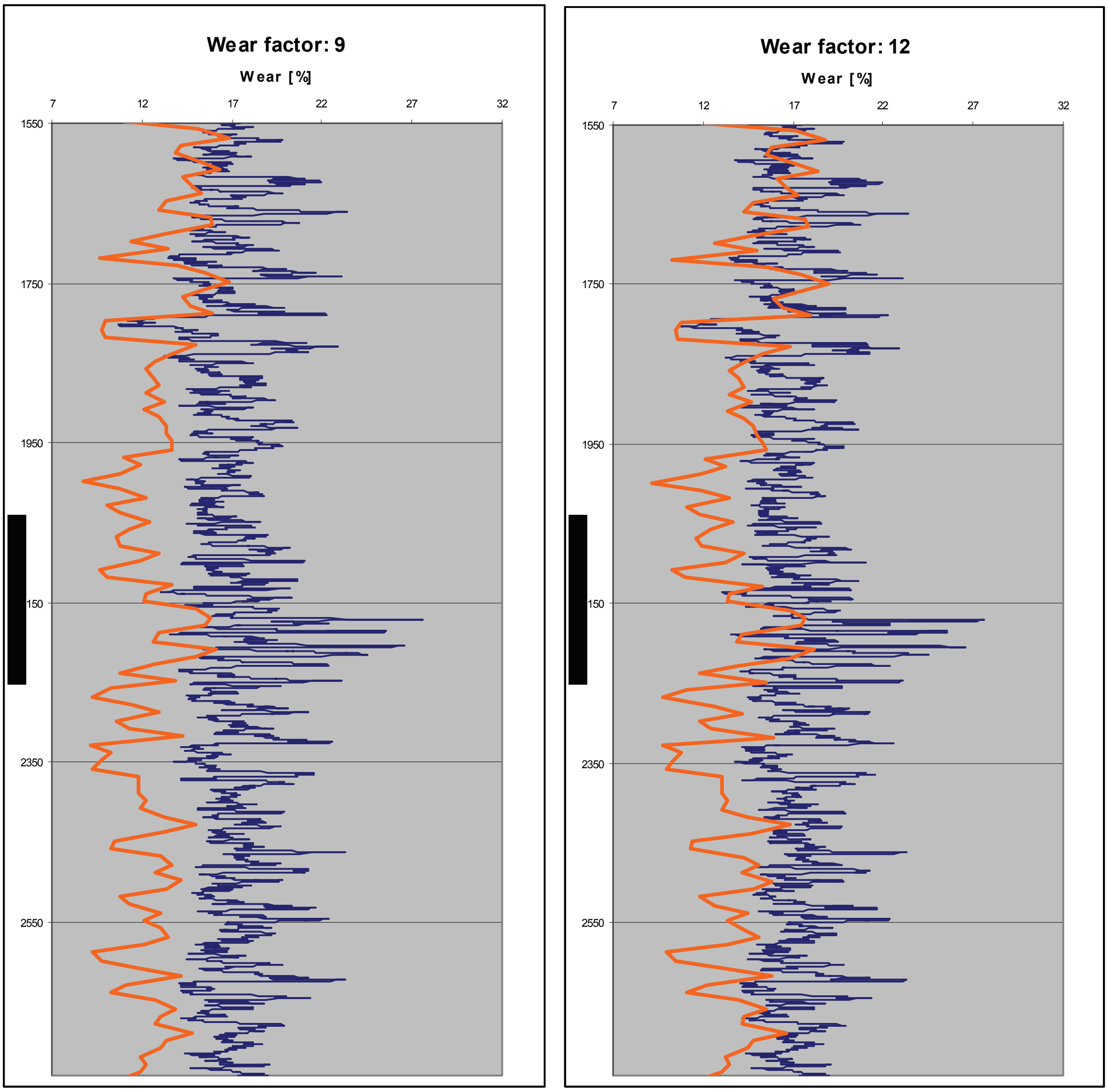

Figure 102: 30/10 B-14A T3 simulations WF 9 and 12

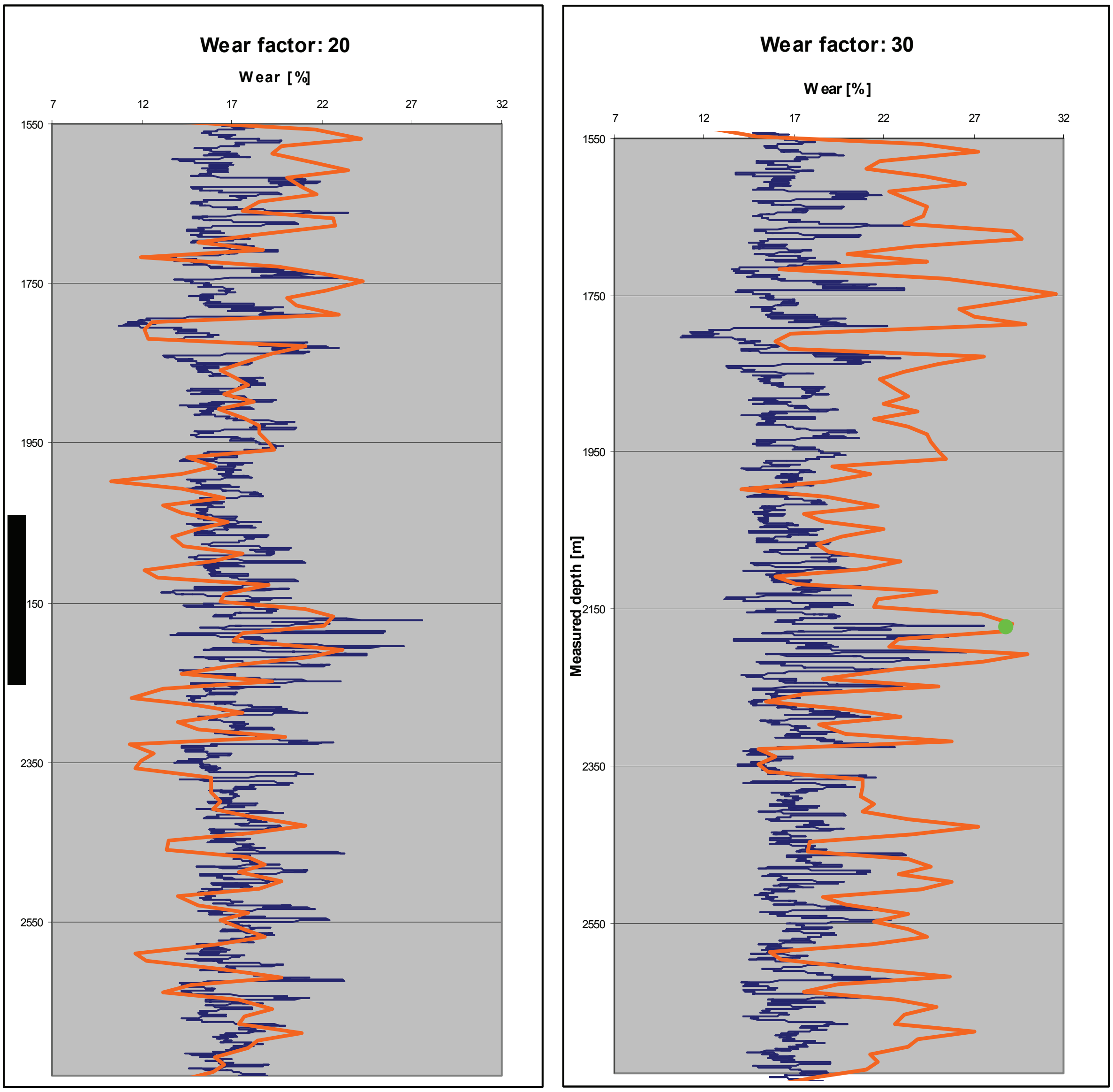

Figure 103: 30/10 B-14A T3 simulations WF 20 and 30

It can be observed that the trend is starting to match with wear factor 20. But there are still many peaks exceeding the simulation. With a wear factor of 30 a good overall coverage of the simulation is achieved. In addition to that the Schlumberger log interpretation of visual maximum wear was indicated by a green dot. This visual interpretation matches exactly the simulated wear.

Schlumberger log interpretation

The logged interval appears to be dominated by the presence of a groove. The groove orientation is not clear as the USIT images are not oriented, but this kind of damage is more likely to have developed towards the low side of the casing. It can be identified at the edges of the thickness image below.

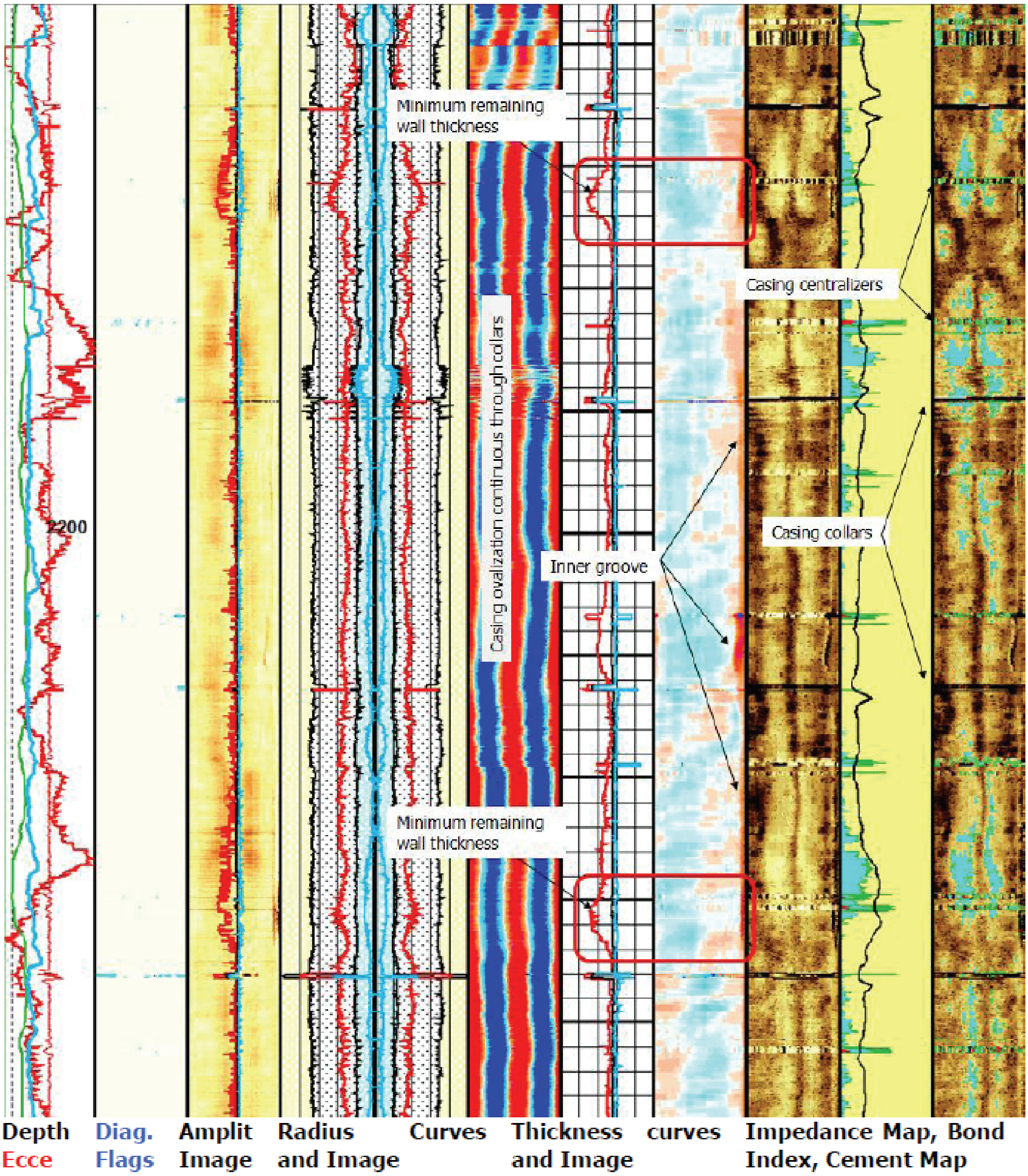

Figure 104: 30/10 B-14A T3 Schlumberger log interpretation [24]

The minimum remaining wall thickness is around 0.34 inch at 2186 metres and 2215 metres. This relative reduction is a combination of manufacturing effects, wear and internal corrosion. This figure translates to a penetration of 29.17% with respect to theoretical nominal dimensions. It should be noted that wear is most serious in absolute terms where it has occurred across areas of pipe wall which was already relatively thin due to the manufacturing process.

The dominant red/blue/red/blue pattern which is evident on the radius image throughout most of the logged interval may be indicative of minor cross sectional pipe distortion in the form of ovality (i.e. a long axis perpendicular to a short axis). The condition must have developed with the pipe in-situ (or during the pipe running procedure) as it can be seen to be continuous through collars. Although the effect is not considered serious in terms of overall pipe integrity it should be taken into account when planning the passage of large diameter hardware and/or packer/whipstock setting within these intervals.

Appendix C: Cwear output for Example well 34/10 B-14A T3

Description Tables

Project Description	
Well	B14AT3
Project	Master thesis Bindl Benedikt
Company	Statoil
Field	Gullfaks
Location	
Date	17.08.2010 08:42:07
Comments	simulation run 4
Input File	\\be-fsB\homeB\BEBIN\Statoil Documents\master thesis\wells\B14A\simulations\run 4\simulation run 4-20.CR7
System of Units	Custom
Operating Mode	Redrill

Table 19: 30/10 B-14A T3 project description

General Data	
Maximum Survey MD	4532,00 (m)
Tool Joint OD	6,625 (in)
Tool Joint Contact Length	25,000 (in)
Drill Pipe Joint Length	13,72 (m)
Max. Lateral Load per Protector	0,0000 (T[metric])
Max. Lateral Load per Tool Joint	0,0000 (T[metric])
Offset Angle	0,00 (deg)
Depth	0,00 (m)
Burst and Collapse Calculation Using	API Equation
Operating Mode	Redrill
Start MD	3714,00 (m)
End MD	4474,00 (m)
Single Wear Factor	30 (E-10/psi)

Table 20: 30/10 B-14A T3 general data

Data Tables

Tabulated Results (Redrill)								
Measured Depth (m)	Wall Thickness (in)	WF Base Rem. Wall (in)	WF Base Wear %	WF Low Rem. Wall (in)	WF Low Wear %	WF High Rem. Wall (in)	WF High Wear %	Pipe Protectors Required
0,00	0,545	0,545	0,0	0,545	0,0	0,545	0,0	0
30,00	0,545	0,545	0,0	0,545	0,0	0,545	0,0	0
39,10	0,545	0,545	0,0	0,545	0,0	0,545	0,0	0
60,00	0,545	0,403	26,1	0,403	26,1	0,403	26,1	0
90,00	0,545	0,403	26,1	0,403	26,1	0,403	26,1	0
120,00	0,545	0,399	26,7	0,399	26,7	0,399	26,7	0
150,00	0,545	0,394	27,7	0,394	27,7	0,394	27,7	0
180,00	0,545	0,387	29,0	0,387	29,0	0,387	29,0	0
210,00	0,545	0,379	30,4	0,379	30,4	0,379	30,4	0
214,55	0,545	0,374	31,4	0,374	31,4	0,374	31,4	0
224,64	0,545	0,462	15,1	0,462	15,1	0,462	15,1	0
234,74	0,545	0,470	13,7	0,470	13,7	0,470	13,7	0
240,00	0,545	0,485	11,0	0,485	11,0	0,485	11,0	0
244,84	0,545	0,485	11,0	0,485	11,0	0,485	11,0	0
254,95	0,545	0,467	14,3	0,467	14,3	0,467	14,3	0
265,06	0,545	0,443	18,7	0,443	18,7	0,443	18,7	0
270,00	0,545	0,473	13,2	0,473	13,2	0,473	13,2	0
275,18	0,545	0,473	13,2	0,473	13,2	0,473	13,2	0
285,30	0,545	0,502	7,9	0,502	7,9	0,502	7,9	0
295,43	0,545	0,467	14,3	0,467	14,3	0,467	14,3	0
300,00	0,545	0,457	16,1	0,457	16,1	0,457	16,1	0
305,56	0,545	0,457	16,1	0,457	16,1	0,457	16,1	0
315,69	0,545	0,460	15,6	0,460	15,6	0,460	15,6	0
325,83	0,545	0,468	14,2	0,468	14,2	0,468	14,2	0
330,00	0,545	0,475	12,9	0,475	12,9	0,475	12,9	0
335,98	0,545	0,475	12,9	0,475	12,9	0,475	12,9	0
346,12	0,545	0,459	15,8	0,459	15,8	0,459	15,8	0
356,27	0,545	0,423	22,4	0,423	22,4	0,423	22,4	0
360,00	0,545	0,437	19,8	0,437	19,8	0,437	19,8	0
366,40	0,545	0,437	19,8	0,437	19,8	0,437	19,8	0
376,54	0,545	0,441	19,0	0,441	19,0	0,441	19,0	0
386,68	0,545	0,424	22,2	0,424	22,2	0,424	22,2	0
390,00	0,545	0,412	24,3	0,412	24,3	0,412	24,3	0
396,83	0,545	0,412	24,3	0,412	24,3	0,412	24,3	0
407,00	0,545	0,403	26,1	0,403	26,1	0,403	26,1	0
417,19	0,545	0,382	30,0	0,382	30,0	0,382	30,0	0
420,00	0,545	0,376	31,1	0,376	31,1	0,376	31,1	0
427,39	0,545	0,376	31,1	0,376	31,1	0,376	31,1	0
437,63	0,545	0,376	31,1	0,376	31,1	0,376	31,1	0
447,90	0,545	0,367	32,7	0,367	32,7	0,367	32,7	0
450,00	0,545	0,366	32,9	0,366	32,9	0,366	32,9	0
458,20	0,545	0,366	32,9	0,366	32,9	0,366	32,9	0
468,55	0,545	0,357	34,5	0,357	34,5	0,357	34,5	0
478,95	0,545	0,346	36,6	0,346	36,6	0,346	36,6	0
480,00	0,545	0,341	37,4	0,341	37,4	0,341	37,4	0
489,42	0,545	0,343	37,1	0,343	37,1	0,343	37,1	0
499,96	0,545	0,335	38,5	0,335	38,5	0,335	38,5	0
510,00	0,545	0,331	39,3	0,331	39,3	0,331	39,3	0

Tabulated Results (Redrill)								
Measured Depth (m)	Wall Thickness (in)	WF Base Rem. Wall (in)	WF Base Wear %	WF Low Rem. Wall (in)	WF Low Wear %	WF High Rem. Wall (in)	WF High Wear %	Pipe Protectors Required
510,60	0,545	0,332	39,1	0,332	39,1	0,332	39,1	0
521,33	0,545	0,332	39,1	0,332	39,1	0,332	39,1	0
532,17	0,545	0,333	39,0	0,333	39,0	0,333	39,0	0
540,00	0,545	0,347	36,4	0,347	36,4	0,347	36,4	0
543,12	0,545	0,347	36,2	0,347	36,2	0,347	36,2	0
554,18	0,545	0,367	32,7	0,367	32,7	0,367	32,7	0
565,35	0,545	0,377	30,8	0,377	30,8	0,377	30,8	0
570,00	0,545	0,385	29,3	0,385	29,3	0,385	29,3	0
576,63	0,545	0,386	29,2	0,386	29,2	0,386	29,2	0
588,01	0,545	0,390	28,4	0,390	28,4	0,390	28,4	0
599,50	0,545	0,392	28,0	0,392	28,0	0,392	28,0	0
600,00	0,545	0,386	29,2	0,386	29,2	0,386	29,2	0
611,12	0,545	0,387	29,0	0,387	29,0	0,387	29,0	0
622,89	0,545	0,370	32,1	0,370	32,1	0,370	32,1	0
630,00	0,545	0,351	35,6	0,351	35,6	0,351	35,6	0
634,84	0,545	0,352	35,4	0,352	35,4	0,352	35,4	0
647,03	0,545	0,344	36,9	0,344	36,9	0,344	36,9	0
659,48	0,545	0,349	35,9	0,349	35,9	0,349	35,9	0
660,00	0,545	0,359	34,2	0,359	34,2	0,359	34,2	0
672,21	0,545	0,361	33,8	0,361	33,8	0,361	33,8	0
685,22	0,545	0,381	30,1	0,381	30,1	0,381	30,1	0
690,00	0,545	0,395	27,5	0,395	27,5	0,395	27,5	0
698,49	0,545	0,395	27,5	0,395	27,5	0,395	27,5	0
712,00	0,545	0,374	31,4	0,374	31,4	0,374	31,4	0
720,00	0,545	0,358	34,3	0,358	34,3	0,358	34,3	0
725,82	0,545	0,358	34,3	0,358	34,3	0,358	34,3	0
739,97	0,545	0,362	33,5	0,362	33,5	0,362	33,5	0
750,00	0,545	0,397	27,2	0,397	27,2	0,397	27,2	0
754,42	0,545	0,397	27,2	0,397	27,2	0,397	27,2	0
769,06	0,545	0,408	25,1	0,408	25,1	0,408	25,1	0
780,00	0,545	0,412	24,3	0,412	24,3	0,412	24,3	0
783,84	0,545	0,412	24,3	0,412	24,3	0,412	24,3	0
798,91	0,545	0,407	25,3	0,407	25,3	0,407	25,3	0
810,00	0,545	0,386	29,2	0,386	29,2	0,386	29,2	0
814,44	0,545	0,387	29,0	0,387	29,0	0,387	29,0	0
830,58	0,545	0,391	28,2	0,391	28,2	0,391	28,2	0
840,00	0,545	0,402	26,3	0,402	26,3	0,402	26,3	0
847,41	0,545	0,403	26,1	0,403	26,1	0,403	26,1	0
864,93	0,545	0,419	23,0	0,419	23,0	0,419	23,0	0
870,00	0,545	0,462	15,1	0,462	15,1	0,462	15,1	0
883,00	0,545	0,463	15,0	0,463	15,0	0,463	15,0	0
900,00	0,545	0,447	18,0	0,447	18,0	0,447	18,0	0
901,32	0,545	0,447	18,0	0,447	18,0	0,447	18,0	0
919,69	0,545	0,440	19,3	0,440	19,3	0,440	19,3	0
930,00	0,545	0,451	17,2	0,451	17,2	0,451	17,2	0
938,36	0,545	0,452	17,1	0,452	17,1	0,452	17,1	0
957,85	0,545	0,418	23,4	0,418	23,4	0,418	23,4	0
960,00	0,545	0,419	23,2	0,419	23,2	0,419	23,2	0
978,53	0,545	0,420	22,9	0,420	22,9	0,420	22,9	0
990,00	0,545	0,439	19,5	0,439	19,5	0,439	19,5	0
1000,59	0,545	0,439	19,5	0,439	19,5	0,439	19,5	0

Tabulated Results (Redrill)								
Measured Depth (m)	Wall Thickness (in)	WF Base Rem. Wall (in)	WF Base Wear %	WF Low Rem. Wall (in)	WF Low Wear %	WF High Rem. Wall (in)	WF High Wear %	Pipe Protectors Required
1020,00	0,545	0,463	15,0	0,463	15,0	0,463	15,0	0
1023,59	0,545	0,462	15,1	0,462	15,1	0,462	15,1	0
1046,53	0,545	0,404	25,9	0,404	25,9	0,404	25,9	0
1050,00	0,545	0,454	16,8	0,454	16,8	0,454	16,8	0
1069,38	0,545	0,454	16,8	0,454	16,8	0,454	16,8	0
1080,00	0,545	0,459	15,8	0,459	15,8	0,459	15,8	0
1093,06	0,545	0,460	15,6	0,460	15,6	0,460	15,6	0
1110,00	0,545	0,449	17,6	0,449	17,6	0,449	17,6	0
1117,72	0,545	0,448	17,7	0,448	17,7	0,448	17,7	0
1140,00	0,545	0,407	25,3	0,407	25,3	0,407	25,3	0
1142,43	0,545	0,407	25,3	0,407	25,3	0,407	25,3	0
1166,94	0,545	0,438	19,7	0,438	19,7	0,438	19,7	0
1170,00	0,545	0,435	20,1	0,435	20,1	0,435	20,1	0
1191,57	0,545	0,435	20,1	0,435	20,1	0,435	20,1	0
1200,00	0,545	0,369	32,2	0,369	32,2	0,369	32,2	0
1215,52	0,545	0,369	32,2	0,369	32,2	0,369	32,2	0
1230,00	0,545	0,356	34,6	0,356	34,6	0,356	34,6	0
1237,95	0,545	0,356	34,6	0,356	34,6	0,356	34,6	0
1259,74	0,545	0,449	17,6	0,449	17,6	0,449	17,6	0
1260,00	0,545	0,468	14,2	0,468	14,2	0,468	14,2	0
1282,19	0,545	0,469	14,0	0,469	14,0	0,469	14,0	0
1290,00	0,545	0,475	12,9	0,475	12,9	0,475	12,9	0
1305,57	0,545	0,474	13,0	0,474	13,0	0,474	13,0	0
1320,00	0,545	0,449	17,6	0,449	17,6	0,449	17,6	0
1329,45	0,545	0,449	17,6	0,449	17,6	0,449	17,6	0
1350,00	0,545	0,463	15,0	0,463	15,0	0,463	15,0	0
1360,00	0,545	0,463	15,0	0,463	15,0	0,463	15,0	0
1370,00	0,545	0,479	12,1	0,479	12,1	0,479	12,1	0
1380,00	0,545	0,457	16,1	0,457	16,1	0,457	16,1	0
1390,00	0,545	0,454	16,8	0,454	16,8	0,454	16,8	0
1400,00	0,545	0,461	15,5	0,461	15,5	0,461	15,5	0
1410,00	0,545	0,456	16,3	0,456	16,3	0,456	16,3	0
1420,00	0,545	0,432	20,8	0,432	20,8	0,432	20,8	0
1430,00	0,545	0,378	30,6	0,378	30,6	0,378	30,6	0
1440,00	0,545	0,419	23,2	0,419	23,2	0,419	23,2	0
1450,00	0,545	0,406	25,5	0,406	25,5	0,406	25,5	0
1460,00	0,545	0,405	25,6	0,405	25,6	0,405	25,6	0
1470,00	0,545	0,405	25,6	0,405	25,6	0,405	25,6	0
1480,00	0,545	0,429	21,3	0,429	21,3	0,429	21,3	0
1490,00	0,545	0,407	25,3	0,407	25,3	0,407	25,3	0
1500,00	0,545	0,390	28,5	0,390	28,5	0,390	28,5	0
1510,00	0,545	0,421	22,7	0,421	22,7	0,421	22,7	0
1520,00	0,545	0,445	18,4	0,445	18,4	0,445	18,4	0
1530,00	0,545	0,440	19,3	0,440	19,3	0,440	19,3	0
1540,00	0,545	0,453	16,9	0,453	16,9	0,453	16,9	0
1550,00	0,545	0,466	14,5	0,466	14,5	0,466	14,5	0
1560,00	0,545	0,453	16,9	0,453	16,9	0,453	16,9	0
1570,00	0,545	0,403	26,1	0,403	26,1	0,403	26,1	0
1580,00	0,545	0,385	29,3	0,385	29,3	0,385	29,3	0
1590,00	0,545	0,415	23,8	0,415	23,8	0,415	23,8	0
1600,00	0,545	0,419	23,0	0,419	23,0	0,419	23,0	0

Tabulated Results (Redrill)								
Measured Depth (m)	Wall Thickness (in)	WF Base Rem. Wall (in)	WF Base Wear %	WF Low Rem. Wall (in)	WF Low Wear %	WF High Rem. Wall (in)	WF High Wear %	Pipe Protector s Required
1610,00	0,545	0,402	26,3	0,402	26,3	0,402	26,3	0
1620,00	0,545	0,390	28,5	0,390	28,5	0,390	28,5	0
1630,00	0,545	0,412	24,3	0,412	24,3	0,412	24,3	0
1640,00	0,545	0,407	25,3	0,407	25,3	0,407	25,3	0
1650,00	0,545	0,401	26,4	0,401	26,4	0,401	26,4	0
1660,00	0,545	0,424	22,2	0,424	22,2	0,424	22,2	0
1670,00	0,545	0,430	21,1	0,430	21,1	0,430	21,1	0
1680,00	0,545	0,397	27,2	0,397	27,2	0,397	27,2	0
1690,00	0,545	0,394	27,7	0,394	27,7	0,394	27,7	0
1700,00	0,545	0,426	21,7	0,426	21,7	0,426	21,7	0
1710,00	0,545	0,447	18,0	0,447	18,0	0,447	18,0	0
1720,00	0,545	0,423	22,4	0,423	22,4	0,423	22,4	0
1730,00	0,545	0,468	14,2	0,468	14,2	0,468	14,2	0
1740,00	0,545	0,417	23,5	0,417	23,5	0,417	23,5	0
1750,00	0,545	0,399	26,7	0,399	26,7	0,399	26,7	0
1760,00	0,545	0,383	29,6	0,383	29,6	0,383	29,6	0
1770,00	0,545	0,398	26,9	0,398	26,9	0,398	26,9	0
1780,00	0,545	0,413	24,2	0,413	24,2	0,413	24,2	0
1790,00	0,545	0,409	25,0	0,409	25,0	0,409	25,0	0
1800,00	0,545	0,393	27,9	0,393	27,9	0,393	27,9	0
1810,00	0,545	0,464	14,8	0,464	14,8	0,464	14,8	0
1820,00	0,545	0,469	14,0	0,469	14,0	0,469	14,0	0
1830,00	0,545	0,465	14,7	0,465	14,7	0,465	14,7	0
1840,00	0,545	0,405	25,6	0,405	25,6	0,405	25,6	0
1850,00	0,545	0,419	23,0	0,419	23,0	0,419	23,0	0
1860,00	0,545	0,430	21,1	0,430	21,1	0,430	21,1	0
1870,00	0,545	0,437	19,8	0,437	19,8	0,437	19,8	0
1880,00	0,545	0,433	20,6	0,433	20,6	0,433	20,6	0
1890,00	0,545	0,428	21,4	0,428	21,4	0,428	21,4	0
1900,00	0,545	0,436	20,0	0,436	20,0	0,436	20,0	0
1910,00	0,545	0,426	21,9	0,426	21,9	0,426	21,9	0
1920,00	0,545	0,439	19,5	0,439	19,5	0,439	19,5	0
1930,00	0,545	0,428	21,4	0,428	21,4	0,428	21,4	0
1940,00	0,545	0,423	22,4	0,423	22,4	0,423	22,4	0
1950,00	0,545	0,422	22,6	0,422	22,6	0,422	22,6	0
1960,00	0,545	0,419	23,0	0,419	23,0	0,419	23,0	0
1970,00	0,545	0,417	23,5	0,417	23,5	0,417	23,5	0
1980,00	0,545	0,452	17,1	0,452	17,1	0,452	17,1	0
1990,00	0,545	0,441	19,2	0,441	19,2	0,441	19,2	0
2000,00	0,545	0,454	16,8	0,454	16,8	0,454	16,8	0
2010,00	0,545	0,479	12,1	0,479	12,1	0,479	12,1	0
2020,00	0,545	0,454	16,8	0,454	16,8	0,454	16,8	0
2030,00	0,545	0,438	19,7	0,438	19,7	0,438	19,7	0
2040,00	0,545	0,461	15,5	0,461	15,5	0,461	15,5	0
2050,00	0,545	0,455	16,6	0,455	16,6	0,455	16,6	0
2060,00	0,545	0,436	20,0	0,436	20,0	0,436	20,0	0
2070,00	0,545	0,448	17,7	0,448	17,7	0,448	17,7	0
2080,00	0,545	0,456	16,3	0,456	16,3	0,456	16,3	0
2090,00	0,545	0,453	16,9	0,453	16,9	0,453	16,9	0
2100,00	0,545	0,431	20,9	0,431	20,9	0,431	20,9	0
2110,00	0,545	0,441	19,0	0,441	19,0	0,441	19,0	0

Tabulated Results (Redrill)								
Measured Depth (m)	Wall Thickness (in)	WF Base Rem. Wall (in)	WF Base Wear %	WF Low Rem. Wall (in)	WF Low Wear %	WF High Rem. Wall (in)	WF High Wear %	Pipe Protector s Required
2120,00	0,545	0,469	14,0	0,469	14,0	0,469	14,0	0
2130,00	0,545	0,462	15,1	0,462	15,1	0,462	15,1	0
2140,00	0,545	0,420	22,9	0,420	22,9	0,420	22,9	0
2150,00	0,545	0,438	19,7	0,438	19,7	0,438	19,7	0
2160,00	0,545	0,439	19,5	0,439	19,5	0,439	19,5	0
2170,00	0,545	0,406	25,5	0,406	25,5	0,406	25,5	0
2180,00	0,545	0,397	27,2	0,397	27,2	0,397	27,2	0
2190,00	0,545	0,400	26,6	0,400	26,6	0,400	26,6	0
2200,00	0,545	0,432	20,8	0,432	20,8	0,432	20,8	0
2210,00	0,545	0,434	20,3	0,434	20,3	0,434	20,3	0
2220,00	0,545	0,392	28,0	0,392	28,0	0,392	28,0	0
2230,00	0,545	0,406	25,5	0,406	25,5	0,406	25,5	0
2240,00	0,545	0,433	20,6	0,433	20,6	0,433	20,6	0
2250,00	0,545	0,455	16,6	0,455	16,6	0,455	16,6	0
2260,00	0,545	0,419	23,0	0,419	23,0	0,419	23,0	0
2270,00	0,545	0,461	15,5	0,461	15,5	0,461	15,5	0
2280,00	0,545	0,472	13,4	0,472	13,4	0,472	13,4	0
2290,00	0,545	0,448	17,9	0,448	17,9	0,448	17,9	0
2300,00	0,545	0,431	20,9	0,431	20,9	0,431	20,9	0
2310,00	0,545	0,455	16,4	0,455	16,4	0,455	16,4	0
2320,00	0,545	0,448	17,9	0,448	17,9	0,448	17,9	0
2330,00	0,545	0,415	23,8	0,415	23,8	0,415	23,8	0
2340,00	0,545	0,474	13,0	0,474	13,0	0,474	13,0	0
2350,00	0,545	0,469	14,0	0,469	14,0	0,469	14,0	0
2360,00	0,545	0,474	13,0	0,474	13,0	0,474	13,0	0
2370,00	0,545	0,471	13,5	0,471	13,5	0,471	13,5	0
2380,00	0,545	0,442	18,8	0,442	18,8	0,442	18,8	0
2390,00	0,545	0,442	18,8	0,442	18,8	0,442	18,8	0
2400,00	0,545	0,443	18,7	0,443	18,7	0,443	18,7	0
2410,00	0,545	0,439	19,5	0,439	19,5	0,439	19,5	0
2420,00	0,545	0,442	18,8	0,442	18,8	0,442	18,8	0
2460,00	0,545	0,458	15,9	0,458	15,9	0,458	15,9	0
2470,00	0,545	0,459	15,8	0,459	15,8	0,459	15,8	0
2480,00	0,545	0,429	21,3	0,429	21,3	0,429	21,3	0
2490,00	0,545	0,422	22,6	0,422	22,6	0,422	22,6	0
2500,00	0,545	0,432	20,8	0,432	20,8	0,432	20,8	0
2510,00	0,545	0,415	23,8	0,415	23,8	0,415	23,8	0
2520,00	0,545	0,425	22,1	0,425	22,1	0,425	22,1	0
2530,00	0,545	0,455	16,6	0,455	16,6	0,455	16,6	0
2540,00	0,545	0,448	17,9	0,448	17,9	0,448	17,9	0
2550,00	0,545	0,429	21,3	0,429	21,3	0,429	21,3	0
2560,00	0,545	0,439	19,5	0,439	19,5	0,439	19,5	0
2570,00	0,545	0,429	21,3	0,429	21,3	0,429	21,3	0
2580,00	0,545	0,423	22,4	0,423	22,4	0,423	22,4	0
2590,00	0,545	0,440	19,3	0,440	19,3	0,440	19,3	0
2600,00	0,545	0,470	13,7	0,470	13,7	0,470	13,7	0
2610,00	0,545	0,467	14,3	0,467	14,3	0,467	14,3	0
2620,00	0,545	0,441	19,0	0,441	19,0	0,441	19,0	0
2630,00	0,545	0,416	23,7	0,416	23,7	0,416	23,7	0
2640,00	0,545	0,450	17,4	0,450	17,4	0,450	17,4	0
2650,00	0,545	0,460	15,6	0,460	15,6	0,460	15,6	0

Tabulated Results (Redrill)								
Measured Depth (m)	Wall Thickness (in)	WF Base Rem. Wall (in)	WF Base Wear %	WF Low Rem. Wall (in)	WF Low Wear %	WF High Rem. Wall (in)	WF High Wear %	Pipe Protectors Required
2660,00	0,545	0,433	20,6	0,433	20,6	0,433	20,6	0
2670,00	0,545	0,420	22,9	0,420	22,9	0,420	22,9	0
2680,00	0,545	0,430	21,1	0,430	21,1	0,430	21,1	0
2690,00	0,545	0,433	20,6	0,433	20,6	0,433	20,6	0
2700,00	0,545	0,409	25,0	0,409	25,0	0,409	25,0	0
2710,00	0,545	0,426	21,9	0,426	21,9	0,426	21,9	0
2720,00	0,545	0,428	21,4	0,428	21,4	0,428	21,4	0
2730,00	0,545	0,441	19,2	0,441	19,2	0,441	19,2	0
2740,00	0,545	0,438	19,7	0,438	19,7	0,438	19,7	0
2750,00	0,545	0,441	19,0	0,441	19,0	0,441	19,0	0
2760,00	0,545	0,456	16,3	0,456	16,3	0,456	16,3	0
2770,00	0,545	0,472	13,4	0,472	13,4	0,472	13,4	0
2780,00	0,545	0,464	14,8	0,464	14,8	0,464	14,8	0
2790,00	0,545	0,434	20,3	0,434	20,3	0,434	20,3	0
2800,00	0,545	0,440	19,3	0,440	19,3	0,440	19,3	0
2810,00	0,545	0,419	23,0	0,419	23,0	0,419	23,0	0
2820,00	0,545	0,420	22,9	0,420	22,9	0,420	22,9	0
2830,00	0,545	0,448	17,9	0,448	17,9	0,448	17,9	0
2840,00	0,545	0,451	17,2	0,451	17,2	0,451	17,2	0
2850,00	0,545	0,447	18,0	0,447	18,0	0,447	18,0	0
2860,00	0,545	0,426	21,9	0,426	21,9	0,426	21,9	0
2870,00	0,545	0,443	18,7	0,443	18,7	0,443	18,7	0
2880,00	0,545	0,446	18,2	0,446	18,2	0,446	18,2	0
2890,00	0,545	0,429	21,3	0,429	21,3	0,429	21,3	0
2900,00	0,545	0,440	19,3	0,440	19,3	0,440	19,3	0
2910,00	0,545	0,447	18,0	0,447	18,0	0,447	18,0	0
2920,00	0,545	0,445	18,4	0,445	18,4	0,445	18,4	0
2930,00	0,545	0,456	16,3	0,456	16,3	0,456	16,3	0
2940,00	0,545	0,434	20,3	0,434	20,3	0,434	20,3	0
2950,00	0,545	0,438	19,7	0,438	19,7	0,438	19,7	0
2960,00	0,545	0,443	18,7	0,443	18,7	0,443	18,7	0
2970,00	0,545	0,427	21,6	0,427	21,6	0,427	21,6	0
2980,00	0,545	0,441	19,2	0,441	19,2	0,441	19,2	0
2987,00	0,545	0,450	17,4	0,450	17,4	0,450	17,4	0
2990,00	0,545	0,450	17,4	0,450	17,4	0,450	17,4	0
3000,00	0,545	0,426	21,9	0,426	21,9	0,426	21,9	0
3011,00	0,545	0,426	21,9	0,426	21,9	0,426	21,9	0
3030,00	0,545	0,469	13,9	0,469	13,9	0,469	13,9	0
3036,00	0,545	0,469	14,0	0,469	14,0	0,469	14,0	0
3060,00	0,545	0,455	16,4	0,455	16,4	0,455	16,4	0
3061,00	0,545	0,455	16,4	0,455	16,4	0,455	16,4	0
3086,00	0,545	0,454	16,8	0,454	16,8	0,454	16,8	0
3090,00	0,545	0,432	20,8	0,432	20,8	0,432	20,8	0
3111,00	0,545	0,432	20,8	0,432	20,8	0,432	20,8	0
3120,00	0,545	0,435	20,1	0,435	20,1	0,435	20,1	0
3136,00	0,545	0,435	20,1	0,435	20,1	0,435	20,1	0
3150,00	0,545	0,432	20,8	0,432	20,8	0,432	20,8	0
3161,00	0,545	0,432	20,8	0,432	20,8	0,432	20,8	0
3180,00	0,545	0,424	22,2	0,424	22,2	0,424	22,2	0
3186,00	0,545	0,424	22,2	0,424	22,2	0,424	22,2	0
3210,00	0,545	0,441	19,2	0,441	19,2	0,441	19,2	0

Tabulated Results (Redrill)								
Measured Depth (m)	Wall Thickness (in)	WF Base Rem. Wall (in)	WF Base Wear %	WF Low Rem. Wall (in)	WF Low Wear %	WF High Rem. Wall (in)	WF High Wear %	Pipe Protectors Required
3211,00	0,545	0,440	19,3	0,440	19,3	0,440	19,3	0
3236,00	0,545	0,455	16,6	0,455	16,6	0,455	16,6	0
3240,00	0,545	0,436	20,0	0,436	20,0	0,436	20,0	0
3261,00	0,545	0,437	19,8	0,437	19,8	0,437	19,8	0
3270,00	0,545	0,433	20,5	0,433	20,5	0,433	20,5	0
3286,00	0,545	0,433	20,5	0,433	20,5	0,433	20,5	0
3300,00	0,545	0,427	21,6	0,427	21,6	0,427	21,6	0
3311,00	0,545	0,427	21,6	0,427	21,6	0,427	21,6	0
3330,00	0,545	0,434	20,3	0,434	20,3	0,434	20,3	0
3336,00	0,545	0,434	20,3	0,434	20,3	0,434	20,3	0
3360,00	0,545	0,447	18,0	0,447	18,0	0,447	18,0	0
3361,00	0,545	0,447	18,0	0,447	18,0	0,447	18,0	0
3386,00	0,545	0,449	17,6	0,449	17,6	0,449	17,6	0
3390,00	0,545	0,421	22,7	0,421	22,7	0,421	22,7	0
3411,00	0,545	0,416	23,7	0,416	23,7	0,416	23,7	0
3420,00	0,545	0,424	22,2	0,424	22,2	0,424	22,2	0
3436,00	0,545	0,424	22,2	0,424	22,2	0,424	22,2	0
3450,00	0,545	0,426	21,7	0,426	21,7	0,426	21,7	0
3461,00	0,545	0,424	22,2	0,424	22,2	0,424	22,2	0
3480,00	0,545	0,441	19,2	0,441	19,2	0,441	19,2	0
3486,00	0,545	0,441	19,2	0,441	19,2	0,441	19,2	0
3510,00	0,545	0,414	24,0	0,414	24,0	0,414	24,0	0
3511,00	0,545	0,414	24,0	0,414	24,0	0,414	24,0	0
3536,00	0,545	0,423	22,4	0,423	22,4	0,423	22,4	0
3540,00	0,545	0,422	22,6	0,422	22,6	0,422	22,6	0
3561,00	0,545	0,422	22,6	0,422	22,6	0,422	22,6	0
3570,00	0,545	0,441	19,0	0,441	19,0	0,441	19,0	0
3586,00	0,545	0,433	20,6	0,433	20,6	0,433	20,6	0
3600,00	0,545	0,418	23,4	0,418	23,4	0,418	23,4	0
3611,00	0,545	0,406	25,5	0,406	25,5	0,406	25,5	0
3630,00	0,545	0,402	26,3	0,402	26,3	0,402	26,3	0
3636,00	0,545	0,401	26,4	0,401	26,4	0,401	26,4	0
3660,00	0,545	0,416	23,7	0,416	23,7	0,416	23,7	0
3661,00	0,545	0,416	23,7	0,416	23,7	0,416	23,7	0
3666,00	0,545	0,415	23,8	0,415	23,8	0,415	23,8	0
3687,00	0,545	0,423	22,4	0,423	22,4	0,423	22,4	0
3690,00	0,545	0,416	23,7	0,416	23,7	0,416	23,7	0
3714,00	0,545	0,426	21,9	0,426	21,9	0,426	21,9	0
3720,00	0,545	0,419	23,2	0,419	23,2	0,419	23,2	0
3742,00	0,545	0,429	21,3	0,429	21,3	0,429	21,3	0
3750,00	0,545	0,427	21,6	0,427	21,6	0,427	21,6	0
3770,00	0,545	0,426	21,9	0,426	21,9	0,426	21,9	0
3780,00	0,545	0,407	25,3	0,407	25,3	0,407	25,3	0
3798,00	0,545	0,407	25,3	0,407	25,3	0,407	25,3	0
3807,00	0,545	0,405	25,6	0,405	25,6	0,405	25,6	0
3810,00	0,545	0,405	25,6	0,405	25,6	0,405	25,6	0
3818,00	0,545	0,389	28,7	0,389	28,7	0,389	28,7	0

Table 21: 30/10 B-14A T3 tabulated wear results

Tabulated Results (Redrill)							
Measured Depth (m)	Inclination Angle (deg)	Azimuth Angle (deg)	Vertical Depth (m)	Dogleg Severity (deg/30m)	Normal Force (N/m)	L-Load per Joint (T[metric])	Axial Drag (T[metric])
0,00	0,00	0,00	0,00	0,00	0,0	0,0000	57,2012
30,00	0,00	0,00	30,00	0,00	0,0	0,0000	56,4200
39,10	0,00	0,00	39,10	0,00	0,0	0,0000	56,1831
60,00	0,93	8,57	60,00	1,33	421,5	0,5896	55,6389
90,00	2,26	20,87	89,99	1,33	423,1	0,5918	54,8580
120,00	3,59	33,17	119,95	1,33	442,1	0,6184	54,0778
150,00	4,92	45,47	149,86	1,33	475,1	0,6645	53,2987
180,00	6,25	57,77	179,72	1,33	518,0	0,7246	52,5213
210,00	7,58	70,06	209,50	1,33	567,6	0,7940	51,7457
214,55	7,78	71,93	214,01	1,33	602,1	0,8421	51,6283
224,64	7,97	72,20	224,01	0,58	134,5	0,1882	51,3681
234,74	8,13	72,01	234,01	0,48	105,4	0,1474	51,1076
240,00	8,18	71,90	239,21	0,31	56,4	0,0789	50,9721
244,84	8,23	71,80	244,00	0,31	56,0	0,0784	50,8473
254,95	8,41	71,65	254,01	0,54	118,7	0,1660	50,5868
265,06	8,71	71,47	264,00	0,89	218,8	0,3061	50,3265
270,00	8,79	71,47	268,89	0,47	97,0	0,1357	50,1994
275,18	8,87	71,47	274,01	0,47	96,3	0,1347	50,0661
285,30	8,93	71,52	284,00	0,18	12,8	0,0179	49,8057
295,43	9,10	71,06	294,01	0,55	118,8	0,1662	49,5452
300,00	9,18	70,68	298,52	0,66	156,5	0,2188	49,4277
305,56	9,28	70,22	304,01	0,66	156,4	0,2188	49,2848
315,69	9,44	69,38	314,00	0,62	145,2	0,2032	49,0245
325,83	9,60	68,83	324,00	0,54	116,7	0,1632	48,7641
330,00	9,66	68,67	328,12	0,46	90,7	0,1268	48,6571
335,98	9,74	68,43	334,01	0,46	90,3	0,1263	48,5036
346,12	9,70	67,52	344,00	0,47	146,3	0,2046	48,2433
356,27	9,45	66,05	354,01	1,03	314,8	0,4403	47,9827
360,00	9,41	65,46	357,69	0,84	246,3	0,3445	47,8869
366,40	9,35	64,44	364,01	0,83	244,4	0,3419	47,7225
376,54	9,49	62,80	374,01	0,90	226,3	0,3165	47,4620
386,68	9,78	60,89	384,01	1,28	316,8	0,4432	47,2017
390,00	9,90	60,19	387,28	1,52	378,5	0,5294	47,1165
396,83	10,14	58,75	394,00	1,53	380,5	0,5322	46,9413
407,00	10,61	56,70	404,01	1,76	434,4	0,6076	46,6808
417,19	11,26	54,51	414,01	2,27	561,4	0,7852	46,4203
420,00	11,45	53,87	416,77	2,41	597,1	0,8351	46,3486
427,39	11,94	52,18	424,01	2,43	599,6	0,8387	46,1601
437,63	12,66	50,12	434,01	2,47	601,2	0,8410	45,8996
447,90	13,50	48,33	444,01	2,72	657,9	0,9202	45,6391
450,00	13,68	48,04	446,05	2,77	665,7	0,9311	45,5860
458,20	14,39	46,89	454,01	2,78	663,8	0,9285	45,3788
468,55	15,43	46,16	464,01	3,06	724,1	1,0129	45,1184
478,95	16,60	45,70	474,01	3,40	799,0	1,1176	44,8581
480,00	16,72	45,65	475,01	3,52	828,6	1,1590	44,8319
489,42	17,82	45,17	484,01	3,52	821,9	1,1496	44,5977
499,96	19,15	44,94	494,00	3,79	878,4	1,2286	44,3374
510,00	20,47	44,96	503,45	3,95	906,6	1,2682	44,0914
510,60	20,55	44,96	504,01	3,95	903,4	1,2636	44,0768
521,33	21,97	45,25	514,01	3,98	903,1	1,2632	43,8164
532,17	23,41	45,57	524,01	4,00	896,1	1,2533	43,5559
540,00	24,36	45,73	531,17	3,65	800,9	1,1202	43,3695

Tabulated Results (Redrill)							
Measured Depth (m)	Inclination Angle (deg)	Azimuth Angle (deg)	Vertical Depth (m)	Dogleg Severity (deg/30m)	Normal Force (N/m)	L-Load per Joint (T[metric])	Axial Drag (T[metric])
543,12	24,74	45,80	534,01	3,65	796,8	1,1145	43,2956
554,18	25,90	46,07	544,01	3,16	667,9	0,9343	43,0353
565,35	26,99	46,33	554,01	2,94	605,6	0,8471	42,7748
570,00	27,41	46,43	558,14	2,76	555,2	0,7765	42,6671
576,63	28,02	46,58	564,01	2,76	550,9	0,7706	42,5143
588,01	29,03	46,72	574,01	2,67	521,8	0,7298	42,2540
599,50	30,05	46,79	584,01	2,66	512,7	0,7172	41,9937
600,00	30,10	46,79	584,44	2,84	552,7	0,7731	41,9824
611,12	31,15	46,85	594,01	2,84	546,6	0,7645	41,7332
622,89	32,46	46,84	604,01	3,34	655,6	0,9170	41,4727
630,00	33,39	46,78	609,98	3,92	785,2	1,0983	41,3173
634,84	34,02	46,74	614,01	3,92	780,0	1,0910	41,2125
647,03	35,72	46,61	624,01	4,19	832,8	1,1649	40,9521
659,48	37,42	46,45	634,01	4,10	800,8	1,1201	40,6917
660,00	37,49	46,44	634,42	3,83	734,3	1,0271	40,6809
672,21	39,04	46,24	644,01	3,83	726,1	1,0156	40,4313
685,22	40,46	45,98	654,01	3,30	593,8	0,8306	40,1708
690,00	40,90	45,75	657,63	2,89	507,3	0,7095	40,0764
698,49	41,67	45,34	664,01	2,90	503,8	0,7047	39,9103
712,00	42,92	44,05	674,01	3,38	631,1	0,8828	39,6501
720,00	43,73	43,13	679,83	3,85	738,1	1,0324	39,4985
725,82	44,32	42,46	684,01	3,86	739,2	1,0339	39,3896
739,97	45,76	40,95	694,01	3,80	711,9	0,9958	39,1292
750,00	46,41	40,07	700,97	2,71	488,2	0,6828	38,9480
754,42	46,69	39,68	704,01	2,71	489,1	0,6841	38,8689
769,06	47,10	38,45	714,01	2,02	405,4	0,5671	38,6084
780,00	47,60	37,61	721,42	2,19	390,3	0,5460	38,4154
783,84	47,78	37,31	724,01	2,19	391,2	0,5472	38,3481
798,91	49,04	36,51	734,01	2,78	438,7	0,6136	38,0876
810,00	50,30	36,11	741,19	3,50	569,3	0,7963	37,9007
814,44	50,80	35,95	744,01	3,50	566,2	0,7919	37,8272
830,58	52,65	35,76	754,01	3,45	539,9	0,7552	37,5669
840,00	53,64	35,90	759,66	3,18	475,5	0,6651	37,4198
847,41	54,42	36,01	764,01	3,18	471,3	0,6592	37,3064
864,93	55,96	36,48	774,01	2,72	374,8	0,5242	37,0460
870,00	56,21	36,58	776,84	1,57	145,0	0,2028	36,9723
883,00	56,86	36,83	784,01	1,57	143,1	0,2001	36,7857
900,00	56,96	36,77	793,29	0,20	177,3	0,2479	36,5440
901,32	56,97	36,77	794,01	0,20	177,4	0,2482	36,5253
919,69	57,06	36,38	804,01	0,55	214,5	0,3001	36,2648
930,00	57,68	36,13	809,57	1,90	201,9	0,2824	36,1201
938,36	58,18	35,92	814,01	1,91	200,2	0,2800	36,0045
957,85	60,07	35,50	824,01	2,96	390,9	0,5468	35,7440
960,00	60,28	35,47	825,08	2,98	387,4	0,5418	35,7162
978,53	62,11	35,24	834,00	2,98	381,3	0,5334	35,4837
990,00	63,08	35,18	839,28	2,53	285,0	0,3986	35,3462
1000,59	63,97	35,12	844,01	2,53	281,3	0,3935	35,2233
1020,00	64,40	35,21	852,46	0,68	100,4	0,1405	35,0032
1023,59	64,48	35,23	854,01	0,68	101,1	0,1414	34,9629
1046,53	63,83	35,55	864,01	0,93	405,1	0,5667	34,7025
1050,00	63,89	35,60	865,54	0,68	142,7	0,1997	34,6626
1069,38	64,25	35,88	874,01	0,68	143,5	0,2007	34,4420

Tabulated Results (Redrill)							
Measured Depth (m)	Inclination Angle (deg)	Azimuth Angle (deg)	Vertical Depth (m)	Dogleg Severity (deg/30m)	Normal Force (N/m)	L-Load per Joint (T[metric])	Axial Drag (T[metric])
1080,00	64,94	36,04	878,57	1,99	170,5	0,2385	34,3234
1093,06	65,79	36,23	884,01	1,99	167,9	0,2349	34,1816
1110,00	66,20	36,68	890,90	1,03	170,6	0,2386	34,0021
1117,72	66,38	36,89	894,01	1,03	171,1	0,2393	33,9213
1140,00	65,92	37,58	903,01	1,05	388,2	0,5429	33,6867
1142,43	65,87	37,65	904,01	1,05	387,5	0,5420	33,6609
1166,94	65,95	37,60	914,01	0,11	214,8	0,3004	33,4003
1170,00	65,97	37,52	915,26	0,77	233,4	0,3264	33,3679
1191,57	66,15	36,94	924,01	0,77	233,3	0,3263	33,1400
1200,00	65,57	36,88	927,46	2,09	626,2	0,8759	33,0502
1215,52	64,49	36,78	934,01	2,09	622,6	0,8709	32,8796
1230,00	63,23	36,87	940,39	2,61	716,9	1,0027	32,7135
1237,95	62,54	36,92	944,01	2,61	713,5	0,9980	32,6191
1259,74	62,81	36,88	954,01	0,38	158,5	0,2217	32,3587
1260,00	62,83	36,88	954,13	1,98	138,8	0,1942	32,3556
1282,19	64,29	36,81	964,01	1,98	134,4	0,1880	32,0983
1290,00	64,55	36,84	967,39	1,01	51,2	0,0717	32,0105
1305,57	65,07	36,90	974,01	1,01	52,8	0,0739	31,8379
1320,00	65,29	37,05	980,07	0,53	158,0	0,2210	31,6802
1329,45	65,43	37,14	984,01	0,53	158,5	0,2218	31,5776
1350,00	65,96	37,09	992,47	0,78	94,6	0,1324	31,3573
1360,00	66,22	37,07	996,52	0,78	95,8	0,1340	31,2518
1370,00	66,81	37,07	1000,51	1,77	80,4	0,1124	31,1480
1380,00	67,51	36,85	1004,39	2,19	174,0	0,2434	31,0470
1390,00	68,30	36,68	1008,15	2,42	200,1	0,2799	30,9490
1400,00	69,05	36,57	1011,79	2,27	167,2	0,2339	30,8543
1410,00	69,57	36,27	1015,32	1,77	151,9	0,2124	30,7623
1420,00	69,70	35,89	1018,80	1,14	253,6	0,3547	30,6717
1430,00	69,19	35,33	1022,31	2,19	575,8	0,8054	30,5803
1440,00	69,08	35,06	1025,87	0,83	324,0	0,4533	30,4875
1450,00	68,88	34,64	1029,46	1,32	398,6	0,5576	30,3941
1460,00	68,59	34,45	1033,09	1,02	399,2	0,5583	30,2997
1470,00	68,28	34,46	1036,76	0,93	397,9	0,5565	30,2040
1480,00	68,23	34,49	1040,47	0,17	263,4	0,3684	30,1075
1490,00	67,94	34,56	1044,20	0,89	387,4	0,5419	30,0103
1500,00	67,45	34,74	1047,99	1,55	494,6	0,6919	29,9115
1510,00	67,33	34,90	1051,84	0,57	306,4	0,4286	29,8114
1520,00	67,46	35,04	1055,68	0,55	182,0	0,2545	29,7113
1530,00	67,55	35,22	1059,51	0,57	208,2	0,2912	29,6116
1540,00	67,76	35,35	1063,31	0,73	143,6	0,2009	29,5126
1550,00	68,09	35,44	1067,07	1,02	82,1	0,1148	29,4148
1560,00	68,30	35,56	1070,78	0,71	143,1	0,2002	29,3181
1570,00	67,96	35,72	1074,51	1,11	413,8	0,5789	29,2211
1580,00	67,61	36,47	1078,29	2,33	537,3	0,7516	29,1226
1590,00	67,53	36,93	1082,10	1,30	347,5	0,4860	29,0232
1600,00	67,44	37,27	1085,93	0,98	320,7	0,4486	28,9235
1610,00	67,07	37,35	1089,80	1,13	419,7	0,5871	28,8229
1620,00	66,53	37,43	1093,74	1,64	501,6	0,7016	28,7203
1630,00	66,28	37,47	1097,74	0,76	357,0	0,4993	28,6160
1640,00	65,96	37,53	1101,79	0,97	390,7	0,5464	28,5106
1650,00	65,57	37,65	1105,89	1,22	425,9	0,5957	28,4037
1660,00	65,45	37,69	1110,04	0,38	291,1	0,4072	28,2958

Tabulated Results (Redrill)							
Measured Depth (m)	Inclination Angle (deg)	Azimuth Angle (deg)	Vertical Depth (m)	Dogleg Severity (deg/30m)	Normal Force (N/m)	L-Load per Joint (T[metric])	Axial Drag (T[metric])
1670,00	65,40	37,72	1114,20	0,17	256,7	0,3591	28,1875
1680,00	64,93	37,65	1118,40	1,42	458,7	0,6417	28,0781
1690,00	64,43	37,61	1122,68	1,50	470,6	0,6582	27,9668
1700,00	64,33	37,58	1127,00	0,31	278,3	0,3893	27,8542
1710,00	64,46	37,56	1131,32	0,39	168,8	0,2361	27,7416
1720,00	64,32	37,55	1135,64	0,42	296,6	0,4148	27,6291
1730,00	64,74	37,56	1139,94	1,26	33,0	0,0462	27,5171
1740,00	64,60	37,55	1144,22	0,42	296,6	0,4148	27,4057
1750,00	64,23	37,61	1148,54	1,12	404,0	0,5652	27,2932
1760,00	63,63	37,61	1152,94	1,80	508,6	0,7114	27,1788
1770,00	63,24	37,71	1157,41	1,20	411,2	0,5752	27,0623
1780,00	63,04	37,75	1161,93	0,61	320,5	0,4484	26,9447
1790,00	62,78	37,71	1166,48	0,79	347,2	0,4856	26,8261
1800,00	62,30	37,70	1171,09	1,44	446,1	0,6240	26,7060
1810,00	62,70	37,76	1175,71	1,21	50,7	0,0709	26,5858
1820,00	63,25	37,84	1180,25	1,66	38,9	0,0544	26,4675
1830,00	63,66	37,87	1184,72	1,23	45,2	0,0632	26,3511
1840,00	63,36	38,01	1189,18	0,98	367,7	0,5143	26,2350
1850,00	63,24	38,05	1193,67	0,38	282,3	0,3949	26,1180
1860,00	63,37	37,99	1198,17	0,42	172,0	0,2406	26,0010
1870,00	63,48	37,97	1202,64	0,33	179,9	0,2516	25,8845
1880,00	63,53	37,94	1207,10	0,17	206,9	0,2894	25,7683
1890,00	63,53	37,97	1211,56	0,08	228,9	0,3202	25,6522
1900,00	63,63	37,94	1216,01	0,31	185,4	0,2593	25,5364
1910,00	63,60	38,04	1220,45	0,28	245,0	0,3427	25,4207
1920,00	63,74	38,13	1224,89	0,48	171,9	0,2404	25,3052
1930,00	63,92	38,10	1229,30	0,55	152,1	0,2127	25,1903
1940,00	64,03	38,15	1233,69	0,36	183,3	0,2564	25,0761
1950,00	64,14	38,06	1238,06	0,41	186,0	0,2601	24,9623
1960,00	64,20	38,07	1242,41	0,18	204,4	0,2859	24,8488
1970,00	64,44	38,02	1246,75	0,73	130,0	0,1818	24,7360
1980,00	64,59	38,06	1251,05	0,46	168,0	0,2350	24,6239
1990,00	64,60	38,06	1255,34	0,03	226,5	0,3168	24,5122
2000,00	64,78	38,12	1259,61	0,56	157,3	0,2201	24,4009
2010,00	65,23	38,13	1263,84	1,35	44,5	0,0623	24,2909
2020,00	65,41	38,06	1268,02	0,57	159,8	0,2235	24,1821
2030,00	65,38	38,09	1272,18	0,12	244,9	0,3425	24,0737
2040,00	65,64	38,10	1276,32	0,78	125,8	0,1760	23,9658
2050,00	65,83	38,07	1280,43	0,58	155,6	0,2177	23,8588
2060,00	65,78	38,09	1284,53	0,16	253,4	0,3545	23,7520
2070,00	65,90	38,08	1288,62	0,36	184,5	0,2581	23,6455
2080,00	66,12	38,09	1292,69	0,66	144,7	0,2025	23,5396
2090,00	66,30	38,12	1296,72	0,55	161,9	0,2264	23,4345
2100,00	66,17	38,14	1300,75	0,39	285,8	0,3997	23,3296
2110,00	66,19	38,17	1304,79	0,10	226,0	0,3161	23,2244
2120,00	66,65	37,98	1308,79	1,48	86,4	0,1208	23,1203
2130,00	66,96	38,08	1312,73	0,97	118,3	0,1655	23,0177
2140,00	66,68	38,10	1316,67	0,84	344,7	0,4822	22,9152
2150,00	66,66	38,16	1320,63	0,18	243,3	0,3403	22,8121
2160,00	66,65	38,18	1324,59	0,06	238,5	0,3336	22,7089
2170,00	66,13	38,27	1328,60	1,58	436,4	0,6105	22,6046
2180,00	65,44	38,41	1332,70	2,11	501,1	0,7009	22,4978

Tabulated Results (Redrill)							
Measured Depth (m)	Inclination Angle (deg)	Azimuth Angle (deg)	Vertical Depth (m)	Dogleg Severity (deg/30m)	Normal Force (N/m)	L-Load per Joint (T[metric])	Axial Drag (T[metric])
2190,00	64,81	38,63	1336,90	1,98	479,3	0,6705	22,3883
2200,00	64,68	38,72	1341,17	0,46	282,3	0,3949	22,2772
2210,00	64,60	38,82	1345,45	0,36	263,4	0,3684	22,1656
2220,00	63,80	38,77	1349,81	2,40	532,3	0,7445	22,0523
2230,00	63,24	38,92	1354,26	1,73	441,8	0,6180	21,9362
2240,00	63,11	38,91	1358,78	0,39	276,5	0,3868	21,8187
2250,00	63,35	39,13	1363,28	0,93	156,9	0,2194	21,7014
2260,00	63,02	39,30	1367,79	1,09	354,4	0,4956	21,5839
2270,00	63,36	39,52	1372,30	1,18	125,8	0,1759	21,4665
2280,00	63,81	39,61	1376,75	1,37	70,7	0,0989	21,3506
2290,00	63,93	39,77	1381,16	0,56	192,9	0,2698	21,2360
2300,00	63,78	39,81	1385,56	0,46	283,8	0,3970	21,1212
2310,00	64,00	39,88	1389,96	0,69	151,9	0,2125	21,0066
2320,00	64,11	39,84	1394,34	0,35	190,8	0,2668	20,8927
2330,00	63,67	39,82	1398,74	1,32	385,9	0,5398	20,7781
2340,00	64,22	39,67	1403,13	1,70	59,1	0,0826	20,6637
2350,00	65,29	39,60	1407,40	3,22	147,2	0,2058	20,5527
2360,00	66,28	39,54	1411,50	2,97	115,2	0,1611	20,4459
2370,00	66,74	39,50	1415,48	1,38	75,2	0,1051	20,3421
2380,00	66,79	39,54	1419,43	0,19	217,8	0,3046	20,2393
2390,00	66,84	39,54	1423,37	0,15	217,6	0,3043	20,1368
2400,00	66,90	39,46	1427,29	0,28	215,8	0,3018	20,0345
2410,00	66,89	39,34	1431,22	0,33	241,3	0,3375	19,9323
2420,00	66,98	39,08	1435,14	0,77	220,0	0,3077	19,8303
2430,00	66,88	38,60	1439,05	1,36	307,4	0,4299	19,7283
2440,00	66,45	37,87	1443,01	2,39	440,9	0,6166	19,6251
2450,00	66,27	37,58	1447,02	0,96	307,2	0,4298	19,5207
2460,00	66,60	37,39	1451,02	1,12	137,2	0,1920	19,4166
2470,00	66,93	37,49	1454,97	1,03	129,2	0,1807	19,3139
2480,00	66,76	37,66	1458,90	0,69	295,3	0,4130	19,2115
2490,00	66,44	37,78	1462,87	1,02	341,0	0,4770	19,1081
2500,00	66,30	37,63	1466,88	0,59	283,1	0,3960	19,0037
2510,00	65,83	37,60	1470,94	1,41	385,6	0,5394	18,8981
2520,00	65,59	37,27	1475,05	1,15	324,8	0,4543	18,7910
2530,00	65,85	37,17	1479,16	0,83	152,5	0,2133	18,6839
2540,00	65,99	37,10	1483,24	0,46	189,8	0,2654	18,5776
2550,00	65,78	36,99	1487,33	0,70	301,2	0,4213	18,4712
2560,00	65,77	36,86	1491,43	0,36	239,0	0,3343	18,3644
2570,00	65,57	36,75	1495,55	0,67	296,9	0,4153	18,2571
2580,00	65,25	36,49	1499,71	1,19	339,7	0,4752	18,1488
2590,00	65,24	36,38	1503,90	0,30	237,1	0,3316	18,0397
2600,00	65,76	36,38	1508,05	1,56	72,8	0,1018	17,9317
2610,00	66,24	36,27	1512,11	1,47	92,1	0,1288	17,8258
2620,00	66,26	36,27	1516,14	0,06	227,7	0,3185	17,7209
2630,00	65,77	36,46	1520,21	1,56	384,7	0,5381	17,6151
2640,00	65,96	36,45	1524,29	0,57	176,2	0,2464	17,5086
2650,00	66,33	36,52	1528,34	1,13	124,8	0,1746	17,4033
2660,00	66,18	36,60	1532,37	0,50	279,1	0,3903	17,2985
2670,00	65,75	36,60	1536,44	1,29	359,8	0,5033	17,1924
2680,00	65,53	36,66	1540,56	0,68	297,5	0,4161	17,0850
2690,00	65,37	36,81	1544,72	0,63	281,6	0,3939	16,9768
2700,00	64,67	36,99	1548,94	2,16	436,2	0,6101	16,8668

Tabulated Results (Redrill)							
Measured Depth (m)	Inclination Angle (deg)	Azimuth Angle (deg)	Vertical Depth (m)	Dogleg Severity (deg/30m)	Normal Force (N/m)	L-Load per Joint (T[metric])	Axial Drag (T[metric])
2710,00	64,36	37,23	1553,24	1,13	325,5	0,4553	16,7548
2720,00	64,11	37,40	1557,59	0,88	304,4	0,4258	16,6416
2730,00	64,11	37,49	1561,96	0,24	230,9	0,3230	16,5279
2740,00	64,05	37,42	1566,33	0,26	247,2	0,3458	16,4141
2750,00	64,07	37,32	1570,70	0,28	225,5	0,3154	16,3002
2760,00	64,43	37,07	1575,05	1,27	144,5	0,2021	16,1870
2770,00	65,13	36,94	1579,31	2,13	50,2	0,0703	16,0761
2780,00	65,62	36,86	1583,48	1,49	100,2	0,1402	15,9676
2790,00	65,48	36,90	1587,61	0,43	270,7	0,3786	15,8598
2800,00	65,46	36,95	1591,77	0,15	238,1	0,3330	15,7517
2810,00	64,97	36,93	1595,96	1,47	363,1	0,5079	15,6425
2820,00	64,49	37,07	1600,23	1,49	360,2	0,5038	15,5314
2830,00	64,65	37,16	1604,52	0,54	189,7	0,2653	15,4196
2840,00	64,92	37,36	1608,78	0,98	167,2	0,2339	15,3086
2850,00	65,05	37,38	1613,01	0,39	197,7	0,2765	15,1985
2860,00	64,69	37,39	1617,26	1,08	324,2	0,4535	15,0879
2870,00	64,75	37,28	1621,53	0,35	217,1	0,3036	14,9767
2880,00	64,87	37,28	1625,78	0,36	200,6	0,2806	14,8659
2890,00	64,58	37,40	1630,05	0,93	305,5	0,4272	14,7547
2900,00	64,57	37,42	1634,35	0,06	233,2	0,3262	14,6429
2910,00	64,73	37,26	1638,63	0,65	194,4	0,2719	14,5314
2920,00	64,83	37,29	1642,89	0,31	206,5	0,2888	14,4205
2930,00	65,22	37,31	1647,11	1,17	136,1	0,1903	14,3105
2940,00	65,08	37,45	1651,31	0,57	267,6	0,3743	14,2011
2950,00	65,01	37,49	1655,53	0,24	248,6	0,3477	14,0912
2960,00	65,09	37,69	1659,75	0,59	216,8	0,3033	13,9814
2970,00	64,74	37,81	1663,99	1,10	315,5	0,4413	13,8710
2980,00	64,74	37,80	1668,26	0,03	231,0	0,3231	13,7599
2987,00	64,92	37,91	1671,23	0,88	174,2	0,2436	13,6824
2990,00	65,00	37,95	1672,50	0,88	171,4	0,2398	13,6493
3000,00	64,59	38,16	1676,76	1,37	330,2	0,4618	13,5384
3011,00	64,13	38,40	1681,52	1,37	328,4	0,4594	13,4144
3030,00	65,62	38,57	1689,59	2,37	57,2	0,0800	13,2044
3036,00	66,09	38,63	1692,04	2,37	59,8	0,0836	13,1405
3060,00	67,92	40,03	1701,42	2,80	136,0	0,1903	12,8963
3061,00	68,00	40,09	1701,79	2,80	137,5	0,1924	12,8866
3086,00	69,70	41,54	1710,82	2,61	148,3	0,2074	12,6517
3090,00	69,80	41,99	1712,20	3,24	292,9	0,4097	12,6156
3111,00	70,33	44,34	1719,36	3,25	291,5	0,4077	12,4292
3120,00	70,25	44,58	1722,40	0,80	263,7	0,3688	12,3502
3136,00	70,12	45,01	1727,82	0,80	263,2	0,3681	12,2089
3150,00	69,96	45,82	1732,60	1,66	286,8	0,4012	12,0845
3161,00	69,83	46,45	1736,38	1,66	286,1	0,4001	11,9860
3180,00	70,20	49,28	1742,87	4,25	347,3	0,4858	11,8169
3186,00	70,32	50,18	1744,90	4,25	346,9	0,4853	11,7642
3210,00	71,16	52,14	1752,82	2,54	230,0	0,3217	11,5580
3211,00	71,19	52,22	1753,14	2,54	230,7	0,3227	11,5496
3236,00	72,56	52,58	1760,92	1,69	138,9	0,1942	11,3471
3240,00	72,62	52,88	1762,12	2,23	254,9	0,3566	11,3159
3261,00	72,96	54,48	1768,33	2,23	254,5	0,3560	11,1541
3270,00	72,83	54,34	1770,98	0,63	273,7	0,3828	11,0852
3286,00	72,59	54,09	1775,73	0,63	273,1	0,3820	10,9614

Tabulated Results (Redrill)							
Measured Depth (m)	Inclination Angle (deg)	Azimuth Angle (deg)	Vertical Depth (m)	Dogleg Severity (deg/30m)	Normal Force (N/m)	L-Load per Joint (T[metric])	Axial Drag (T[metric])
3300,00	72,08	54,64	1779,98	1,56	318,6	0,4457	10,8507
3311,00	71,68	55,07	1783,40	1,56	317,3	0,4439	10,7617
3330,00	71,54	54,18	1789,40	1,35	268,6	0,3756	10,6056
3336,00	71,49	53,90	1791,30	1,35	268,2	0,3752	10,5560
3360,00	73,54	55,99	1798,51	3,58	173,8	0,2431	10,3683
3361,00	73,63	56,08	1798,79	3,58	175,2	0,2451	10,3609
3386,00	75,19	57,26	1805,51	2,32	158,5	0,2217	10,1859
3390,00	75,09	56,74	1806,54	3,86	362,8	0,5075	10,1592
3411,00	74,59	53,99	1812,03	3,86	360,0	0,5036	10,0163
3420,00	74,30	54,08	1814,44	1,00	301,0	0,4210	9,9534
3436,00	73,79	54,23	1818,84	1,00	299,9	0,4195	9,8389
3450,00	73,49	54,53	1822,79	0,88	282,5	0,3951	9,7362
3461,00	73,26	54,76	1825,93	0,88	281,8	0,3942	9,6543
3480,00	74,34	54,71	1831,23	1,71	152,8	0,2137	9,5162
3486,00	74,68	54,69	1832,84	1,71	154,1	0,2155	9,4745
3510,00	73,96	57,86	1839,32	3,92	356,7	0,4990	9,3056
3511,00	73,93	57,99	1839,60	3,92	356,0	0,4980	9,2984
3515,00	73,90	57,66	1840,71	2,41	288,2	0,4031	9,2695
3536,00	73,72	55,91	1846,57	2,41	584,4	0,8174	8,9222
3540,00	73,59	55,77	1847,69	1,40	608,9	0,8518	8,8555
3561,00	72,92	55,02	1853,74	1,40	605,7	0,8472	8,4967
3570,00	73,67	55,32	1856,33	2,66	441,2	0,6171	8,3432
3586,00	74,99	55,84	1860,65	2,66	447,6	0,6261	8,0869
3600,00	74,90	55,32	1864,29	1,08	572,4	0,8006	7,8712
3611,00	74,83	54,92	1867,16	1,08	571,9	0,8000	7,7009
3630,00	74,54	55,60	1872,18	1,14	582,0	0,8141	7,4033
3636,00	74,45	55,82	1873,78	1,14	581,2	0,8130	7,3081
3660,00	74,25	56,45	1880,26	0,80	570,9	0,7986	6,9241
3661,00	74,24	56,48	1880,53	0,80	570,6	0,7981	6,9080
3666,00	74,27	56,92	1881,88	2,55	561,7	0,7857	6,8276
3680,00	74,89	57,31	1885,61	1,55	511,6	0,7156	6,6068
3687,00	75,20	57,50	1887,41	1,55	933,5	1,3057	6,4197
3690,00	75,18	57,56	1888,18	0,58	990,6	1,3856	6,3402
3708,00	75,04	57,89	1892,80	0,58	570,2	0,7976	6,0659
3711,00	75,02	57,94	1893,58	0,58	989,4	1,3839	5,9857
3714,00	75,00	58,00	1894,36	0,58	132,3	0,1851	5,9756
3720,00	75,19	57,72	1895,90	1,66	101,7	0,1422	5,9554
3742,00	75,90	56,70	1901,39	1,66	102,0	0,1427	5,8839
3750,00	76,01	56,90	1903,33	0,84	112,4	0,1572	5,8586
3770,00	76,30	57,40	1908,12	0,84	112,6	0,1575	5,7962
3780,00	76,44	57,22	1910,47	0,67	111,5	0,1559	5,7655
3798,00	76,70	56,90	1914,65	0,67	111,7	0,1562	5,7110
3807,00	76,60	56,30	1916,73	1,97	149,2	0,2087	5,6839
3810,00	76,54	56,36	1917,43	0,81	143,7	0,2010	5,6748
3818,00	76,40	56,52	1919,30	0,81	143,5	0,2008	5,6504
3840,00	75,99	56,97	1924,55	0,81	143,1	0,2002	5,5820
3858,70	75,64	57,35	1929,13	0,81	142,7	0,1996	5,5223
3870,00	75,21	57,36	1931,98	1,15	159,7	0,2233	5,4852
3886,40	74,58	57,38	1936,25	1,15	159,0	0,2224	5,4295
3900,00	74,19	57,20	1939,91	0,95	150,3	0,2102	5,3818
3914,00	73,78	57,01	1943,78	0,95	149,8	0,2095	5,3314
3930,00	73,11	57,16	1948,33	1,29	160,5	0,2246	5,2720

Tabulated Results (Redrill)							
Measured Depth (m)	Inclination Angle (deg)	Azimuth Angle (deg)	Vertical Depth (m)	Dogleg Severity (deg/30m)	Normal Force (N/m)	L-Load per Joint (T[metric])	Axial Drag (T[metric])
3941,70	72,62	57,27	1951,78	1,29	159,8	0,2236	5,2271
3960,00	72,42	57,27	1957,28	0,34	131,8	0,1844	5,1554
3969,40	72,31	57,27	1960,13	0,34	131,6	0,1841	5,1183
3990,00	72,02	57,03	1966,44	0,54	134,2	0,1877	5,0361
3997,00	71,92	56,95	1968,60	0,54	134,0	0,1875	5,0078
4020,00	71,70	56,64	1975,78	0,47	129,8	0,1816	4,9142
4024,70	71,66	56,58	1977,26	0,47	129,7	0,1814	4,8950
4050,00	70,92	56,37	1985,38	0,91	145,3	0,2032	4,7892
4052,30	70,85	56,35	1986,13	0,91	145,0	0,2028	4,7794
4080,00	70,40	56,13	1995,32	0,54	133,7	0,1870	4,6596
4107,70	69,96	55,78	2004,71	0,60	132,9	0,1859	4,5372
4110,00	69,89	55,75	2005,50	0,93	142,8	0,1997	4,5269
4135,30	69,16	55,47	2014,35	0,93	141,9	0,1985	4,4116
4140,00	69,08	55,46	2016,02	0,55	133,0	0,1861	4,3897
4163,00	68,66	55,39	2024,32	0,55	132,5	0,1853	4,2816
4170,00	68,59	55,31	2026,87	0,42	126,4	0,1768	4,2484
4190,60	68,39	55,09	2034,42	0,42	126,1	0,1764	4,1500
4200,00	68,21	55,12	2037,90	0,59	132,5	0,1853	4,1046
4218,30	67,85	55,18	2044,74	0,59	132,0	0,1846	4,0154
4230,00	67,72	55,15	2049,17	0,33	125,7	0,1758	3,9578
4246,00	67,55	55,11	2055,25	0,33	125,4	0,1754	3,8784
4260,00	67,17	54,91	2060,64	0,91	136,0	0,1902	3,8082
4273,60	66,80	54,71	2065,96	0,91	135,3	0,1893	3,7389
4290,00	66,26	54,37	2072,49	1,14	138,3	0,1935	3,6537
4301,30	65,89	54,13	2077,07	1,14	137,6	0,1924	3,5940
4320,00	65,31	53,95	2084,80	0,97	135,2	0,1891	3,4933
4328,90	65,03	53,87	2088,54	0,97	134,5	0,1881	3,4446
4350,00	64,44	53,43	2097,54	1,01	131,9	0,1845	3,3272
4353,00	64,36	53,37	2098,84	1,01	131,5	0,1839	3,3103
4356,60	64,26	53,29	2100,40	1,01	556,5	0,7784	3,2148
4380,00	63,53	52,99	2110,70	1,01	553,1	0,7736	2,5844
4384,30	63,39	52,93	2112,62	1,01	550,4	0,7699	2,4668
4410,00	62,60	52,68	2124,29	0,96	544,2	0,7612	1,7524
4411,90	62,54	52,66	2125,16	0,96	541,9	0,7580	1,6989
4439,60	61,96	52,71	2138,06	0,63	534,6	0,7478	0,9093
4440,00	61,96	52,71	2138,25	0,00	531,7	0,7437	0,8978
4465,00	61,67	52,65	2150,06	0,34	529,6	0,7408	0,1750
4467,00	61,65	52,64	2151,01	0,34	731,9	1,0238	0,0946
4467,20	61,65	52,64	2151,10	0,34	528,6	0,7394	0,0887
4468,00	61,63	52,64	2151,48	0,83	528,7	0,7395	0,0655
4469,00	61,60	52,63	2151,96	0,83	1188,6	1,6625	0,0000

Table 22: 30/10 B-14A T3 tabulated loads and forces

Tabulated Results (Redrill)									
Measured Depth (m)	WF Base Rem. Wall (in)	WF Base Burst (kPa)	WF Base Collapse (kPa)	WF Low Rem. Wall (in)	WF Low Burst (kPa)	WF Low Collapse (kPa)	WF High Rem. Wall (in)	WF High Burst (kPa)	WF High Collapse (kPa)
0,00	0,545	54658,6	45625,8	0,545	54658,6	45625,8	0,545	54658,6	45625,8
30,00	0,545	54658,6	45625,8	0,545	54658,6	45625,8	0,545	54658,6	45625,8
39,10	0,545	54658,6	45625,8	0,545	54658,6	45625,8	0,545	54658,6	45625,8
60,00	0,403	40393,5	22166,7	0,403	40393,5	22166,7	0,403	40393,5	22166,7
90,00	0,403	40393,5	22166,7	0,403	40393,5	22166,7	0,403	40393,5	22166,7
120,00	0,399	40041,3	21764,7	0,399	40041,3	21764,7	0,399	40041,3	21764,7
150,00	0,394	39512,9	21161,6	0,394	39512,9	21161,6	0,394	39512,9	21161,6
180,00	0,387	38808,5	20357,5	0,387	38808,5	20357,5	0,387	38808,5	20357,5
210,00	0,379	38016,0	19452,9	0,379	38016,0	19452,9	0,379	38016,0	19452,9
214,55	0,374	37487,7	18849,9	0,374	37487,7	18849,9	0,374	37487,7	18849,9
224,64	0,462	46381,3	31101,5	0,462	46381,3	31101,5	0,462	46381,3	31101,5
234,74	0,470	47173,8	32492,1	0,470	47173,8	32492,1	0,470	47173,8	32492,1
240,00	0,485	48670,7	35118,8	0,485	48670,7	35118,8	0,485	48670,7	35118,8
244,84	0,485	48670,7	35118,8	0,485	48670,7	35118,8	0,485	48670,7	35118,8
254,95	0,467	46821,5	31874,0	0,467	46821,5	31874,0	0,467	46821,5	31874,0
265,06	0,443	44444,0	27702,2	0,443	44444,0	27702,2	0,443	44444,0	27702,2
270,00	0,473	47437,9	32955,6	0,473	47437,9	32955,6	0,473	47437,9	32955,6
275,18	0,473	47437,9	32955,6	0,473	47437,9	32955,6	0,473	47437,9	32955,6
285,30	0,502	50343,7	38054,5	0,502	50343,7	38054,5	0,502	50343,7	38054,5
295,43	0,467	46821,5	31874,0	0,467	46821,5	31874,0	0,467	46821,5	31874,0
300,00	0,457	45852,9	30174,4	0,457	45852,9	30174,4	0,457	45852,9	30174,4
305,56	0,457	45852,9	30174,4	0,457	45852,9	30174,4	0,457	45852,9	30174,4
315,69	0,460	46117,1	30637,9	0,460	46117,1	30637,9	0,460	46117,1	30637,9
325,83	0,468	46909,6	32028,5	0,468	46909,6	32028,5	0,468	46909,6	32028,5
330,00	0,475	47614,0	33264,6	0,475	47614,0	33264,6	0,475	47614,0	33264,6
335,98	0,475	47614,0	33264,6	0,475	47614,0	33264,6	0,475	47614,0	33264,6
346,12	0,459	46029,0	30483,4	0,459	46029,0	30483,4	0,459	46029,0	30483,4
356,27	0,423	42418,8	24478,5	0,423	42418,8	24478,5	0,423	42418,8	24478,5
360,00	0,437	43827,6	26620,6	0,437	43827,6	26620,6	0,437	43827,6	26620,6
366,40	0,437	43827,6	26620,6	0,437	43827,6	26620,6	0,437	43827,6	26620,6
376,54	0,441	44267,9	27393,2	0,441	44267,9	27393,2	0,441	44267,9	27393,2
386,68	0,424	42506,8	24579,0	0,424	42506,8	24579,0	0,424	42506,8	24579,0
390,00	0,412	41362,1	23272,3	0,412	41362,1	23272,3	0,412	41362,1	23272,3
396,83	0,412	41362,1	23272,3	0,412	41362,1	23272,3	0,412	41362,1	23272,3
407,00	0,403	40393,5	22166,7	0,403	40393,5	22166,7	0,403	40393,5	22166,7
417,19	0,382	38280,2	19754,5	0,382	38280,2	19754,5	0,382	38280,2	19754,5
420,00	0,376	37663,8	19050,9	0,376	37663,8	19050,9	0,376	37663,8	19050,9
427,39	0,376	37663,8	19050,9	0,376	37663,8	19050,9	0,376	37663,8	19050,9
437,63	0,376	37663,8	19050,9	0,376	37663,8	19050,9	0,376	37663,8	19050,9
447,90	0,367	36783,2	18045,8	0,367	36783,2	18045,8	0,367	36783,2	18045,8
450,00	0,366	36695,2	17945,3	0,366	36695,2	17945,3	0,366	36695,2	17945,3
458,20	0,366	36695,2	17945,3	0,366	36695,2	17945,3	0,366	36695,2	17945,3
468,55	0,357	35814,6	16940,2	0,357	35814,6	16940,2	0,357	35814,6	16940,2
478,95	0,346	34669,9	15633,5	0,346	34669,9	15633,5	0,346	34669,9	15633,5
480,00	0,341	34229,6	15131,0	0,341	34229,6	15131,0	0,341	34229,6	15131,0
489,42	0,343	34405,7	15332,0	0,343	34405,7	15332,0	0,343	34405,7	15332,0
499,96	0,335	33613,2	14427,4	0,335	33613,2	14427,4	0,335	33613,2	14427,4
510,00	0,331	33172,9	13924,8	0,331	33172,9	13924,8	0,331	33172,9	13924,8
510,60	0,332	33261,0	14025,3	0,332	33261,0	14025,3	0,332	33261,0	14025,3
521,33	0,332	33261,0	14025,3	0,332	33261,0	14025,3	0,332	33261,0	14025,3
532,17	0,333	33349,1	14125,9	0,333	33349,1	14125,9	0,333	33349,1	14125,9
540,00	0,347	34757,9	15734,0	0,347	34757,9	15734,0	0,347	34757,9	15734,0

Tabulated Results (Redrill)									
Measure d Depth (m)	WF Base Rem. Wall (in)	WF Base Burst (kPa)	WF Base Collapse (kPa)	WF Low Rem. Wall (in)	WF Low Burst (kPa)	WF Low Collapse (kPa)	WF High Rem. Wall (in)	WF High Burst (kPa)	WF High Collapse (kPa)
543,12	0,347	34846,0	15834,5	0,347	34846,0	15834,5	0,347	34846,0	15834,5
554,18	0,367	36783,2	18045,8	0,367	36783,2	18045,8	0,367	36783,2	18045,8
565,35	0,377	37839,9	19251,9	0,377	37839,9	19251,9	0,377	37839,9	19251,9
570,00	0,385	38632,4	20156,5	0,385	38632,4	20156,5	0,385	38632,4	20156,5
576,63	0,386	38720,4	20257,0	0,386	38720,4	20257,0	0,386	38720,4	20257,0
588,01	0,390	39160,7	20759,6	0,390	39160,7	20759,6	0,390	39160,7	20759,6
599,50	0,392	39336,8	20960,6	0,392	39336,8	20960,6	0,392	39336,8	20960,6
600,00	0,386	38720,4	20257,0	0,386	38720,4	20257,0	0,386	38720,4	20257,0
611,12	0,387	38808,5	20357,5	0,387	38808,5	20357,5	0,387	38808,5	20357,5
622,89	0,370	37135,4	18447,8	0,370	37135,4	18447,8	0,370	37135,4	18447,8
630,00	0,351	35198,2	16236,6	0,351	35198,2	16236,6	0,351	35198,2	16236,6
634,84	0,352	35286,3	16337,1	0,352	35286,3	16337,1	0,352	35286,3	16337,1
647,03	0,344	34493,8	15432,5	0,344	34493,8	15432,5	0,344	34493,8	15432,5
659,48	0,349	35022,1	16035,6	0,349	35022,1	16035,6	0,349	35022,1	16035,6
660,00	0,359	35990,7	17141,2	0,359	35990,7	17141,2	0,359	35990,7	17141,2
672,21	0,361	36166,8	17342,2	0,361	36166,8	17342,2	0,361	36166,8	17342,2
685,22	0,381	38192,1	19654,0	0,381	38192,1	19654,0	0,381	38192,1	19654,0
690,00	0,395	39601,0	21262,1	0,395	39601,0	21262,1	0,395	39601,0	21262,1
698,49	0,395	39601,0	21262,1	0,395	39601,0	21262,1	0,395	39601,0	21262,1
712,00	0,374	37487,7	18849,9	0,374	37487,7	18849,9	0,374	37487,7	18849,9
720,00	0,358	35902,7	17040,7	0,358	35902,7	17040,7	0,358	35902,7	17040,7
725,82	0,358	35902,7	17040,7	0,358	35902,7	17040,7	0,358	35902,7	17040,7
739,97	0,362	36342,9	17543,2	0,362	36342,9	17543,2	0,362	36342,9	17543,2
750,00	0,397	39777,1	21463,1	0,397	39777,1	21463,1	0,397	39777,1	21463,1
754,42	0,397	39777,1	21463,1	0,397	39777,1	21463,1	0,397	39777,1	21463,1
769,06	0,408	40921,8	22769,8	0,408	40921,8	22769,8	0,408	40921,8	22769,8
780,00	0,412	41362,1	23272,3	0,412	41362,1	23272,3	0,412	41362,1	23272,3
783,84	0,412	41362,1	23272,3	0,412	41362,1	23272,3	0,412	41362,1	23272,3
798,91	0,407	40833,8	22669,3	0,407	40833,8	22669,3	0,407	40833,8	22669,3
810,00	0,386	38720,4	20257,0	0,386	38720,4	20257,0	0,386	38720,4	20257,0
814,44	0,387	38808,5	20357,5	0,387	38808,5	20357,5	0,387	38808,5	20357,5
830,58	0,391	39248,8	20860,1	0,391	39248,8	20860,1	0,391	39248,8	20860,1
840,00	0,402	40305,4	22066,2	0,402	40305,4	22066,2	0,402	40305,4	22066,2
847,41	0,403	40393,5	22166,7	0,403	40393,5	22166,7	0,403	40393,5	22166,7
864,93	0,419	42066,5	24076,4	0,419	42066,5	24076,4	0,419	42066,5	24076,4
870,00	0,462	46381,3	31101,5	0,462	46381,3	31101,5	0,462	46381,3	31101,5
883,00	0,463	46469,3	31256,0	0,463	46469,3	31256,0	0,463	46469,3	31256,0
900,00	0,447	44796,3	28320,3	0,447	44796,3	28320,3	0,447	44796,3	28320,3
901,32	0,447	44796,3	28320,3	0,447	44796,3	28320,3	0,447	44796,3	28320,3
919,69	0,440	44091,8	27084,2	0,440	44091,8	27084,2	0,440	44091,8	27084,2
930,00	0,451	45236,5	29092,8	0,451	45236,5	29092,8	0,451	45236,5	29092,8
938,36	0,452	45324,6	29247,3	0,452	45324,6	29247,3	0,452	45324,6	29247,3
957,85	0,418	41890,4	23875,4	0,418	41890,4	23875,4	0,418	41890,4	23875,4
960,00	0,419	41978,5	23975,9	0,419	41978,5	23975,9	0,419	41978,5	23975,9
978,53	0,420	42154,6	24176,9	0,420	42154,6	24176,9	0,420	42154,6	24176,9
990,00	0,439	44003,8	26929,6	0,439	44003,8	26929,6	0,439	44003,8	26929,6
1000,59	0,439	44003,8	26929,6	0,439	44003,8	26929,6	0,439	44003,8	26929,6
1020,00	0,463	46469,3	31256,0	0,463	46469,3	31256,0	0,463	46469,3	31256,0
1023,59	0,462	46381,3	31101,5	0,462	46381,3	31101,5	0,462	46381,3	31101,5
1046,53	0,404	40481,5	22267,2	0,404	40481,5	22267,2	0,404	40481,5	22267,2
1050,00	0,454	45500,7	29556,3	0,454	45500,7	29556,3	0,454	45500,7	29556,3
1069,38	0,454	45500,7	29556,3	0,454	45500,7	29556,3	0,454	45500,7	29556,3

Tabulated Results (Redrill)									
Measured Depth (m)	WF Base Rem. Wall (in)	WF Base Burst (kPa)	WF Base Collapse (kPa)	WF Low Rem. Wall (in)	WF Low Burst (kPa)	WF Low Collapse (kPa)	WF High Rem. Wall (in)	WF High Burst (kPa)	WF High Collapse (kPa)
1080,00	0,459	46029,0	30483,4	0,459	46029,0	30483,4	0,459	46029,0	30483,4
1093,06	0,460	46117,1	30637,9	0,460	46117,1	30637,9	0,460	46117,1	30637,9
1110,00	0,449	45060,4	28783,8	0,449	45060,4	28783,8	0,449	45060,4	28783,8
1117,72	0,448	44972,4	28629,3	0,448	44972,4	28629,3	0,448	44972,4	28629,3
1140,00	0,407	40833,8	22669,3	0,407	40833,8	22669,3	0,407	40833,8	22669,3
1142,43	0,407	40833,8	22669,3	0,407	40833,8	22669,3	0,407	40833,8	22669,3
1166,94	0,438	43915,7	26775,1	0,438	43915,7	26775,1	0,438	43915,7	26775,1
1170,00	0,435	43651,5	26311,6	0,435	43651,5	26311,6	0,435	43651,5	26311,6
1191,57	0,435	43651,5	26311,6	0,435	43651,5	26311,6	0,435	43651,5	26311,6
1200,00	0,369	37047,4	18347,3	0,369	37047,4	18347,3	0,369	37047,4	18347,3
1215,52	0,369	37047,4	18347,3	0,369	37047,4	18347,3	0,369	37047,4	18347,3
1230,00	0,356	35726,5	16839,6	0,356	35726,5	16839,6	0,356	35726,5	16839,6
1237,95	0,356	35726,5	16839,6	0,356	35726,5	16839,6	0,356	35726,5	16839,6
1259,74	0,449	45060,4	28783,8	0,449	45060,4	28783,8	0,449	45060,4	28783,8
1260,00	0,468	46909,6	32028,5	0,468	46909,6	32028,5	0,468	46909,6	32028,5
1282,19	0,469	46997,6	32183,1	0,469	46997,6	32183,1	0,469	46997,6	32183,1
1290,00	0,475	47614,0	33264,6	0,475	47614,0	33264,6	0,475	47614,0	33264,6
1305,57	0,474	47526,0	33110,1	0,474	47526,0	33110,1	0,474	47526,0	33110,1
1320,00	0,449	45060,4	28783,8	0,449	45060,4	28783,8	0,449	45060,4	28783,8
1329,45	0,449	45060,4	28783,8	0,449	45060,4	28783,8	0,449	45060,4	28783,8
1350,00	0,463	46469,3	31256,0	0,463	46469,3	31256,0	0,463	46469,3	31256,0
1360,00	0,463	46469,3	31256,0	0,463	46469,3	31256,0	0,463	46469,3	31256,0
1370,00	0,479	48054,3	34037,2	0,479	48054,3	34037,2	0,479	48054,3	34037,2
1380,00	0,457	45852,9	30174,4	0,457	45852,9	30174,4	0,457	45852,9	30174,4
1390,00	0,454	45500,7	29556,3	0,454	45500,7	29556,3	0,454	45500,7	29556,3
1400,00	0,461	46205,1	30792,5	0,461	46205,1	30792,5	0,461	46205,1	30792,5
1410,00	0,456	45764,9	30019,9	0,456	45764,9	30019,9	0,456	45764,9	30019,9
1420,00	0,432	43299,3	25693,5	0,432	43299,3	25693,5	0,432	43299,3	25693,5
1430,00	0,378	37927,9	19352,4	0,378	37927,9	19352,4	0,378	37927,9	19352,4
1440,00	0,419	41978,5	23975,9	0,419	41978,5	23975,9	0,419	41978,5	23975,9
1450,00	0,406	40745,7	22568,8	0,406	40745,7	22568,8	0,406	40745,7	22568,8
1460,00	0,405	40657,7	22468,2	0,405	40657,7	22468,2	0,405	40657,7	22468,2
1470,00	0,405	40657,7	22468,2	0,405	40657,7	22468,2	0,405	40657,7	22468,2
1480,00	0,429	43035,1	25230,0	0,429	43035,1	25230,0	0,429	43035,1	25230,0
1490,00	0,407	40833,8	22669,3	0,407	40833,8	22669,3	0,407	40833,8	22669,3
1500,00	0,390	39072,7	20659,1	0,390	39072,7	20659,1	0,390	39072,7	20659,1
1510,00	0,421	42242,6	24277,4	0,421	42242,6	24277,4	0,421	42242,6	24277,4
1520,00	0,445	44620,1	28011,2	0,445	44620,1	28011,2	0,445	44620,1	28011,2
1530,00	0,440	44091,8	27084,2	0,440	44091,8	27084,2	0,440	44091,8	27084,2
1540,00	0,453	45412,6	29401,8	0,453	45412,6	29401,8	0,453	45412,6	29401,8
1550,00	0,466	46733,5	31719,5	0,466	46733,5	31719,5	0,466	46733,5	31719,5
1560,00	0,453	45412,6	29401,8	0,453	45412,6	29401,8	0,453	45412,6	29401,8
1570,00	0,403	40393,5	22166,7	0,403	40393,5	22166,7	0,403	40393,5	22166,7
1580,00	0,385	38632,4	20156,5	0,385	38632,4	20156,5	0,385	38632,4	20156,5
1590,00	0,415	41626,3	23573,9	0,415	41626,3	23573,9	0,415	41626,3	23573,9
1600,00	0,419	42066,5	24076,4	0,419	42066,5	24076,4	0,419	42066,5	24076,4
1610,00	0,402	40305,4	22066,2	0,402	40305,4	22066,2	0,402	40305,4	22066,2
1620,00	0,390	39072,7	20659,1	0,390	39072,7	20659,1	0,390	39072,7	20659,1
1630,00	0,412	41362,1	23272,3	0,412	41362,1	23272,3	0,412	41362,1	23272,3
1640,00	0,407	40833,8	22669,3	0,407	40833,8	22669,3	0,407	40833,8	22669,3
1650,00	0,401	40217,4	21965,7	0,401	40217,4	21965,7	0,401	40217,4	21965,7
1660,00	0,424	42506,8	24579,0	0,424	42506,8	24579,0	0,424	42506,8	24579,0

Tabulated Results (Redrill)									
Measured Depth (m)	WF Base Rem. Wall (in)	WF Base Burst (kPa)	WF Base Collapse (kPa)	WF Low Rem. Wall (in)	WF Low Burst (kPa)	WF Low Collapse (kPa)	WF High Rem. Wall (in)	WF High Burst (kPa)	WF High Collapse (kPa)
1670,00	0,430	43123,2	25384,5	0,430	43123,2	25384,5	0,430	43123,2	25384,5
1680,00	0,397	39777,1	21463,1	0,397	39777,1	21463,1	0,397	39777,1	21463,1
1690,00	0,394	39512,9	21161,6	0,394	39512,9	21161,6	0,394	39512,9	21161,6
1700,00	0,426	42771,0	24880,5	0,426	42771,0	24880,5	0,426	42771,0	24880,5
1710,00	0,447	44796,3	28320,3	0,447	44796,3	28320,3	0,447	44796,3	28320,3
1720,00	0,423	42418,8	24478,5	0,423	42418,8	24478,5	0,423	42418,8	24478,5
1730,00	0,468	46909,6	32028,5	0,468	46909,6	32028,5	0,468	46909,6	32028,5
1740,00	0,417	41802,4	23774,9	0,417	41802,4	23774,9	0,417	41802,4	23774,9
1750,00	0,399	40041,3	21764,7	0,399	40041,3	21764,7	0,399	40041,3	21764,7
1760,00	0,383	38456,3	19955,5	0,383	38456,3	19955,5	0,383	38456,3	19955,5
1770,00	0,398	39953,2	21664,2	0,398	39953,2	21664,2	0,398	39953,2	21664,2
1780,00	0,413	41450,2	23372,8	0,413	41450,2	23372,8	0,413	41450,2	23372,8
1790,00	0,409	41009,9	22870,3	0,409	41009,9	22870,3	0,409	41009,9	22870,3
1800,00	0,393	39424,9	21061,1	0,393	39424,9	21061,1	0,393	39424,9	21061,1
1810,00	0,464	46557,4	31410,5	0,464	46557,4	31410,5	0,464	46557,4	31410,5
1820,00	0,469	46997,6	32183,1	0,469	46997,6	32183,1	0,469	46997,6	32183,1
1830,00	0,465	46645,4	31565,0	0,465	46645,4	31565,0	0,465	46645,4	31565,0
1840,00	0,405	40657,7	22468,2	0,405	40657,7	22468,2	0,405	40657,7	22468,2
1850,00	0,419	42066,5	24076,4	0,419	42066,5	24076,4	0,419	42066,5	24076,4
1860,00	0,430	43123,2	25384,5	0,430	43123,2	25384,5	0,430	43123,2	25384,5
1870,00	0,437	43827,6	26620,6	0,437	43827,6	26620,6	0,437	43827,6	26620,6
1880,00	0,433	43387,4	25848,1	0,433	43387,4	25848,1	0,433	43387,4	25848,1
1890,00	0,428	42947,1	25081,5	0,428	42947,1	25081,5	0,428	42947,1	25081,5
1900,00	0,436	43739,6	26466,1	0,436	43739,6	26466,1	0,436	43739,6	26466,1
1910,00	0,426	42682,9	24780,0	0,426	42682,9	24780,0	0,426	42682,9	24780,0
1920,00	0,439	44003,8	26929,6	0,439	44003,8	26929,6	0,439	44003,8	26929,6
1930,00	0,428	42947,1	25081,5	0,428	42947,1	25081,5	0,428	42947,1	25081,5
1940,00	0,423	42418,8	24478,5	0,423	42418,8	24478,5	0,423	42418,8	24478,5
1950,00	0,422	42330,7	24378,0	0,422	42330,7	24378,0	0,422	42330,7	24378,0
1960,00	0,419	42066,5	24076,4	0,419	42066,5	24076,4	0,419	42066,5	24076,4
1970,00	0,417	41802,4	23774,9	0,417	41802,4	23774,9	0,417	41802,4	23774,9
1980,00	0,452	45324,6	29247,3	0,452	45324,6	29247,3	0,452	45324,6	29247,3
1990,00	0,441	44179,9	27238,7	0,441	44179,9	27238,7	0,441	44179,9	27238,7
2000,00	0,454	45500,7	29556,3	0,454	45500,7	29556,3	0,454	45500,7	29556,3
2010,00	0,479	48054,3	34037,2	0,479	48054,3	34037,2	0,479	48054,3	34037,2
2020,00	0,454	45500,7	29556,3	0,454	45500,7	29556,3	0,454	45500,7	29556,3
2030,00	0,438	43915,7	26775,1	0,438	43915,7	26775,1	0,438	43915,7	26775,1
2040,00	0,461	46205,1	30792,5	0,461	46205,1	30792,5	0,461	46205,1	30792,5
2050,00	0,455	45588,8	29710,9	0,455	45588,8	29710,9	0,455	45588,8	29710,9
2060,00	0,436	43739,6	26466,1	0,436	43739,6	26466,1	0,436	43739,6	26466,1
2070,00	0,448	44972,4	28629,3	0,448	44972,4	28629,3	0,448	44972,4	28629,3
2080,00	0,456	45764,9	30019,9	0,456	45764,9	30019,9	0,456	45764,9	30019,9
2090,00	0,453	45412,6	29401,8	0,453	45412,6	29401,8	0,453	45412,6	29401,8
2100,00	0,431	43211,3	25539,0	0,431	43211,3	25539,0	0,431	43211,3	25539,0
2110,00	0,441	44267,9	27393,2	0,441	44267,9	27393,2	0,441	44267,9	27393,2
2120,00	0,469	46997,6	32183,1	0,469	46997,6	32183,1	0,469	46997,6	32183,1
2130,00	0,462	46381,3	31101,5	0,462	46381,3	31101,5	0,462	46381,3	31101,5
2140,00	0,420	42154,6	24176,9	0,420	42154,6	24176,9	0,420	42154,6	24176,9
2150,00	0,438	43915,7	26775,1	0,438	43915,7	26775,1	0,438	43915,7	26775,1
2160,00	0,439	44003,8	26929,6	0,439	44003,8	26929,6	0,439	44003,8	26929,6
2170,00	0,406	40745,7	22568,8	0,406	40745,7	22568,8	0,406	40745,7	22568,8
2180,00	0,397	39777,1	21463,1	0,397	39777,1	21463,1	0,397	39777,1	21463,1

Tabulated Results (Redrill)									
Measured Depth (m)	WF Base Rem. Wall (in)	WF Base Burst (kPa)	WF Base Collapse (kPa)	WF Low Rem. Wall (in)	WF Low Burst (kPa)	WF Low Collapse (kPa)	WF High Rem. Wall (in)	WF High Burst (kPa)	WF High Collapse (kPa)
2190,00	0,400	40129,3	21865,2	0,400	40129,3	21865,2	0,400	40129,3	21865,2
2200,00	0,432	43299,3	25693,5	0,432	43299,3	25693,5	0,432	43299,3	25693,5
2210,00	0,434	43563,5	26157,1	0,434	43563,5	26157,1	0,434	43563,5	26157,1
2220,00	0,392	39336,8	20960,6	0,392	39336,8	20960,6	0,392	39336,8	20960,6
2230,00	0,406	40745,7	22568,8	0,406	40745,7	22568,8	0,406	40745,7	22568,8
2240,00	0,433	43387,4	25848,1	0,433	43387,4	25848,1	0,433	43387,4	25848,1
2250,00	0,455	45588,8	29710,9	0,455	45588,8	29710,9	0,455	45588,8	29710,9
2260,00	0,419	42066,5	24076,4	0,419	42066,5	24076,4	0,419	42066,5	24076,4
2270,00	0,461	46205,1	30792,5	0,461	46205,1	30792,5	0,461	46205,1	30792,5
2280,00	0,472	47349,9	32801,1	0,472	47349,9	32801,1	0,472	47349,9	32801,1
2290,00	0,448	44884,3	28474,8	0,448	44884,3	28474,8	0,448	44884,3	28474,8
2300,00	0,431	43211,3	25539,0	0,431	43211,3	25539,0	0,431	43211,3	25539,0
2310,00	0,455	45676,8	29865,4	0,455	45676,8	29865,4	0,455	45676,8	29865,4
2320,00	0,448	44884,3	28474,8	0,448	44884,3	28474,8	0,448	44884,3	28474,8
2330,00	0,415	41626,3	23573,9	0,415	41626,3	23573,9	0,415	41626,3	23573,9
2340,00	0,474	47526,0	33110,1	0,474	47526,0	33110,1	0,474	47526,0	33110,1
2350,00	0,469	46997,6	32183,1	0,469	46997,6	32183,1	0,469	46997,6	32183,1
2360,00	0,474	47526,0	33110,1	0,474	47526,0	33110,1	0,474	47526,0	33110,1
2370,00	0,471	47261,8	32646,6	0,471	47261,8	32646,6	0,471	47261,8	32646,6
2380,00	0,442	44356,0	27547,7	0,442	44356,0	27547,7	0,442	44356,0	27547,7
2390,00	0,442	44356,0	27547,7	0,442	44356,0	27547,7	0,442	44356,0	27547,7
2400,00	0,443	44444,0	27702,2	0,443	44444,0	27702,2	0,443	44444,0	27702,2
2410,00	0,439	44003,8	26929,6	0,439	44003,8	26929,6	0,439	44003,8	26929,6
2420,00	0,442	44356,0	27547,7	0,442	44356,0	27547,7	0,442	44356,0	27547,7
2430,00	0,428	42947,1	25081,5	0,428	42947,1	25081,5	0,428	42947,1	25081,5
2440,00	0,407	40833,8	22669,3	0,407	40833,8	22669,3	0,407	40833,8	22669,3
2450,00	0,427	42859,0	24981,0	0,427	42859,0	24981,0	0,427	42859,0	24981,0
2460,00	0,458	45941,0	30328,9	0,458	45941,0	30328,9	0,458	45941,0	30328,9
2470,00	0,459	46029,0	30483,4	0,459	46029,0	30483,4	0,459	46029,0	30483,4
2480,00	0,429	43035,1	25230,0	0,429	43035,1	25230,0	0,429	43035,1	25230,0
2490,00	0,422	42330,7	24378,0	0,422	42330,7	24378,0	0,422	42330,7	24378,0
2500,00	0,432	43299,3	25693,5	0,432	43299,3	25693,5	0,432	43299,3	25693,5
2510,00	0,415	41626,3	23573,9	0,415	41626,3	23573,9	0,415	41626,3	23573,9
2520,00	0,425	42594,9	24679,5	0,425	42594,9	24679,5	0,425	42594,9	24679,5
2530,00	0,455	45588,8	29710,9	0,455	45588,8	29710,9	0,455	45588,8	29710,9
2540,00	0,448	44884,3	28474,8	0,448	44884,3	28474,8	0,448	44884,3	28474,8
2550,00	0,429	43035,1	25230,0	0,429	43035,1	25230,0	0,429	43035,1	25230,0
2560,00	0,439	44003,8	26929,6	0,439	44003,8	26929,6	0,439	44003,8	26929,6
2570,00	0,429	43035,1	25230,0	0,429	43035,1	25230,0	0,429	43035,1	25230,0
2580,00	0,423	42418,8	24478,5	0,423	42418,8	24478,5	0,423	42418,8	24478,5
2590,00	0,440	44091,8	27084,2	0,440	44091,8	27084,2	0,440	44091,8	27084,2
2600,00	0,470	47173,8	32492,1	0,470	47173,8	32492,1	0,470	47173,8	32492,1
2610,00	0,467	46821,5	31874,0	0,467	46821,5	31874,0	0,467	46821,5	31874,0
2620,00	0,441	44267,9	27393,2	0,441	44267,9	27393,2	0,441	44267,9	27393,2
2630,00	0,416	41714,3	23674,4	0,416	41714,3	23674,4	0,416	41714,3	23674,4
2640,00	0,450	45148,5	28938,3	0,450	45148,5	28938,3	0,450	45148,5	28938,3
2650,00	0,460	46117,1	30637,9	0,460	46117,1	30637,9	0,460	46117,1	30637,9
2660,00	0,433	43387,4	25848,1	0,433	43387,4	25848,1	0,433	43387,4	25848,1
2670,00	0,420	42154,6	24176,9	0,420	42154,6	24176,9	0,420	42154,6	24176,9
2680,00	0,430	43123,2	25384,5	0,430	43123,2	25384,5	0,430	43123,2	25384,5
2690,00	0,433	43387,4	25848,1	0,433	43387,4	25848,1	0,433	43387,4	25848,1
2700,00	0,409	41009,9	22870,3	0,409	41009,9	22870,3	0,409	41009,9	22870,3

Tabulated Results (Redrill)									
Measured Depth (m)	WF Base Rem. Wall (in)	WF Base Burst (kPa)	WF Base Collapse (kPa)	WF Low Rem. Wall (in)	WF Low Burst (kPa)	WF Low Collapse (kPa)	WF High Rem. Wall (in)	WF High Burst (kPa)	WF High Collapse (kPa)
2710,00	0,426	42682,9	24780,0	0,426	42682,9	24780,0	0,426	42682,9	24780,0
2720,00	0,428	42947,1	25081,5	0,428	42947,1	25081,5	0,428	42947,1	25081,5
2730,00	0,441	44179,9	27238,7	0,441	44179,9	27238,7	0,441	44179,9	27238,7
2740,00	0,438	43915,7	26775,1	0,438	43915,7	26775,1	0,438	43915,7	26775,1
2750,00	0,441	44267,9	27393,2	0,441	44267,9	27393,2	0,441	44267,9	27393,2
2760,00	0,456	45764,9	30019,9	0,456	45764,9	30019,9	0,456	45764,9	30019,9
2770,00	0,472	47349,9	32801,1	0,472	47349,9	32801,1	0,472	47349,9	32801,1
2780,00	0,464	46557,4	31410,5	0,464	46557,4	31410,5	0,464	46557,4	31410,5
2790,00	0,434	43563,5	26157,1	0,434	43563,5	26157,1	0,434	43563,5	26157,1
2800,00	0,440	44091,8	27084,2	0,440	44091,8	27084,2	0,440	44091,8	27084,2
2810,00	0,419	42066,5	24076,4	0,419	42066,5	24076,4	0,419	42066,5	24076,4
2820,00	0,420	42154,6	24176,9	0,420	42154,6	24176,9	0,420	42154,6	24176,9
2830,00	0,448	44884,3	28474,8	0,448	44884,3	28474,8	0,448	44884,3	28474,8
2840,00	0,451	45236,5	29092,8	0,451	45236,5	29092,8	0,451	45236,5	29092,8
2850,00	0,447	44796,3	28320,3	0,447	44796,3	28320,3	0,447	44796,3	28320,3
2860,00	0,426	42682,9	24780,0	0,426	42682,9	24780,0	0,426	42682,9	24780,0
2870,00	0,443	44444,0	27702,2	0,443	44444,0	27702,2	0,443	44444,0	27702,2
2880,00	0,446	44708,2	28165,7	0,446	44708,2	28165,7	0,446	44708,2	28165,7
2890,00	0,429	43035,1	25230,0	0,429	43035,1	25230,0	0,429	43035,1	25230,0
2900,00	0,440	44091,8	27084,2	0,440	44091,8	27084,2	0,440	44091,8	27084,2
2910,00	0,447	44796,3	28320,3	0,447	44796,3	28320,3	0,447	44796,3	28320,3
2920,00	0,445	44620,1	28011,2	0,445	44620,1	28011,2	0,445	44620,1	28011,2
2930,00	0,456	45764,9	30019,9	0,456	45764,9	30019,9	0,456	45764,9	30019,9
2940,00	0,434	43563,5	26157,1	0,434	43563,5	26157,1	0,434	43563,5	26157,1
2950,00	0,438	43915,7	26775,1	0,438	43915,7	26775,1	0,438	43915,7	26775,1
2960,00	0,443	44444,0	27702,2	0,443	44444,0	27702,2	0,443	44444,0	27702,2
2970,00	0,427	42859,0	24981,0	0,427	42859,0	24981,0	0,427	42859,0	24981,0
2980,00	0,441	44179,9	27238,7	0,441	44179,9	27238,7	0,441	44179,9	27238,7
2987,00	0,450	45148,5	28938,3	0,450	45148,5	28938,3	0,450	45148,5	28938,3
2990,00	0,450	45148,5	28938,3	0,450	45148,5	28938,3	0,450	45148,5	28938,3
3000,00	0,426	42682,9	24780,0	0,426	42682,9	24780,0	0,426	42682,9	24780,0
3011,00	0,426	42682,9	24780,0	0,426	42682,9	24780,0	0,426	42682,9	24780,0
3030,00	0,469	47085,7	32337,6	0,469	47085,7	32337,6	0,469	47085,7	32337,6
3036,00	0,469	46997,6	32183,1	0,469	46997,6	32183,1	0,469	46997,6	32183,1
3060,00	0,455	45676,8	29865,4	0,455	45676,8	29865,4	0,455	45676,8	29865,4
3061,00	0,455	45676,8	29865,4	0,455	45676,8	29865,4	0,455	45676,8	29865,4
3086,00	0,454	45500,7	29556,3	0,454	45500,7	29556,3	0,454	45500,7	29556,3
3090,00	0,432	43299,3	25693,5	0,432	43299,3	25693,5	0,432	43299,3	25693,5
3111,00	0,432	43299,3	25693,5	0,432	43299,3	25693,5	0,432	43299,3	25693,5
3120,00	0,435	43651,5	26311,6	0,435	43651,5	26311,6	0,435	43651,5	26311,6
3136,00	0,435	43651,5	26311,6	0,435	43651,5	26311,6	0,435	43651,5	26311,6
3150,00	0,432	43299,3	25693,5	0,432	43299,3	25693,5	0,432	43299,3	25693,5
3161,00	0,432	43299,3	25693,5	0,432	43299,3	25693,5	0,432	43299,3	25693,5
3180,00	0,424	42506,8	24579,0	0,424	42506,8	24579,0	0,424	42506,8	24579,0
3186,00	0,424	42506,8	24579,0	0,424	42506,8	24579,0	0,424	42506,8	24579,0
3210,00	0,441	44179,9	27238,7	0,441	44179,9	27238,7	0,441	44179,9	27238,7
3211,00	0,440	44091,8	27084,2	0,440	44091,8	27084,2	0,440	44091,8	27084,2
3236,00	0,455	45588,8	29710,9	0,455	45588,8	29710,9	0,455	45588,8	29710,9
3240,00	0,436	43739,6	26466,1	0,436	43739,6	26466,1	0,436	43739,6	26466,1
3261,00	0,437	43827,6	26620,6	0,437	43827,6	26620,6	0,437	43827,6	26620,6
3270,00	0,433	43475,4	26002,6	0,433	43475,4	26002,6	0,433	43475,4	26002,6
3286,00	0,433	43475,4	26002,6	0,433	43475,4	26002,6	0,433	43475,4	26002,6

Tabulated Results (Redrill)									
Measured Depth (m)	WF Base Rem. Wall (in)	WF Base Burst (kPa)	WF Base Collapse (kPa)	WF Low Rem. Wall (in)	WF Low Burst (kPa)	WF Low Collapse (kPa)	WF High Rem. Wall (in)	WF High Burst (kPa)	WF High Collapse (kPa)
3300,00	0,427	42859,0	24981,0	0,427	42859,0	24981,0	0,427	42859,0	24981,0
3311,00	0,427	42859,0	24981,0	0,427	42859,0	24981,0	0,427	42859,0	24981,0
3330,00	0,434	43563,5	26157,1	0,434	43563,5	26157,1	0,434	43563,5	26157,1
3336,00	0,434	43563,5	26157,1	0,434	43563,5	26157,1	0,434	43563,5	26157,1
3360,00	0,447	44796,3	28320,3	0,447	44796,3	28320,3	0,447	44796,3	28320,3
3361,00	0,447	44796,3	28320,3	0,447	44796,3	28320,3	0,447	44796,3	28320,3
3386,00	0,449	45060,4	28783,8	0,449	45060,4	28783,8	0,449	45060,4	28783,8
3390,00	0,421	42242,6	24277,4	0,421	42242,6	24277,4	0,421	42242,6	24277,4
3411,00	0,416	41714,3	23674,4	0,416	41714,3	23674,4	0,416	41714,3	23674,4
3420,00	0,424	42506,8	24579,0	0,424	42506,8	24579,0	0,424	42506,8	24579,0
3436,00	0,424	42506,8	24579,0	0,424	42506,8	24579,0	0,424	42506,8	24579,0
3450,00	0,426	42771,0	24880,5	0,426	42771,0	24880,5	0,426	42771,0	24880,5
3461,00	0,424	42506,8	24579,0	0,424	42506,8	24579,0	0,424	42506,8	24579,0
3480,00	0,441	44179,9	27238,7	0,441	44179,9	27238,7	0,441	44179,9	27238,7
3486,00	0,441	44179,9	27238,7	0,441	44179,9	27238,7	0,441	44179,9	27238,7
3510,00	0,414	41538,2	23473,4	0,414	41538,2	23473,4	0,414	41538,2	23473,4
3511,00	0,414	41538,2	23473,4	0,414	41538,2	23473,4	0,414	41538,2	23473,4
3536,00	0,423	42418,8	24478,5	0,423	42418,8	24478,5	0,423	42418,8	24478,5
3540,00	0,422	42330,7	24378,0	0,422	42330,7	24378,0	0,422	42330,7	24378,0
3561,00	0,422	42330,7	24378,0	0,422	42330,7	24378,0	0,422	42330,7	24378,0
3570,00	0,441	44267,9	27393,2	0,441	44267,9	27393,2	0,441	44267,9	27393,2
3586,00	0,433	43387,4	25848,1	0,433	43387,4	25848,1	0,433	43387,4	25848,1
3600,00	0,418	41890,4	23875,4	0,418	41890,4	23875,4	0,418	41890,4	23875,4
3611,00	0,406	40745,7	22568,8	0,406	40745,7	22568,8	0,406	40745,7	22568,8
3630,00	0,402	40305,4	22066,2	0,402	40305,4	22066,2	0,402	40305,4	22066,2
3636,00	0,401	40217,4	21965,7	0,401	40217,4	21965,7	0,401	40217,4	21965,7
3660,00	0,416	41714,3	23674,4	0,416	41714,3	23674,4	0,416	41714,3	23674,4
3661,00	0,416	41714,3	23674,4	0,416	41714,3	23674,4	0,416	41714,3	23674,4
3666,00	0,415	41626,3	23573,9	0,415	41626,3	23573,9	0,415	41626,3	23573,9
3687,00	0,423	42418,8	24478,5	0,423	42418,8	24478,5	0,423	42418,8	24478,5
3690,00	0,416	41714,3	23674,4	0,416	41714,3	23674,4	0,416	41714,3	23674,4
3714,00	0,426	42682,9	24780,0	0,426	42682,9	24780,0	0,426	42682,9	24780,0
3720,00	0,419	41978,5	23975,9	0,419	41978,5	23975,9	0,419	41978,5	23975,9
3742,00	0,429	43035,1	25230,0	0,429	43035,1	25230,0	0,429	43035,1	25230,0
3750,00	0,427	42859,0	24981,0	0,427	42859,0	24981,0	0,427	42859,0	24981,0
3770,00	0,426	42682,9	24780,0	0,426	42682,9	24780,0	0,426	42682,9	24780,0
3780,00	0,407	40833,8	22669,3	0,407	40833,8	22669,3	0,407	40833,8	22669,3
3798,00	0,407	40833,8	22669,3	0,407	40833,8	22669,3	0,407	40833,8	22669,3
3807,00	0,405	40657,7	22468,2	0,405	40657,7	22468,2	0,405	40657,7	22468,2
3810,00	0,405	40657,7	22468,2	0,405	40657,7	22468,2	0,405	40657,7	22468,2
3818,00	0,389	38984,6	20558,5	0,389	38984,6	20558,5	0,389	38984,6	20558,5

Table 23: 30/10 B-14A T3 tabulated pressures

Tabulated Results (Redrill)	
Wear Information	
Casing Top, MD= 0,00	
Wear Percent (%)	0,0
Remaining Thickness (in)	0,545
Burst Limit (kPa)	54658,6
Collapse Limit (kPa)	45625,8
Maximum Wear %, MD= 510,00	
Wear Percent (%)	39,3
Remaining Thickness (in)	0,331
Burst Limit (kPa)	33172,9
Collapse Limit (kPa)	13924,8

Table 24: 30/10 B-14A T3 results

Output Graphs

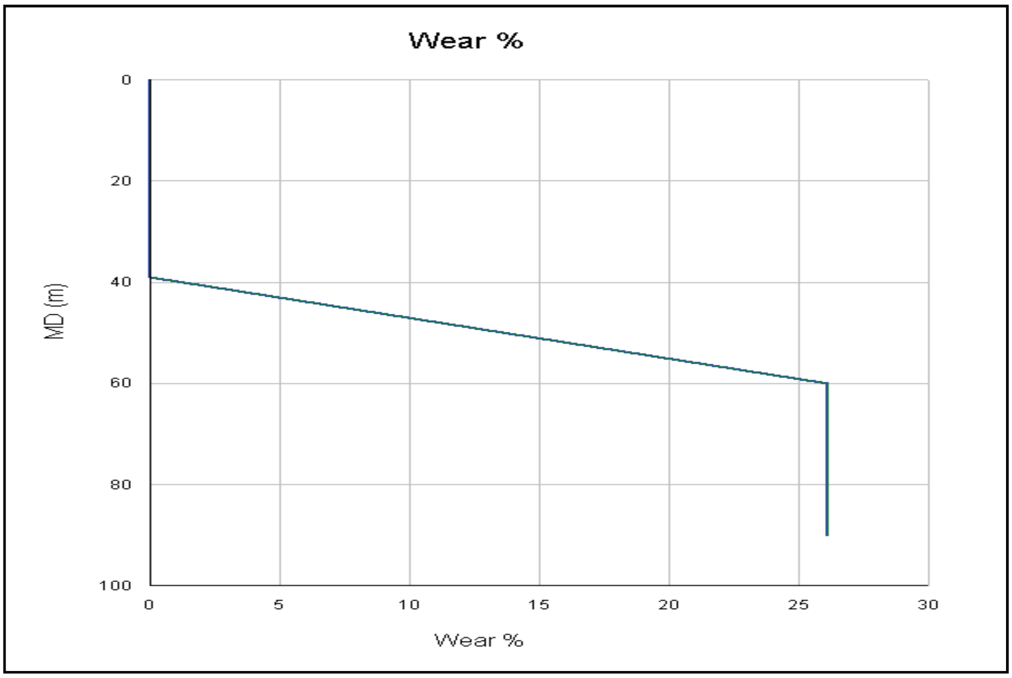

Figure 105: 30/10 B-14A T3 Output graph I

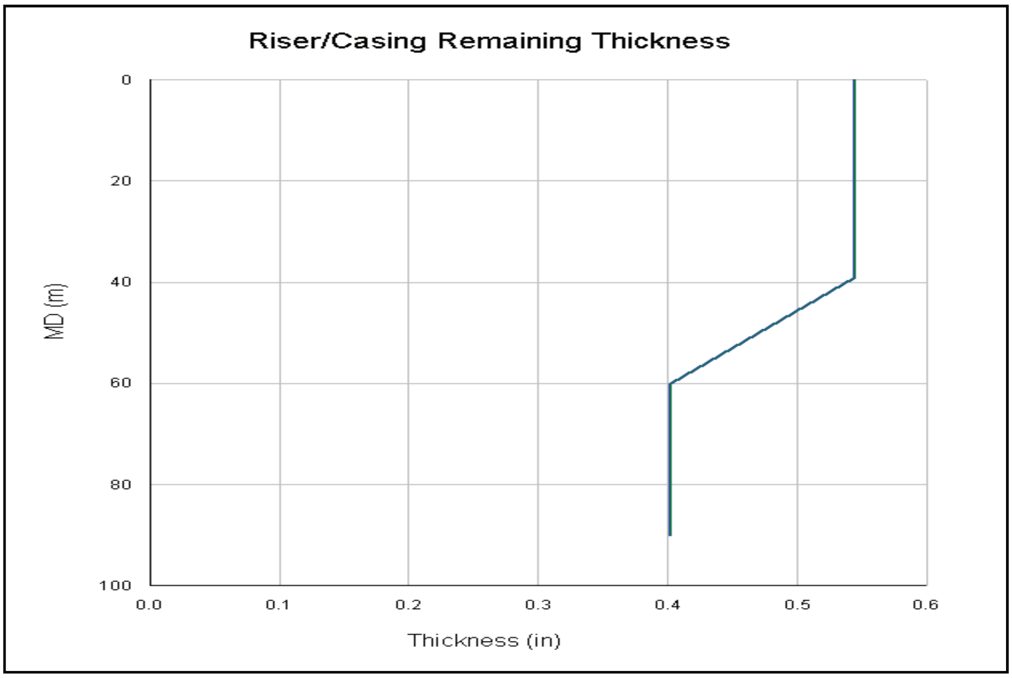

Figure 106: 30/10 B-14A T3 Output graph II

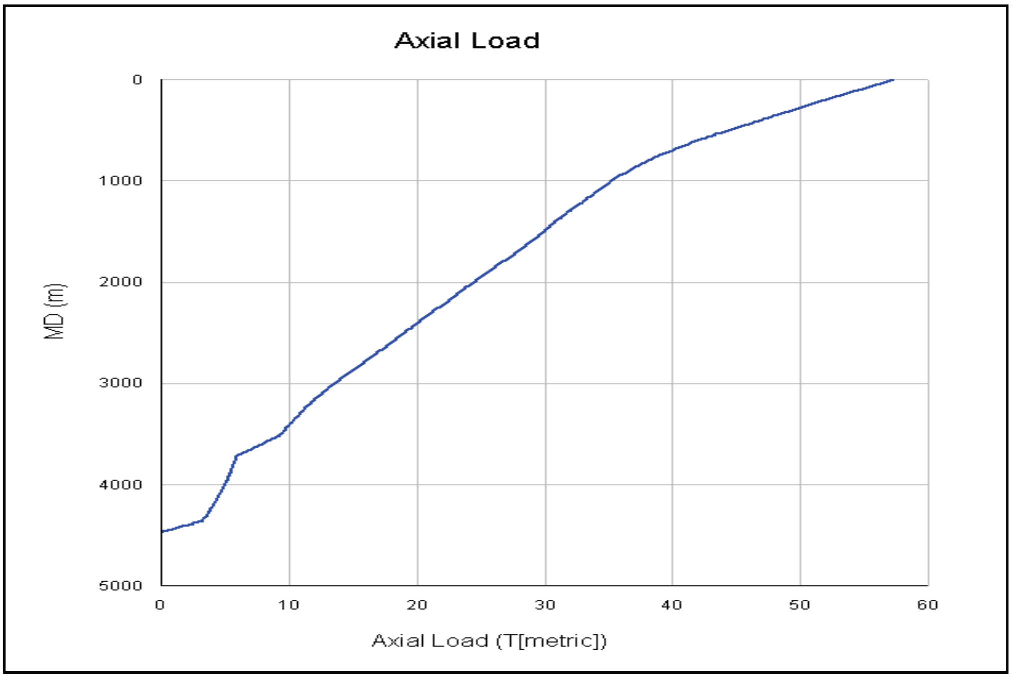

Figure 107: 30/10 B-14A T3 Output graph III

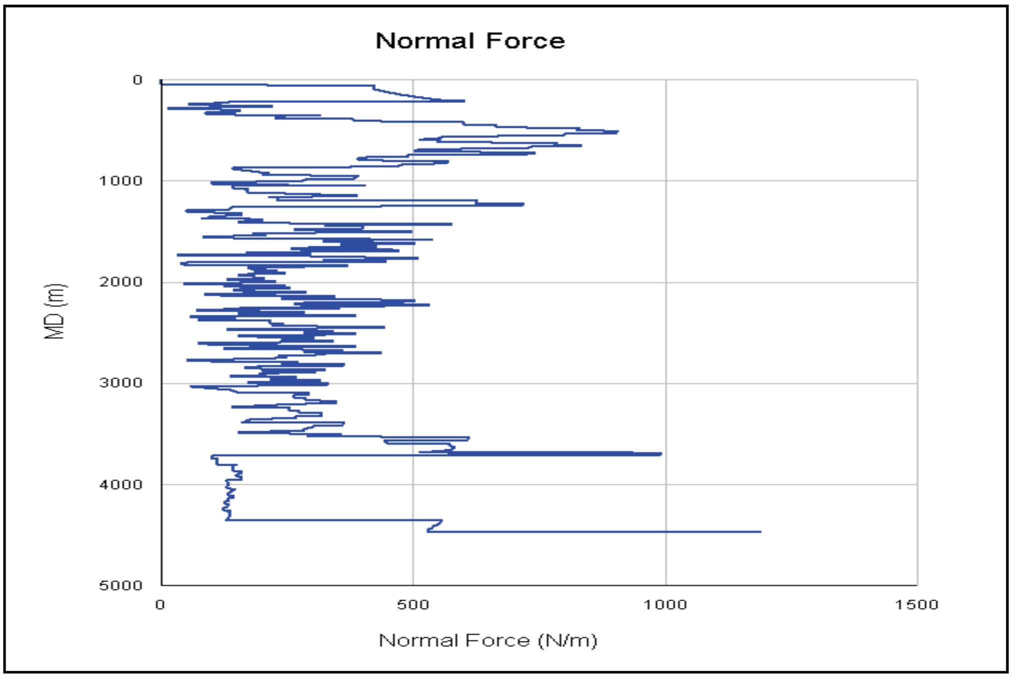

Figure 108: 30/10 B-14A T3 Output graph IV

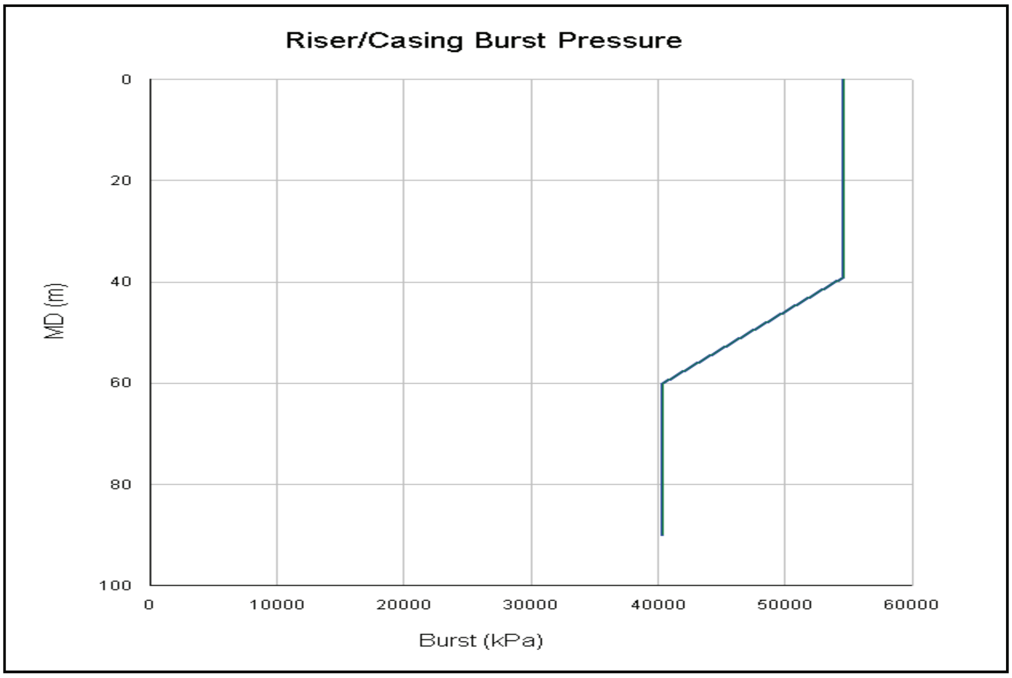

Figure 109: 30/10 B-14A T3 Output graph V

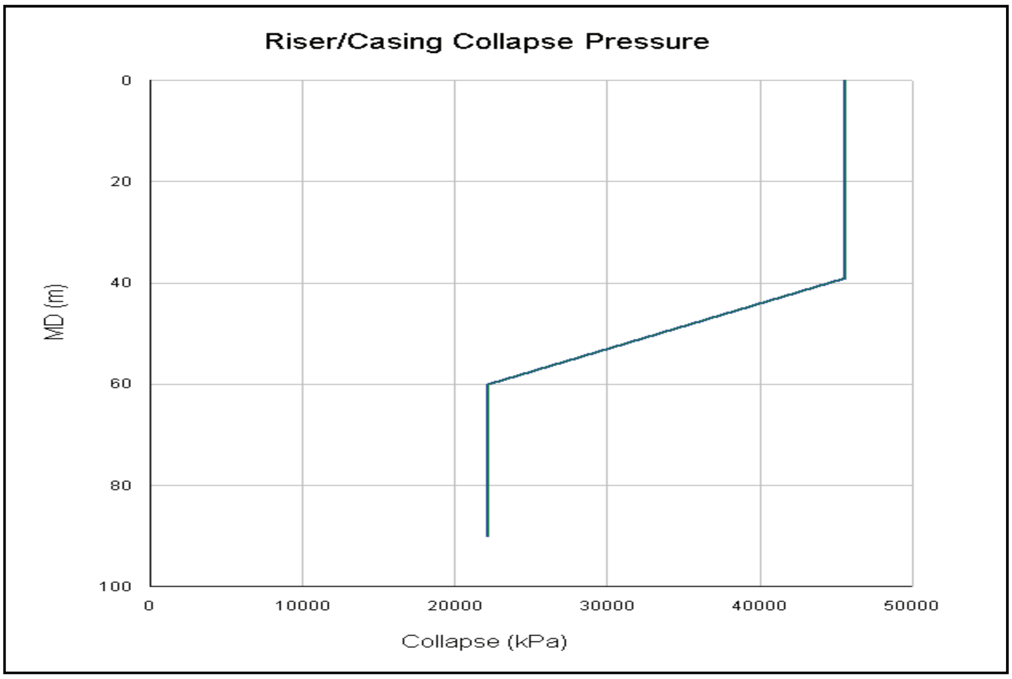

Figure 110: 30/10 B-14A T3 Output graph VI